

**ADVANCED SUSCEPTIBILITY AND DIFFUSION
WEIGHTED IMAGING IN THE DIAGNOSIS OF
MULTIPLE SCLEROSIS: FROM RESEARCH TO
CLINICAL APPLICATIONS**



Caterina Lapucci

Department of Neuroscience, Rehabilitation,
Ophthalmology, Genetics, and Maternal and Children's
Sciences (DINOEMI) University of Genova

Supervisors

Prof. Luca Roccatagliata

Prof. Matilde Inglese

Publications

Journal Articles

Published

- [1] Cellerino M, Cordano C, Boffa G, Bommarito G, Petracca M, Sbragia E, Novi G, **Lapucci C**, Capello E, Uccelli A, Inglese M. Relationship between retinal inner nuclear layer, age, and disease activity in progressive MS. *Neurol Neuroimmunol Neuroinflamm.* 2019 Aug 12;6(5): e596. doi: 10.1212/NXI.0000000000000596. Print 2019 Sep. PMID: 31454778
- [2] **Lapucci C**, Benedetti L, Tavarelli C, Serrati C, Godani M, Schenone A, Franciotta D. "Limbic encephalitis with acute onset and Hu antibodies treated with rituximab: Paraneoplastic or non-paraneoplastic disorder?" *Clin Neurol Neurosurg.* 2019 Sep; 184:105424. doi: 10.1016/j.clineuro.2019.105424. Epub 2019 Jul 12. PMID: 31330415
- [3] Frau J, Saccà F, Signori A, Baroncini D, Fenu G, Annovazzi P, Capobianco M, Signoriello E, Laroni A, La Gioia S, Sartori A, Maniscalco GT, Bonavita S, Clerico M, Russo CV, Gallo A, **Lapucci C**, Carotenuto A, Sormani MP, Cocco E; i-MuST study group. Outcomes after fingolimod to alemtuzumab treatment shift in relapsing-remitting MS patients: a multicentre cohort study. *J Neurol.* 2019 Oct;266(10):2440-2446. doi: 10.1007/s00415-019-09424-8. Epub 2019 Jun 17. PMID: 31209573
- [4] **Lapucci C**, Boffa G, Massa F, Franciotta D, Castelletti L, Uccelli A, Morbelli S, Nobili F, Benedetti L, Roccatagliata L. Could arterial spin labelling perfusion imaging uncover the invisible in N-methyl-d-aspartate receptor

- encephalitis? *Eur J Neurol.* 2019 Oct;26(10): e86-e87. doi: 10.1111/ene.13977. Epub 2019 May 17. PMID: 31099961
- [5] Boffa G, **Lapucci C**, Morbelli SD, Nobili FM. Two-way crossed cerebellar diaschisis in a clinically isolated syndrome suggestive of multiple sclerosis. *Q J Nucl Med Mol Imaging.* 2019 Jun;63(2):225-226. doi: 10.23736/S1824-4785.19.03171-6. Epub 2019 May 8. PMID: 31089076
- [6] **Lapucci C**, Baroncini D, Cellerino M, Boffa G, Callegari I, Pardini M, Novi G, Sormani MP, Mancardi GL, Ghezzi A, Zaffaroni M, Uccelli A, Inglese M, Roccatagliata L. Different MRI patterns in MS worsening after stopping fingolimod. *Neurol Neuroimmunol Neuroinflamm.* 2019 Apr 16;6(4): e566. doi: 10.1212/NXI.0000000000000566. eCollection 2019 Jul. PMID: 31086807
- [7] **Lapucci C**, Serrati C, Delucchi S, Mannironi A, Benedetti L. Are basketball players more likely to develop Hirayama disease? Cabona C, Beronio A, Martinelli I, Briani C. *J Neurol Sci.* 2019 May 15; 400:142-144. doi: 10.1016/j.jns.2019.03.020. Epub 2019 Mar 21. PMID: 30951991
- [8] **Lapucci C**, Saitta L, Bommarito G, Sormani MP, Pardini M, Bonzano L, Mancardi GL, Gasperini C, Giorgio A, Inglese M, De Stefano N, Roccatagliata L. How much do periventricular lesions assist in distinguishing migraine with aura from CIS? *Neurology.* 2019 Apr 9;92(15): e1739-e1744. doi: 10.1212/WNL.0000000000007266. Epub 2019 Mar 8. PMID: 30850445
- [9] **Lapucci C**, Romano N, Schiavi S, Saitta L, Uccelli A, Boffa G, Pardini M, Signori A, Castellan L, Inglese M, Roccatagliata L. Degree of microstructural changes within T1-SE versus T1-GE hypointense lesions in multiple sclerosis: relevance for the definition of "black holes". *Eur Radiol.* 2020 Jul;30(7):3843-3851. doi: 10.1007/s00330-020-06761-5

- [10] Boffa G*, **Lapucci C***, Sbragia E, Varaldo R, Raiola AM, Currò D, Roccatagliata L, Capello E, Laroni A, Mikulska M, Gualandi F, Uccelli A, Angelucci E, Mancardi GL, Inglese M. Aggressive multiple sclerosis: a single-centre, real-world treatment experience with autologous haematopoietic stem cell transplantation and alemtuzumab. *Eur J Neurol.* 2020 May 17. doi: 10.1111/ene.14324
- [11] Coccia A., **Lapucci C.**, Bandettini di Poggio M., Grazzini M. 2, Inglese M. 2, Finocchi C. A longitudinal clinical and MRI evaluation of the treatment with erenumab *Neurol Sci* 2020 Aug 26;1-2. doi: 10.1007/s10072-020-04660-7
- [12] Carmisciano L, Signori A, Pardini M, Novi G, **Lapucci C**, Nesi L, Gallo E, Laroni A, Cellerino M, Meli R, Sbragia E, Filippi L, Uccelli A, Inglese M, Sormani MP. Assessing upper limb function in multiple sclerosis using an engineered glove. *Eur J Neurol.* 2020 Aug 17. doi: 10.1111/ene.14482
- [13] Novi G, Bovis F, Fabbri S, Tazza F, Gazzola P, Maietta I, Currò D, Bruschi N, Roccatagliata L, Boffa G, **Lapucci C**, Pesce G, Cellerino M, Solaro C, Laroni A, Capello E, Mancardi G, Sormani M, Inglese M, Uccelli A. Tailoring B cell depletion therapy in MS according to memory B cell monitoring. *Neurol Neuroimmunol Neuroinflamm.* 2020 Aug 4;7(5): e845. doi: 10.1212/NXI.0000000000000845.
- [14] Gastaldi M, Mariotto S, Giannoccaro MP, Iorio R, Zoccarato M, Nosadini M, Benedetti L, Casagrande S, Di Filippo M, Valeriani M, Ricci S, Bova S, Arbasino C, Mauri M, Versino M, Vigevano F, Papetti L, Romoli M, **Lapucci C**, Massa F, Sartori S, Zuliani L, Barilaro A, De Gaspari P, Spagni G, Evoli A, Liguori R, Ferrari S, Marchioni E, Giometto B, Massacesi L, Franciotta D. Subgroup comparison according to clinical phenotype and serostatus in

- autoimmune encephalitis: a multicenter retrospective study. *Eur J Neurol*. 2020 Apr;27(4):633-643. doi: 10.1111/ene.14139
- [15] Bauckneht M, Capitanio S, Raffa S, Roccatagliata L, Pardini M, **Lapucci C**, Marini C, Sambuceti G, Inglese M, Gallo P, Cecchin D, Nobili F, Morbelli S. Molecular imaging of multiple sclerosis: from the clinical demand to novel radiotracers. *EJNMMI Radiopharm Chem*. 2019 Apr 8;4(1):6. doi: 10.1186/s41181-019-0058-3.
- [16] Pardini M, Nobili F, Arnaldi D, Morbelli S, Bauckneht M, Rissotto R, Serrati C, Serafini G, **Lapucci C**, Ghio L, Amore M, Massucco D, Sassos D, Bonzano L, Mancardi GL, Roccatagliata L; Disease Management Team on Dementia of the IRCCS Ospedale Policlinico San Martino, Genoa. 123I-FP-CIT SPECT validation of nigro-putaminal MRI tractography in dementia with Lewy bodies. *Eur Radiol Exp*. 2020 May 4;4(1):27. doi: 10.1186/s41747-020-00153-6.
- [17] Boffa G, Bruschi N, Cellerino M, **Lapucci C**, Novi G, Sbragia E, Capello E, Uccelli A, Inglese M. Fingolimod and Dimethyl-Fumarate-Derived Lymphopenia is not Associated with Short-Term Treatment Response and Risk of Infections in a Real-Life MS Population. *CNS Drugs*. 2020 Apr;34(4):425-432. doi: 10.1007/s40263-020-00714-8.
- [18] Signori A, Sormani MP, **Lapucci C**, Uccelli A, Bove M, Bonzano L. Effects of aging on finger movements in multiple sclerosis. *Mult Scler Relat Disord*. 2020 Jan; 37:101449. doi: 10.1016/j.msard.2019.101449.
- [19] Cellerino M, Ivaldi F, Pardini M, Rotta G, Vila G, Bäcker-Koduah P, Berge T, Laroni A, **Lapucci C**, Novi G, Boffa G, Sbragia E, Palmeri S, Asseyer S, Høgestøl E, Campi C, Piana M, Inglese M, Paul F, Harbo HF, Villoslada P, Kerlero de Rosbo N, Uccelli A. Impact of treatment on cellular

- immunophenotype in MS: A cross-sectional study. *Neurol Neuroimmunol Neuroinflamm.* 2020 Mar 5;7(3): e693. doi: 10.1212/NXI.0000000000000693.
- [20] Koudriavtseva T., Stefanile A., Fiorelli M., **Lapucci C.**, Lorenzano L., Pimpinelli F., Zannino S., D'Agosto G., Giannarelli D., Mandoj C., Conti L., Donzelli S., Blandino G., Salvetti M., Inglese M. Coagulation/complement activation and cerebral hypoperfusion in relapsing-remitting multiple sclerosis. *Frontiers in Immunology* (2020).
- [21] Palmeri S, Ponzano M, Ivaldi F, Signori A, **Lapucci C**, Casella V, Ferrò MT, Vigo T, Inglese M, Mancardi GL, Uccelli A, Laroni A. Impact of Natural Killer (NK) Cells on Immune Reconstitution, and Their Potential as a Biomarker of Disease Activity, in Alemtuzumab-Treated Patients with Relapsing Remitting Multiple Sclerosis: An Observational Study. *CNS Drugs.* 2022 Jan;36(1):83-96. doi: 10.1007/s40263-021-00875-0. Epub 2021 Dec 11. PMID: 34894339
- [22] Sormani MP, Schiavetti I, Carmisciano L, Cordioli C, Filippi M, Radaelli M, Immovilli P, Capobianco M, De Rossi N, Bricchetto G, Cocco E, Scandellari C, Cavalla P, Pesci I, Zito A, Confalonieri P, Marfia GA, Perini P, Inglese M, Trojano M, Brescia Morra V, Tedeschi G, Comi G, Battaglia MA, Patti F, Salvetti M; MuSC-19 Study Group. COVID-19 Severity in Multiple Sclerosis: Putting Data into Context. *Neurol Neuroimmunol Neuroinflamm.* 2021 Nov 9;9(1): e1105. doi: 10.1212/NXI.0000000000001105. Print 2022 Jan. PMID: 34753829
- [23] Bergamaschi R, Ponzano M, Schiavetti I, Carmisciano L, Cordioli C, Filippi M, Radaelli M, Immovilli P, Capobianco M, De Rossi N, Bricchetto G, Cocco E, Scandellari C, Cavalla P, Pesci I, Zito A, Confalonieri P, Marfia GA, Perini P, Inglese M, Trojano M, Brescia Morra V, Pisoni E, Tedeschi G, Comi G, Battaglia MA, Patti F, Salvetti M, Sormani MP; MuSC-19 study group. The

effect of air pollution on COVID-19 severity in a sample of patients with multiple sclerosis. *Eur J Neurol.* 2022 Feb;29(2):535-542. doi: 10.1111/ene.15167. Epub 2021 Nov 15. PMID: 34735749

[24] Sormani MP, Inglese M, Schiavetti I, Carmisciano L, Laroni A, **Lapucci C**, Da Rin G, Serrati C, Gandoglia I, Tassinari T, Perego G, Bricchetto G, Gazzola P, Mannironi A, Stromillo ML, Cordioli C, Landi D, Clerico M, Signoriello E, Frau J, Ferrò MT, Di Sapio A, Pasquali L, Ulivelli M, Marinelli F, Callari G, Iodice R, Liberatore G, Caleri F, Repice AM, Cordera S, Battaglia MA, Salvetti M, Franciotta D, Uccelli A; CovaXiMS study group on behalf of the Italian Covid-19 Alliance in MS. Effect of SARS-CoV-2 mRNA vaccination in MS patients treated with disease modifying therapies. *EBioMedicine.* 2021 Oct; 72:103581. doi: 10.1016/j.ebiom.2021.103581. Epub 2021 Sep 22. PMID: 34563483

[25] Russo CV, Saccà F, Frau J, Annovazzi P, Signoriello E, Bonavita S, Grasso R, Clerico M, Cordioli C, Laroni A, Capobianco M, Torri Clerici V, Sartori A, Cavalla P, Maniscalco GT, La Gioia S, Caleri F, Giugno A, Iodice R, Carotenuto A, Cocco E, Fenu G, Zaffaroni M, Baroncini D, Lus G, Gallo A, De Mercanti SF, **Lapucci C**, Di Francescantonio V, Brambilla L, Sormani MP, Signori A. A real-world study of alemtuzumab in a cohort of Italian patients. *Eur J Neurol.* 2022 Jan;29(1):257-266. doi: 10.1111/ene.15121. Epub 2021 Oct 5. PMID: 34558755

[26] Cellerino M, Boffa G, **Lapucci C**, Tazza F, Sbragia E, Mancuso E, Bruschi N, Minguzzi S, Ivaldi F, Poirè I, Laroni A, Mancardi G, Capello E, Uccelli A, Novi G, Inglese M. Predictors of Ocrelizumab Effectiveness in Patients with Multiple Sclerosis. *Neurotherapeutics.* 2021 Oct;18(4):2579-2588. doi: 10.1007/s13311-021-01104-8. Epub 2021 Sep 22. PMID: 34553320

- [27] Sormani MP, Schiavetti I, Landi D, Carmisciano L, De Rossi N, Cordioli C, Moiola L, Radaelli M, Immovilli P, Capobianco M, Brescia Morra V, Trojano M, Tedeschi G, Comi G, Battaglia MA, Patti F, Fragoso YD, Sen S, Siva A, Furlan R, Salvetti M; MuSC-19 Study Group. SARS-CoV-2 serology after COVID-19 in multiple sclerosis: An international cohort study. *Mult Scler*. 2021 Jul 30;13524585211035318. doi: 10.1177/13524585211035318.
- [28] Sormani MP, Salvetti M, Labauge P, Schiavetti I, Zephir H, Carmisciano L, Bensa C, De Rossi N, Pelletier J, Cordioli C, Vukusic S, Moiola L, Kerschen P, Radaelli M, Théaudin M, Immovilli P, Casez O, Capobianco M, Ciron J, Trojano M, Stankoff B, Créange A, Tedeschi G, Clavelou P, Comi G, Thouvenot E, Battaglia MA, Moreau T, Patti F, De Sèze J, Louapre C; Musc-19; Covisep study groups. DMTs and Covid-19 severity in MS: a pooled analysis from Italy and France. *Ann Clin Transl Neurol*. 2021 Aug;8(8):1738-1744. doi: 10.1002/acn3.51408. Epub 2021 Jul 7. PMID: 34240579
- [29] Tazza F*, **Lapucci C***, Cellerino M, Boffa G, Novi G, Poire I, Mancuso E, Bruschi N, Sbragia E, Laroni A, Capello E, Inglese M. Personalizing ocrelizumab treatment in Multiple Sclerosis: What can we learn from Sars-Cov2 pandemic? *J Neurol Sci*. 2021 Aug 15; 427:117501. doi: 10.1016/j.jns.2021.117501. Epub 2021 May 20. PMID: 34044238
- [30] Sbragia E, Colombo E, Pollio C, Cellerino M, **Lapucci C**, Inglese M, Mancardi G, Boffa G. Embracing resilience in multiple sclerosis: a new perspective from COVID-19 pandemic. *Psychol Health Med*. 2022 Feb;27(2):352-360. doi: 10.1080/13548506.2021.1916964. Epub 2021 Apr 25. PMID: 33899615
- [31] Cellerino M, Priano L, Bruschi N, Boffa G, Petracca M, Novi G, **Lapucci C**, Sbragia E, Uccelli A, Inglese M. Relationship Between Retinal Layer Thickness and Disability Worsening in Relapsing-Remitting and Progressive

Multiple Sclerosis. J Neuroophthalmol. 2021 Sep 1;41(3):329-334. doi: 10.1097/WNO.0000000000001165.PMID: 33399416

[32]Demichelis C, Balestra A, **Lapucci C**, Zuppa A, Grisanti SG, Prada V, Pesce G, Grasso I, Queirolo P, Schenone A, Benedetti L, Grandis M. Neuromuscular complications following targeted therapy in cancer patients: beyond the immune checkpoint inhibitors. Case reports and review of the literature. Neurol Sci. 2021 Apr;42(4):1405-1409. doi: 10.1007/s10072-020-04604-1. Epub 2020 Aug 11. PMID: 32783159.

Submitted:

- The role of disconnection in explaining disability in Multiple Sclerosis (accepted on 10 Apr 2022 in European Radiology Experimental)
- The role of central vein sign and diffusion MRI to differentiate microstructural features within white matter lesions of multiple sclerosis patients with comorbidities (under review)
- The Central Vein Sign to differentiate multiple sclerosis from migraine (under review)
- Breakthrough SARS-CoV-2 infections after COVID-19 mRNA vaccination in MS patients on disease modifying therapies (under review)

Conferences

- [1] **C. Lapucci**, S. Schiavi, E. Sbragia, G. Bommarito, M. Cellerino, L. Roccatagliata, A. Uccelli, M. Inglese, M. Pardini The Role Of Disconnection In Explaining Disability In Multiple Sclerosis. Ectrims 2019
- [2] **C. Lapucci**, S. Schiavi, E. Sbragia, G. Bommarito, M. Cellerino, L. Roccatagliata, A. Uccelli, M. Inglese, M. Pardini. The Role of Disconnection In Explaining Disability In Multiple Sclerosis. Sin 2019
- [3] **C. Lapucci**, N. Romano, S. Schiavi, L. Saitta, G. Boffa, M. Pardini, A. Signori, M. Sormani, A. Uccelli, M. Inglese, L. Roccatagliata **T1** Gradient-Echo And T1 Spin-Echo Sequences Detection Of Hypointense Lesions In Multiple Sclerosis. Relevance For the Definition Of “Black Holes”. Sin 2019
- [4] **C. Lapucci**, D. Baroncini, M. Cellerino, G. Boffa, I. Callegari, M. Pardini, G. Novi, M. Sormani, G. Mancardi, A. Ghezzi, M. Zaffaroni, A. Uccelli, M. Inglese, L. Roccatagliata Different Mri Patterns In Multiple Sclerosis Worsening After Stopping Fingolimod. Sin 2019
- [5] T. Koudriavtseva, S. Zannino, M. Filippi, A. Cortese, C. Piantadosi, **C. Lapucci**, M. Fiorelli, D. Giannarelli, C. Mandoj, A. Stefanile, E. Galie, L. Conti, M. Salvetti, M. Inglese. Coagulation Activation and Cerebral Hypoperfusion In Relapsing-Remitting Multiple Sclerosis. Sin 2019
- [6] **C Lapucci**, Romano N, Schiavi S, Saitta L., Boffa G, Pardini M, Sormani Mp, Signori A, Inglese M, Roccatagliata L. Are FSPGR More Sensitive Than T1 Spin-Echo

Sequences in Detecting Brain Hypointense Lesions In Multiple Sclerosis? Relevance For the Definition Of «Black Holes». Airmm 2019

[7] **C Lapucci**, Boffa G, Cellerino M, Novi G, Sbragia E, Bruschi N, Mancuso E, Tazza F, Laroni A, Capello E, Uccelli A, Inglese M. Ocrelizumab Treatment in Patients With Relapsing-Remitting Multiple Sclerosis: A Single-Center Real-World Experience. Ectrims 2020

[8] **C. Lapucci**, Frau J., Cocco E., Vercellino M., Cavalla P., Petracca M., Lanzillo R., Grossi P., Ferrò M.T., Guaschino C., Zaffaroni M., Tazza F., Novi G., Uccelli A., Inglese M. Short-Term Evaluation of Alemtuzumab To Ocrelizumab Switch In Ms Patients With Disease Activity After Alemtuzumab: An Italian Multicentric Study. Ectrims 2020

[9] **C. Lapucci**, G. Boffa, E. Sbragia, E. Capello, D. Currò, A. Laroni, L. Roccatagliata, A. Uccelli, F. Gualandi, G. Mancardi, M. Inglese Therapeutic Strategies for Aggressive Multiple Sclerosis: A Single Center Experience With Alemtuzumab And Autologous Hematopoietic Stem Cells Transplantation. Aan 2020

[10] **C. Lapucci**, Frau J. Cocco E, Vercellino M., Cavalla P., Grossi P., Ferrò M.T., Guaschino C., Zaffaroni M., Tazza F., Novi G., Uccelli A., Inglese M. Short-Term Safety and Efficacy Of The Switch From Alemtuzumab To Ocrelizumab In Ms Patients With Disease Activity After Two Alemtuzumab Courses: An Italian Multicentric, Real-Life Study. Ean 2020

[11] **C. Lapucci**, Boffa G, Cellerino M, Novi G, Sbragia E, Bruschi N, Mancuso E, Tazza F, Laroni A, Capello E, Uccelli A, Inglese M. Ocrelizumab Treatment in Patients

With Relapsing-Remitting Multiple Sclerosis: A Single-Center Real-World Experience.

Aan 2021

- [12] **C. Lapucci**, Frau J., Cocco E., Vercellino M., Cavalla P., Petracca M., Lanzillo R., Grossi P., Ferrò M.T., Guaschino C., Zaffaroni M., Tazza F., Novi G., Uccelli A., Inglese M. Short-Term Evaluation of Alemtuzumab To Ocrelizumab Switch In Ms Patients With Disease Activity After Alemtuzumab: An Italian Multicentric Study. Aan 2021

- [13] **C. Lapucci**, Fiorelli M, Stefanile A, Zannino S, Filippi Mm, Cortese A, Piantadosi C, Salvetti M, And Koudriavtseva T And Inglese M An Increased Normal Appearing White Matter Perfusion: A Possible Radiological Inflammatory Marker in Relapsing-Remitting Multiple Sclerosis Actrims 2021, Ismrm 2021, Ean 2021

Funding

Part of the work presented in this thesis has been financed by the Italian Minister of Health ('5 per mille' public funding) and by Dipartimento di Eccellenza (DINOGMI) funding.

Contents

1 Introduction	1
1.1 Rational and Objectives	1
1.2 Overview of the Thesis	3
2. Background	4
2.1 Multiple sclerosis	4
2.1.1 Classification	4
2.1.2. Epidemiology	5
2.1.3 Risk factors	7
2.1.4 Pathogenesis	9
2.1.5 Clinical features	12
2.1.6 Diagnosis	12
2.1.7 Treatment	13
2.1.8 Differential Diagnosis and Misdiagnosis	15
2.2 Susceptibility Weighted Imaging: The “Central Vein Sign”	24
2.2.1 Central Veins in MS plaques: From Pathology to Imaging	24
2.2.2 Detecting the Central Vein in MRI: Technical Aspects	25
2.2.3 Detecting the Central Vein in MRI: Clinical Application, Definition and Challenges	27
2.3 Advanced Diffusion MRI in Multiple Sclerosis	36
2.3.1 Diffusion Tensor Imaging (DTI)	36
2.3.2 Neurite Orientation Dispersion and Density Imaging (NODDI)	38
2.3.3 Spherical Mean Technique (SMT)	40
3. The Central Vein Sign to differentiate multiple sclerosis from migraine	42
3.1 Introduction	42
3.2 Material and Methods	43

3.3 Results	47
3.4 Discussion	56
4. White matter lesions and comorbidities in multiple sclerosis: central vein sign and diffusion MRI	61
4.1 Introduction	61
4.2 Material and Methods.....	63
4.3 Results	68
4.4 Discussion	80
5. Bibliography	86

List of Figures

Figure 1 The contemporary spectrum of Multiple Sclerosis misdiagnosis	18
Figure 2 Main causes of MS misdiagnosis	21
Figure 3 Duration of MS misdiagnosis.....	21
Figure 4 Consequences of misdiagnosis	22
Figure 5 Perivenous distribution of Multiple Sclerosis lesions	30
Figure 6 Inclusion and exclusion criteria for Central Vein Sign assessment	33
Figure 7 Microstructural maps derived from NODDI and SMT models	41
Figure 8 3D-FLAIR*creation from 3D-epiT2* and 3D-FLAIR images	45
Figure 9 Central Vein Sign in multiple sclerosis and migraine.....	49
Figure 10 Brain location of WM lesions exhibiting the Central Vein Sign in MS.....	51
Figure 11 ROC curve of CVS+ lesion thresholds differentiating MS from migraine.....	54
Figure 12 CVS+ and CVS- lesion distribution according to Age Groups and brain subregions	75
Figure 13 Association between patient's age and the frequency of CVS+ lesions	77
Figure 14 Selected sagittal FLAIR* and SMT-derived EXTRAMD, EXTRATRANS and INTRA maps of a 62-year-old patient diagnosed with Multiple Sclerosis.....	79

List of Tables

Table 1 Demographic and clinical features of MS and migraine patients' cohorts.....	47
Table 2 Total white matter and CVS+ lesions number and volume in migraine and MS patients	52
Table 3. Performance of different CVS+ lesion thresholds and absolute number of CVS+ lesions	55
Table 4 Baseline demographic and clinical characteristics	70
Table 5 Volume and topography of CVS+ and CVS- lesions in the whole cohort and according to Age Groups	72
Table 6 CVS+ lesions percentage comparisons among Age Groups, MS phenotype, RFs for SVD and migraine.....	74
Table 7 SMT metrics comparisons between CVS+ and CVS- lesions.....	78

Chapter 1

1 Introduction

1.1 Rational and Objectives

In 2015, the Institute of Medicine described the need to study the phenomenon of misdiagnosis as a “moral, professional, and public health imperative”.

Despite the periodic updates of diagnostic criteria for MS, the risk of diagnosing as having MS patients with other disease involving the Central Nervous System (CNS) remains still not negligible. Indeed, diagnosis of MS may be straightforward, but a rapid and accurate diagnosis of MS can also be an issue, particularly due to the lack of specific biomarkers.

Alongside developments that enabled earlier diagnosis of MS, the introduction of disease-modifying therapies (DMTs) for MS provided increasing evidence that earlier treatment is associated with better long-term outcomes. This evidence leads to an increasing pressure for the physician to make a diagnosis of MS as early as possible. This pressure, in turn, creates a tension between the benefits of an early MS diagnosis and the risk of an inaccurate diagnosis that may cause serious, sometimes life-threatening, health and financial consequences.

Among MS mimics, migraine (alone or in combination with additional diagnoses) has been reported as the most common alternative diagnosis in patients misdiagnosed with MS (reported in 22% of misdiagnosed patients). Interestingly, in the patients with migraine, it was reported that often migraineurs symptoms mistaken for demyelinating attacks were incorrectly used to satisfy Dissemination in Time (DIT) criteria for MS. On the other side, migraine-associated white matter

(WM) hyperintensity were often considered in the fulfilment of Dissemination in Space (DIS) imaging criteria for MS.

Nevertheless, the differential diagnosis between MS and its mimics is not the only challenge. In a treatment era when also the only evidence of radiological disease activity in clinically stable patients may be the trigger to escalate MS therapy, the presence of comorbidities in a patient with MS introduces an extra challenge, represented by the need to distinguish whether a new T2 lesion is due to MS or to comorbidities. The high prevalence of small vessel disease (SVD)-related white matter hyperintensities in people over 50 years of migraine in general population including MS patients and the similar features shared with MS in conventional MRI sequences regardless of their different histopathological substrates, makes this issue not negligible.

The identification of specific and sensitive biomarkers able to distinguish MS from other diseases represent an unmet need. Several cerebrospinal fluid and serum biomarkers of MS have been studied, but no tests with high specificity and sensitivity are now available. Another issue is represented by the fact that many proposed biomarkers have only been explored in the context of cross-sectional studies, while their longitudinal evaluation is essential.

As concerns MRI biomarkers, the “Central Vein Sign” inside WM lesions has been proposed as a very promising biomarker of inflammatory demyelination and, thus, may aid the diagnosis of MS and differentiation from its mimics. On the other hand, multi-compartments diffusion models have been demonstrated their potential in investigating tissue abnormalities inside MS lesions and Normal Appearing White Matter (NAWM), as demyelination, fibre loss and axonal degeneration.

The work described in this thesis aimed at investigating the application of the Central Vein Sign detected on advanced susceptibility weighted images to

differentiate MS from migraine and then, at applying the Central Vein Sign associated with advanced diffusion weighted images, to explore the impact of ageing and comorbidities on WM lesions architecture in MS.

1.2 Overview of the Thesis

- Chapter 2 includes a description of multiple sclerosis, with a final focus on MS mimics and their challenging differentiation from MS.
- In the chapter 2 an overview of the state of the art of advanced susceptibility and diffusion weighted imaging methods used to investigate brain structure is provided, together with a summary of previous studies that used these techniques in MS.
- In the chapter 3 the first study, aiming at investigating the performance of the Central Vein Sign (CVS) in the differential diagnosis between MS and migraine is described.
- The chapter 4 illustrates the second study, exploring the performance of the CVS and spherical Mean Technique (SMT) model in differentiating MS lesions from white matter hyperintensities related to ageing, concomitant small vessel disease and migraine in a cohort of patients with MS.

The chapters 3 and 4 contain sections including the background, aims, methods and discussion specific for each study.

Chapter 2

2. Background

2.1 Multiple sclerosis

Multiple sclerosis (MS) is defined as a chronic immune-mediated, demyelinating disease of the central nervous system (CNS).

2.1.1 Classification

The most common phenotype is the relapsing-remitting course and affects about 85% of patients; the onset, in this case, is characterized by an acute episode of neurological deficit (clinically isolated syndrome (CIS)) lasting at least 24 hours and in most cases interesting the optic nerve, brainstem, spinal cord or cerebellum, followed by a remission period of clinical recovery¹. The clinical course of relapsing remitting (RR) MS is typically characterized by recurring phases of relapses and remissions. Relapses are characterized by focal inflammation and demyelination within the CNS. Approximately 15-30% of these patients develop secondary progressive (SP) MS, over a long-term follow-up. About 10-15% of patients with MS are diagnosed with primary progressive (PP) disease, which is characterized by a progressive disability from the outset in absence of relapses¹.

A new phenotype classification has been introduced, for the three forms (RR, PP and SP), which further subdivides them according to disease activity and progression².

2.1.2. Epidemiology

Multiple sclerosis is the most common demyelinating disease seen in developed countries, and the main cause of non-traumatic chronic disability in young adults, with the average age at diagnosis being 30 years³.

2.1.2.1 Prevalence and incidence.

The global prevalence of MS has been estimated, in 2016, as 30.1 cases per 100000 population. Its prevalence increased from 1990 to 2016, in particular in east Asia and Canada. The highest rates have been registered in North America (164.6), western Europe (127.0) and Australasia (91.1) while the lowest in eastern and central sub-Saharan Africa (3.3 and 2.8, respectively) and Oceania (2.0). In a recent systematic analysis, a significant association was found between prevalence and both latitude and the socio-demographic status⁴. The constant increase in MS prevalence^{4,5} is probably related to concomitant factors: the higher rate in survival, the higher incidence due to improvements in the diagnosis⁵. The global median incidence of MS is 2.5 per 100000, with higher rates in Europe (3.8), Eastern Mediterranean (2), Americas (1.5), Western Pacific and Africa. Early epidemiological studies and reviews described a north to south and a high- to low-income gradient in MS prevalence. However, despite the differences among continents, the traditional view of a latitudinal gradient has been questioned, in particular in Europe and North America, where, when considering the incidence instead of prevalence, no correlation is found with latitude⁶.

2.1.2.2 Gender ratio.

MS was always considered a disease affecting predominantly females. In the last decades the gender ratio (female: male) showed an increase in both Europe and Canada, where it increased from 1.9 between 1936 and 1940 to 3.2 for patients born between 1976 and 1980⁷. Gender ratio negatively correlates with latitude but increases with incidence and time⁶. Reasons to explain the increase in gender ratio over time may be the improvements in access to healthcare and the higher prevalence of benign MS in women.

2.1.2.3 Mortality.

According to a previous study⁸, 70–88% of patients are still alive 25 years after clinical onset, and the median time from onset to death ranges from 24 years to over 45 years. The age-standardised mortality decreased from 1990 to 2016 by 11.5%, at a global level⁴. Features associated with a better prognosis include a relapsing–remitting phenotype, MS clinical onset before 25 or 30 years of age, initial symptoms such as optic neuritis and sensory problems, a low level of disability during the first years of the disease, and a long-time lag between the first and second neurological episode⁹.

2.1.3 Risk factors.

Multiple sclerosis does not have a single cause, with both genetic susceptibility and environmental exposure playing a role in the onset of the disease.

2.1.3.1 Environmental risk factors.

Multiple environmental factors have been associated with MS. Belbasis et al. examined the meta-analyses of observational studies and identified three risk factors associated with MS with no suggestion of bias: immunoglobulin G (IgG) seropositivity to Epstein Barr virus (EBV) nuclear antigen¹⁰; infectious mononucleosis; smoking. Conversely, the association between several vaccinations (tetanus, diphtheria, influenza, BCG, mumps, measles and rubella, poliomyelitis, hepatitis B virus, and typhoid fever), biochemical factors, presence of dental amalgam, past surgeries and traumatic events (tonsillectomy, adenoidectomy, and traumatic injury), and presence of allergies, eczema, and chronic cerebrospinal venous insufficiency and the onset of MS was found to be null or almost null. The authors also concluded that the evidence for low 25 – (OH) – D levels to be a risk factor for MS is weak and deserves further studies¹¹.

Environmental factors could contribute to MS development by different mechanisms such as molecular mimicry, generation of new autoantigens, release of segregated CNS autoantigens in the periphery or determining a proinflammatory environment. Two main mechanisms have been proposed to explain the causative role of EBV in determining MS: according to the first one a reactivation of the virus within the CNS

would activate B cells, while the second one implies a general dysregulation of the immune response¹².

2.1.3.2 Genetics. Genetic factors play a significant role in causing MS, as demonstrated by the higher concordance for MS in monozygotic twin pairs (25.9%), compared to dizygotic ones (2.3%)¹³. The association between MS and variations in the genes encoding human leukocyte antigens (HLAs) within the major histocompatibility complex was first observed several decades ago. The HLA-DRB1 gene, and in particular the HLA-DRB1*15:01 allele common in European population, showed to have the strongest association with MS with an average odds ratio of about 3 for this allele¹⁴. MS patients carrying the DRB1*15:01 haplotype are more likely to be female and an earlier disease onset, but it's not associated to disease severity or progression. Moreover, this haplotype is associated with presence of oligoclonal bands and IgG levels in the cerebrospinal fluid of MS patients. Instead, alleles which have a protective effect include class I HLA-A*02:01 and class II DRB1*14:01¹⁴. More than 150 single nucleotide polymorphisms been associated with MS, in genes including the ones encoding for the α -chains of interleukin-7 and interleukin-2 receptors¹². Probably, both central tolerance mechanisms and changes in the threshold of peripheral immune cell activation contribute to this genetically determined pathogenetic pathways. Recently, differences in the expression of genes involved in inflammatory and immunological pathways have been found between patients with mild relapsing-remitting MS and patients

with primary progressive MS, further underlining the gap between these two clinical phenotypes of MS¹⁵.

2.1.4 Pathogenesis

MS is considered, in the traditional way, an autoimmune inflammatory disease affecting the CNS. The hallmark of the disease are focal inflammatory lesions, mostly perivenular¹⁶, caused by the disruption of the blood-brain barrier, resulting in lymphocytes infiltrates, microglia activation, demyelination, axonal damage and alteration of the neuronal signalling. In broad terms, MS develops in genetically susceptible subjects who occur to be exposed to environmental risk factors, triggering an autoimmune response against the CNS. The *primum movens* is still uncertain and disentangling the role inflammatory cells have in triggering or sustaining the pathological process is difficult. Two different models implicate that the immune response initiates in the periphery or in the CNS itself. In the former one, autoreactive T cells are activated in peripheral blood and then move to the CNS with activated B cells and monocytes. On the contrary, in the “CNS-intrinsic” model, events (i.e., viral infection or neurodegeneration) occurring within the CNS trigger the immune response, releasing CNS antigens in the periphery which secondly attracts autoreactive lymphocytes. Within this “central” model frame, some authors claim that MS is primarily a degenerative disorder, and that inflammation is secondary to neurodegeneration¹⁷. Observations supporting this hypothesis are, among others, the lack of effect of the available disease modifying drugs (DMD) on the primary progressive clinical phenotypes of the disease and the independence of the inflammatory

relapse activity and the degeneration, as they were driven by two different processes¹⁸. According to this hypothesis, PP MS would be the primary disease and RR and SP phenotypes would represent variants with an abnormal inflammatory response. Instead, traditionally, neurodegeneration is considered as secondary to both acute and chronic inflammation phase of the disease and PP MS a clinical variant with a feeblers inflammatory component. In both cases, whether the process starts in the periphery or within the CNS, antigens released from the CNS reach the periphery and activate a further immune response and the invasion of CNS by lymphocytes. Microglia activation contributes to the initiation of tissue damage and to the protraction of the disease. Inflammation is present at all stages of MS, but it is more pronounced in acute phases than in chronic phases. Perivenular inflammatory lesions are the ones characterizing the disease, showing an infiltrate of macrophages and CD8+ T cells, and a lower number of CD4+ T cells, B cells and plasma cells. Oligodendrocyte and demyelination occur as result of inflammation. In the progressive phase of the disease, the immune response is more confined to the CNS and tissue damage consist in diffuse demyelination, axonal injury, microglia activation and cortical involvement with the formation of tertiary lymphoid structures. This results in a more pronounced atrophy of the grey and white matter. Axonal and neuronal loss are the main responsible of the permanent clinical disability, axonal damage occurring both in the acute and later stages while neuronal loss is mainly due to the deficit of myelin trophic support and mitochondrial dysfunction¹².

2.1.4.1 Pathology The focal lesions are characterized by primary demyelination and astrocytic scarring, but also by axonal and neuronal injury and they affect not only in the WM but also the grey matter, deep nuclei, brainstem and spinal cord. Remyelination to variable extent is present in focal lesions. Focal lesions can be divided in classical active lesions, chronic active or slowly expanding lesions with a low degree of demyelination and no major BBB damage and representing about 30% of lesions in patients in the progressive phase, inactive lesions and remyelinated shadow plaques. Cortical lesions have been recently recognized as a major substrate of MS pathology but, *in vivo*, only the 10-15% of cortical lesions can be identified by MR imaging. Most lesions involve the cortex and the WM (cortico-subcortical lesions) but also intracortical and subpial lesions have been identified. Subpial lesions are associated with meningeal inflammation and tertiary lymph follicles can be observed, especially in patients with SP MS and PP MS with rapid disease progression. Active cortical demyelination starts on surface with an outside-in gradient and is associated with a severe axonal and neuronal degeneration. Focal grey matter lesion and a diffuse neuronal loss interest also the deep gray matter nuclei since the initial stages of the disease and their number and size only moderately increases over time. Diffuse injury is found in the “normal appearing” white and grey matter, in particular in the progressive stage of the disease. In the WM, the injury consists of small perivascular inflammatory infiltrates, diffuse axonal injury, astrocytic scarring and microglia activation. However, the extent of the cortical demyelination is even more severe in the progressive stage, characterized by neuronal loss, thus driving additional axonal neurodegeneration in the white matter¹⁶.

2.1.5 Clinical features

Clinical onset and symptoms from relapses broadly vary, based on the spatial dissemination of lesions within the CNS and the degenerative process over time. Common clinically isolated syndrome presentations include acute unilateral optic neuritis, a partial myelitis, or a brainstem syndrome¹⁹. On the contrary, the onset of primary progressive MS by contrast is characterized by slowly progressive symptoms, most often an asymmetric paraparesis that evolves over months or years or, less commonly, a progressive hemiparesis or cerebellar ataxia or very rarely, visual failure or dementia. However, the symptomatology and the clinical course of the disease are very heterogeneous and a univocal pathogenetic and pathophysiological corresponding pattern to each of the clinical phenotypes is still lacking. Prognosis, in terms of disability accumulation, depends on age at diagnosis, gender, higher disability at baseline and brain atrophy.

2.1.6 Diagnosis

The diagnosis of MS is based on the integration of clinical, imaging and laboratory features and on the demonstration of dissemination of the disease in space (DIS) and time (DIT). The reference criteria for MS diagnosis are the McDonald criteria which are periodically revised. The current diagnostic criteria for MS are the revised McDonald criteria of 2017¹. The diagnosis of MS requires objective evidence of CNS lesions disseminated in time and space, that there is no better explanation for the clinical presentation and that alternative diagnoses are considered and excluded. Using the McDonald 2017

criteria, a diagnosis of MS can still be made on clinical grounds alone. However, MR imaging role gained increased importance in the disease diagnosis since criteria for both Multiple sclerosis DIS and DIT include the presence of new lesions in specific brain and spinal cord regions and the simultaneous presence of a gadolinium enhancing and non-enhancing lesions, respectively. Additionally, MR imaging has a complementary main contribute to the exclusion of alternative diagnoses that can mimic MS (see Section 2.1.8 Differential Diagnosis). In most patients with typical clinical and MR imaging findings, examination of cerebrospinal fluid (CSF) is not usually necessary but can provide supportive evidence of MS and its importance has been highlighted in the last 2017 McDonald criteria, where the presence of CSF oligoclonal bands can represent DIT, thus allowing the diagnosis if also DIS criteria is satisfied. CSF findings include a normal or mildly raised white cell count (< 25 cells per cm^3 ; predominantly lymphocytes) and protein (usually < 1 g/L), a raised IgG index, and IgG oligoclonal bands do not present in serum. Neurophysiological testing of evoked potentials in visual, sensory, or auditory pathways can also provide supportive evidence of MS through identification of a clinically silent lesion in the CNS, indicating dissemination in space and the urgency for studies validating the visual evoked potentials as a tool to fulfil DIS has been stressed in the last revision.

2.1.7 Treatment

In the last ten years, several drugs have been approved for patients with RR MS. Their main target is the inflammatory component of the disease, with

limited effects on the neurodegenerative component and thus on the progressive forms of MS. The disease-modifying drugs for MS (DMD) currently approved for use in the EU for the treatment of RR MS include interferon-beta (IFN- β), glatiramer acetate (GA), teriflunomide, dimethyl fumarate (DMF), fingolimod, natalizumab, alemtuzumab, cladribine, ocrelizumab and siponimod. The latter drugs have been approved also for progressive (primary and secondary respectively) MS patients, showing an effect on slowing progression. Two main strategies are used in choosing and prescribing the more appropriate drug: an escalation and an induction strategy, the first consisting in starting with a first-line treatment and then changing in case of no response, the second providing a higher effective drug as first choice to obtain a fast disease remission, mostly used in patients with a disease characterized by high activity since the beginning. Autologous haemopoietic stem cell transplantation has been used in patients not responding to DMD. Guidelines to help in the choice of the most appropriate drugs have been recently published²⁰. Rehabilitation has been used since the first phases of the disease²¹.

2.1.8 Differential Diagnosis and Misdiagnosis

The practicing neurologist frequently visits patients for whom MS is among the possible diagnosis. At times, diagnosis may be straightforward, but a rapid and accurate diagnosis of MS can also be an issue, particularly due to the lack of specific biomarkers. MS diagnostic criteria evolved substantially over time²²⁻²⁴ but are always centred on the principle of identifying episodes of CNS dysfunction separated in space and time, in the context of a specific clinical history and an abnormal neurological examination, for which other potential causes are excluded. Since the clinicopathological definition of MS performed by Charcot in the 19th century, MRI of the brain, spine and optic nerves changed diagnosis of MS and deepened our knowledge of the disease²⁵⁻²⁷. Over the past 30 years, the sensitivity of MRI allowed to identify individuals with clinically isolated syndrome (CIS) and a high risk of developing additional clinical or radiographic features fulfilling the formal diagnostic criteria for MS^{28,29}.

Furthermore, patients who perform MRI for symptoms that are seemingly unrelated to MS may be identified as exhibiting MRI features that suggest presymptomatic MS — a phenomenon called radiologically isolated syndrome (RIS)^{30,31}.

Furthermore, the introduction of disease-modifying therapies (DMTs) for MS provided increasing evidence that earlier treatment is associated with better long-term clinical outcomes^{32,33}. This evidence generates an increasing pressure for the physician to make a diagnosis of MS as early as possible. This pressure, in turn, creates a tension between the positives of an early MS diagnosis and the risk of an inaccurate diagnosis that may cause serious, sometimes life-threatening, health and financial consequences.

As a matter of fact, in 2015, the Institute of Medicine described the need to study misdiagnosis as a “moral, professional, and public health imperative.”³⁴

2.1.8.1 Incidence of misdiagnosis of MS.

The incidence of misdiagnosis of MS (that is, a diagnosis of MS given incorrectly), as in the case for many other diseases in which methodological issues may occur, may be a real challenge ^{35,36}. Previous estimates indicate that 5–10% of all patients who are initially diagnosed with MS are really misdiagnosed³⁷. These estimates derive from studies^{38,39} performed in the 1980s and earlier, which used previous versions of MS diagnostic criteria, did not specify MS phenotype, often included patients with a diagnoses of possible or probable MS, were performed before a standardization on the clinical use of MRI, were frequently represented by case reports (with a significant risk of over-representing rare or unusual clinical manifestations). Thus, these issues explain the unreliability of such studies for application to current practice.

2.1.8.2 Misdiagnosis of MS: what?

Beyond individual case reports, the most recent study about the characteristics of patients misdiagnosed with MS was published 20 years ago³⁸⁻⁴¹. More recently, a study published in 2012⁴² revealed that 95% of participating physicians recalled having assessed one or more patients over the preceding year who they felt had been misdiagnosed with MS for 1 year or longer. One-third of participants

recalled seeing six or more such patients during the year before the survey. In another study published in 2016³⁷, demographic and clinical data from four MS centres concerning 110 patients who, according to their MS specialists, received a wrong diagnosis of MS, were collected. The five most frequent alternative diagnoses included 66% of the misdiagnosed patients (**Figure 1**) and were represented by migraine alone or in combination with additional diagnoses, fibromyalgia, nonspecific or non-localizing neurologic symptoms with abnormal MRI, conversion or psychogenic disorder, and Neuromyelitis Optica Spectrum Disorder (NMOSD).

	No. (%)
Migraine alone or in combination with other diagnoses	24 (22)
Fibromyalgia	16 (15)
Nonspecific or nonlocalizing neurologic symptoms with abnormal MRI	13 (12)
Conversion or psychogenic disorder	12 (11)
Neuromyelitis optica spectrum disorder	7 (6)
Clinically isolated syndrome	3 (3)
Neurodegenerative cerebellar syndrome	2 (2)
MRI changes caused by vascular disease	2 (2)
Parkinsonism with nonspecific white matter abnormalities	2 (2)
“Radiologically isolated syndrome”	2 (2)
Cervical spondylosis with myelopathy	2 (2)
Genetic leukodystrophy	2 (2)
Idiopathic transverse myelitis	2 (2)
Noninflammatory myelopathy	2 (2)
Nonspecific symptoms with positive CSF OCBs	2 (2)
Stroke, nonembolic	2 (2)
Anti-Ma2 paraneoplastic syndrome	1 (1)
Acute disseminated encephalomyelitis	1 (1)
Astrocytoma	1 (1)
Mitochondrial disorder	1 (1)
Neurosarcoidosis	1 (1)
Moyamoya disease	1 (1)
Hypertension and alcohol abuse	1 (1)
Neuropathy	1 (1)
Unclear diagnosis; complaints of paresthesias	1 (1)
Nonspecific or nonlocalizing neurologic symptoms with normal MRI	1 (1)
Viral meningoencephalitis with subsequent abnormal MRI and acute labyrinthitis	1 (1)
White matter lesions due to TNF- α inhibitor use for psoriasis	1 (1)
Behçet syndrome	1 (1)
CADASIL	1 (1)
Degenerative joint disease of lumbar spine	1 (1)

FIGURE 1 THE CONTEMPORARY SPECTRUM OF MULTIPLE SCLEROSIS MISDIAGNOSIS
from Solomon et al., “The contemporary spectrum of multiple sclerosis misdiagnosis
A multicenter study”, *Neurology* 2016

Migraine (alone or in combination with additional diagnoses) was the most common alternative diagnosis in patients misdiagnosed with MS and was reported in 22% of patients. Additional diagnoses in combination with migraine included psychiatric disease, fibromyalgia, small vessel disease, acute labyrinthitis, spells of uncertain aetiology, rheumatoid arthritis, vitamin B12 deficiency, and small fibre neuropathy. Imaging abnormalities related to tobacco use, vitamin B12 deficiency, and small vessel ischemic disease in patients with migraine were also described. Interestingly, it was reported that often migraineurs symptoms mistaken for demyelinating attacks were incorrectly used to satisfy DIT criteria for MS. On the other side, migraine-associated WM hyperintensity were often considered in the fulfilment of DIS imaging criteria for MS.

2.1.8.3 Misdiagnosis of MS: why?

Clinical and radiographic heterogeneity^{2,43} of misdiagnosis of MS and the significant number of pathological entities that can mimic its features^{44,45} makes them particularly challenging to diagnose.

Except for anti-aquaporin-4 antibody-positive NMOSD, the conditions that seem to be most frequently confused with MS lack specific biomarkers, and their recognition is based on clinical suspicion and an appropriate knowledge of MS diagnostic criteria to facilitate correct interpretation of clinical and radiographic features.

Misdiagnosis of MS is often caused by a misinterpretation of MRI abnormalities in the context of nonspecific symptoms and/or signs, that are atypical for MS³⁷. MRI has high sensitivity for lesions suggestive

of MS, but in many other MS mimics, such as migraine or small vessel disease, morphological features lack of specificity and thus may be confused with those typically associated with MS⁴⁵⁻⁴⁷. Similarly, the presence of intrathecal synthesis of immunoglobulins, used as a diagnostic criteria in MS for over 50 years, has high sensitivity, but its specificity for MS is not unmistakable⁴⁸⁻⁵⁰.

Nevertheless, it should be highlighted that MRI criteria for MS were not developed to differentiate MS from other disease in absence of clinical syndromes that are typical for a demyelinating event, such as optic neuritis, brainstem syndromes, and transverse myelitis^{46,47,51,52}. Therefore, confidence on the MS diagnostic criteria alone when evaluating patients with clinically atypical features decreases specificity for MS and may unequivocally lead to misdiagnosis. A clinical history suggestive of demyelination is crucial for a reliable diagnosis of MS, but the role of confirmatory objective signs at the neurological exam⁵³ is essential to correctly apply MS diagnostic criteria. Unfortunately, this need is often neglected or misinterpreted⁵⁴, particularly when historical episodes of symptoms suggestive of a demyelinating event are considered⁵⁵.

Furthermore, the wrong attribution of MRI lesion location may represent another cause leading to misdiagnosis⁵⁵.

As a matter of fact, both misinterpretation and misapplication of current MS diagnostic criteria has been defined as a contemporary problem⁵⁵⁻

⁵⁷ (Figure 2)

	Yes	No	Unknown
	n (%)	n (%)	n (%)
Inappropriate application to MS diagnostic criteria of neurologic symptoms atypical for a demyelinating attack	72 (65)	24 (22)	14 (13)
Inappropriate application to diagnostic criteria of a historical episode of neurologic dysfunction without corroborating objective evidence of a lesion (on neurologic examination, evoked potentials, or imaging)	53 (48)	38 (35)	19 (17)
Overreliance on the presence of MRI abnormalities meeting DIS to confirm a diagnosis of MS in a patient with "nonspecific neurologic symptoms"	66 (60)	28 (25)	16 (15)
Erroneous determination of juxtacortical or periventricular lesion location to fulfill DIS	36 (33)	43 (39)	31 (28)
Erroneous determination of DIT because of variability of MRI slice orientation (i.e., MRIs performed on different scanners leading to the appearance of new lesions)	13 (12)	64 (58)	33 (30)

FIGURE 2 MAIN CAUSES OF MS MISDIAGNOSIS

from Solomon et al., "The contemporary spectrum of multiple sclerosis misdiagnosis: A multicenter study", Neurology 2016

2.1.8.4 Misdiagnosis: which consequences?

a) Delay in reaching the correct diagnosis. **Figure 3** shows the approximate duration of misdiagnosis in all the patients involved in the abovementioned study

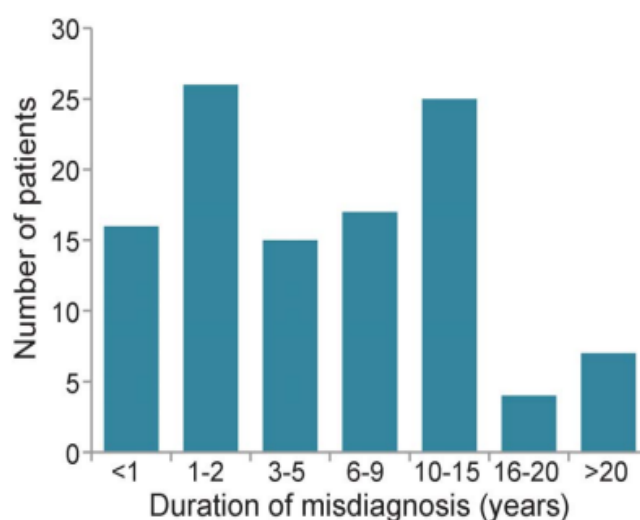


FIGURE 3 DURATION OF MS MISDIAGNOSIS

from Solomon et al., "The contemporary spectrum of multiple sclerosis misdiagnosis: A multicenter study", Neurology 2016

b) Exposure to immunomodulatory therapy. Seventy-seven patients (70%) received one or more immunomodulatory DMTs for MS.

Figure 4 shows the approximate cumulative time of exposure to immunomodulatory and/or immunosuppressive treatment for MS and the different types of DMTs performed in misdiagnosed patients⁵⁵.

Furthermore, among the consequences of misdiagnosis of MS, we must cite also significant and inappropriate costs⁵⁸, psychological impact on misdiagnosed patients, potential implications in the results emerging from clinical trials, and the risk of developing adverse and potentially life-threatening adverse events due to the biological effect of DMTs, particularly in case of second-line treatments ^{59,60}.

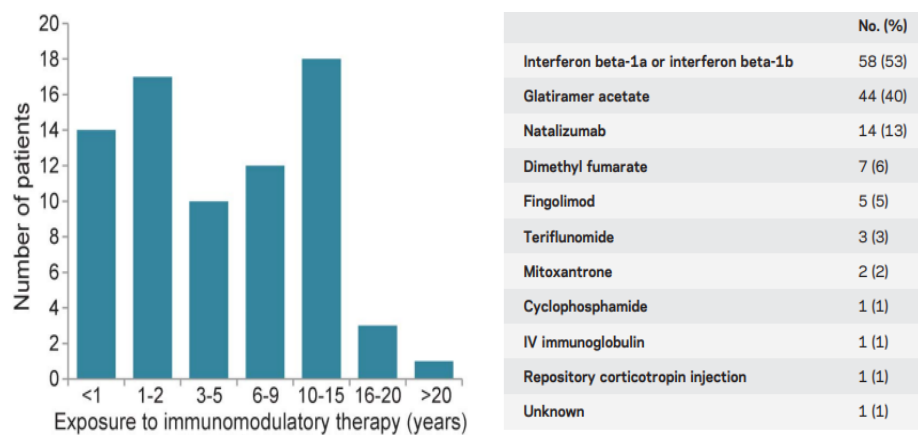


FIGURE 4 CONSEQUENCES OF MISDIAGNOSIS
 from Solomon et al., “The contemporary spectrum of multiple sclerosis misdiagnosis: A multicenter study”, Neurology 2016

2.1.8.5 Misdiagnosis: how to solve?

The identification of specific and sensitive biomarkers able to distinguish MS from other diseases represent an unmet need. Several cerebrospinal fluid and serum biomarkers of MS have been studied⁶¹⁻⁶⁴, but no tests with high specificity and sensitivity are now available. Another issue is represented by the fact that many proposed biomarkers have only been explored in the context of cross-sectional studies, while their longitudinal evaluation is essential.

As concerns MRI biomarkers, the central vein inside WM lesions has been proposed as a biomarker of inflammatory demyelination and, thus, may help in the diagnosis of MS⁶⁵.

In the following Sections, the use of the Central Vein Sign (CVS) and of microstructural metrics in the differential diagnosis between MS and its mimics and in the characterization of MS lesions, obtained by advanced susceptibility weighted and diffusion weighted images respectively, will be discussed.

2.2 Susceptibility Weighted Imaging: The “Central Vein Sign”

2.2.1 Central Veins in MS plaques: From Pathology to Imaging

Central vessels (predominantly veins and venules) in MS lesions have been described in pathological studies since the 1820s⁶⁶. The perivascular space surrounding these veins seemed to be a privileged site for immune cells interaction with antigen-presenting cells, thus leading to an inflammatory cascade and lesions development around the veins^{67,68}.

The development of susceptibility-based magnetic resonance venography in the late 1990s⁶⁹ allowed to observe these central veins in MS plaques in vivo, as showed by Tan et al.⁷⁰.

This first in-vivo demonstration of the perivenous location of MS lesions was further confirmed in 2008 through ultra-high-field MRI^{71,72}. Follow-up imaging studies confirmed this finding in RRMS, SPMS and PPMS^{73,74}. In an imaging study, Kilsdonk et al. found that 78% of the lesions were located around a central vessel⁷⁴. Furthermore, MS clinical phenotype seemed to be not related to the proportion of lesions with a central vein⁷³. However, when lesions were classified according to their location, central veins appeared to be most prevalent in periventricular lesions (94%). This finding was confirmed in different studies^{70,71}, and could be explained by the high density of venous structures in periventricular regions. The proportion of CVS positive lesions decreased with proximity to the neocortex (deep WM lesions: 84%; juxtacortical lesions: 66%; mixed GM and WM lesions: 52%; and intracortical lesions: 25%). Although most studies investigated the supratentorial brain only, central veins within MS lesions have also been detected in the thalamus, cerebellum and pons^{74,75}. Conversely, no in vivo reports are available on central

veins in MS lesions located in the spinal cord, although pathological evidence of this phenomenon have been reported⁷⁶.

Interestingly, Kilsdonk et al.⁷⁴ described a significantly lower percentage of perivenular deep WM lesions (73%) in MS patients aged ≥ 40 years compared with younger patients (92%). One possible explanation for this discrepancy is the presence of age-related WM lesions without central veins. These findings supported the contribution of comorbidities to the brain lesion load in patients with MS^{77,78}.

2.2.2 Detecting the Central Vein in MRI: Technical Aspects

The T2*-based contrast mechanism represent the best approach to investigate the small cerebral veins. This technique is based on the magnetic properties of blood⁶⁹. The paramagnetic deoxyhaemoglobin inside venous blood perturbs the local magnetic field and generates reduced signal intensity in voxels containing a vein, causing veins to appear hypointense on T2*-weighted images^{69,79}.

Since the first in vivo observation of central veins in the brains of patients with MS⁷⁰, a variety of T2*-based acquisitions have been used and improved at different magnetic field strengths to detect veins within MS plaques^{71,75,80–83}. Several studies used a conventional 2D gradient-echo (GRE) sequence, which allows submillimetre in-plane resolution, especially at 7T^{72,73,83–85}. However, 2D GRE acquisitions are very time-consuming (>10 min), characterized by an only partial covering of the supratentorial brain, and provide poor image resolution in the inferior–superior plane owing to thick slices and/or slice gaps.

Some studies utilized a 3D T2*-weighted GRE sequence to overcome this issue and applied parallel imaging to shorten scan time, maintaining high image resolution (typically $0.5 \times 0.5 \times 1–3\text{mm}$)^{82,86,87}. These T2*-weighted images can be post-

processed by the susceptibility-weighted imaging (SWI) technique to further increase venous conspicuity⁸⁸. The 3D GRE sequence can also be set up to have a multi-echo read-out⁸⁹. The multi-echo acquisition can then provide quantitative (and/or multi-contrast) imaging through the use of advanced post-processing techniques^{90,91}.

Another variant of the 3D GRE sequence is based on a segmented echo planar imaging (3D EPI) read-out to accelerate the acquisition. It is capable to provide more-efficient brain coverage and isotropic voxel size⁹². Isotropic resolution is particularly useful to reformat images in the three orthogonal planes and allows a better visualization of the veins regardless of their orientation. Moreover, the use of small isotropic voxel dimensions increases the sensitivity to small parenchymal veins within lesions⁹³ and at the same time it can reduce the sensitivity to artefacts due to background field inhomogeneities. Among the positives, a shorter scan is also beneficial for limiting the head motion that can occur during the acquisition.

Recently, the 3D EPI sequence was demonstrated to image perivenous MS lesions throughout the brain at submillimetre resolution (0.55 mm isotropic) particularly when optimized T2* protocols are used. Another way to increase vein detection on T2*-weighted images is to inject an intravascular contrast agent (a chelate of gadolinium, which is paramagnetic) during the MRI acquisition^{70,80,94}. This solution is straightforward to implement, as MRI protocols for MS often involve the injection of contrast agent.

Unlike T2-weighted fluid-attenuated inversion recovery (FLAIR) images, T2*-weighted and SWI images lack CSF suppression and are, therefore, less able to highlight the contrast between lesions and normal appearing white matter (NAWM) - both of which are extremely helpful for detection of MS lesions by clinicians - making the detection of lesions more difficult. To overcome these

issues, the combination of FLAIR and T2* images in a single image have been performed^{75,86}. In particular, Grabner et al.⁸⁶ introduced a method that transforms FLAIR images using SWI phase masks from T2*- weighted images, creating a FLAIR–SWI contrast. The other approach, proposed by Sati et al.⁷⁵ and known as FLAIR*, uses 1 mm isotropic 3D FLAIR (for lesion detection) and 0.55 mm isotropic 3D EPI (for vein detection) sequences — both acquired in <10 min and provides high-resolution isotropic images of the whole brain. High-quality FLAIR* images of the brain were thus produced at 3.0 T MRI, yielding conspicuous lesions and veins. Lesion-to NAWM and NAWM-to-vein Contrast to Noise Ratio (CNR) values were significantly higher for FLAIR* images than for T2-weighted FLAIR images, allowing an easier detection of intralesional veins for lesions located throughout the brain.

2.2.3 Detecting the Central Vein in MRI: Clinical Application, Definition and Challenges

Over the past few years, several researchers used MRI to evaluate the detect the central veins inside WM lesions in patients suffering from various neurological diseases, including NMOSD, systemic autoimmune diseases (SAD), cerebral small vessel disease (CSVD), Susac syndrome and migraine (Figure 5).

2.2.3.1 Neuromyelitis Optica spectrum disorder (NMOSD)

NMOSD is an autoimmune disease of the CNS predominantly affecting optic nerves and spinal cord. NMOSD and MS share common radiological and

clinical features and the early differential diagnosis between them may be a challenge. Sinnecker et al.⁸⁴ demonstrated that in AQP4-IgG+ NMOSD patients, only 35% of WM lesions were near — and rarely centred on — blood vessels. In a different AQP4-IgG+ NMOSD cohort, Kister et al.⁸⁵ showed that only 9% of WM lesions were traversed by a central vessel, further suggesting that the CVS may be considered a useful tool to distinguish NMOSD from MS. To date, data about AQP4-IgG-seronegative negative patients with NMOSD are lacking.

2.2.3.2 Systemic autoimmune diseases (SAD)

WM lesions are commonly detected in SAD, especially in patients exhibiting clinical manifestations. A pilot study⁹⁵ recruiting patients with MS and SAD, including Behçet syndrome, systemic lupus erythematosus and antiphospholipid syndrome, showed that patients included in SAD group seemed to have a significantly lower proportion of CVS+ lesions with respect to the MS group. Interestingly, patients with a diagnosis of Behçet syndrome showed the highest percentage of perivenular lesions.

2.2.3.3 Cerebral small vessel disease (CSVD)

CSVD includes pathological changes in small brain vessels (small arteries, arterioles, capillaries and small veins) due to different aetiologies. CSVD is commonly described in ageing and patients with significant vascular risk factors. CSVD usually determines the development of brain WM lesions able to mimic MS. Although an early study by Lummel et al.⁹⁶ reported no differences between patients with MS and CSVD in terms of the proportion

of WM lesions with a central vein, more recent studies described a significantly lower proportion (45% at most) of venocentric WM lesions in CSVD^{97–101}.

2.2.3.4 Susac syndrome

Susac syndrome is an autoimmune vasculopathy characterized by occlusion of small vessels in the brain, retina and inner ear. A previous study described the presence of a vessel within the 54% of WM lesions¹⁰². Interestingly, the identified blood vessels were most located at the lesion periphery.

2.2.3.5 Migraine

Radiological features in migraine can be mistaken for MS. A recent study found that the proportion of CVS+ lesions was significantly lower in migraine than in MS¹⁰³.

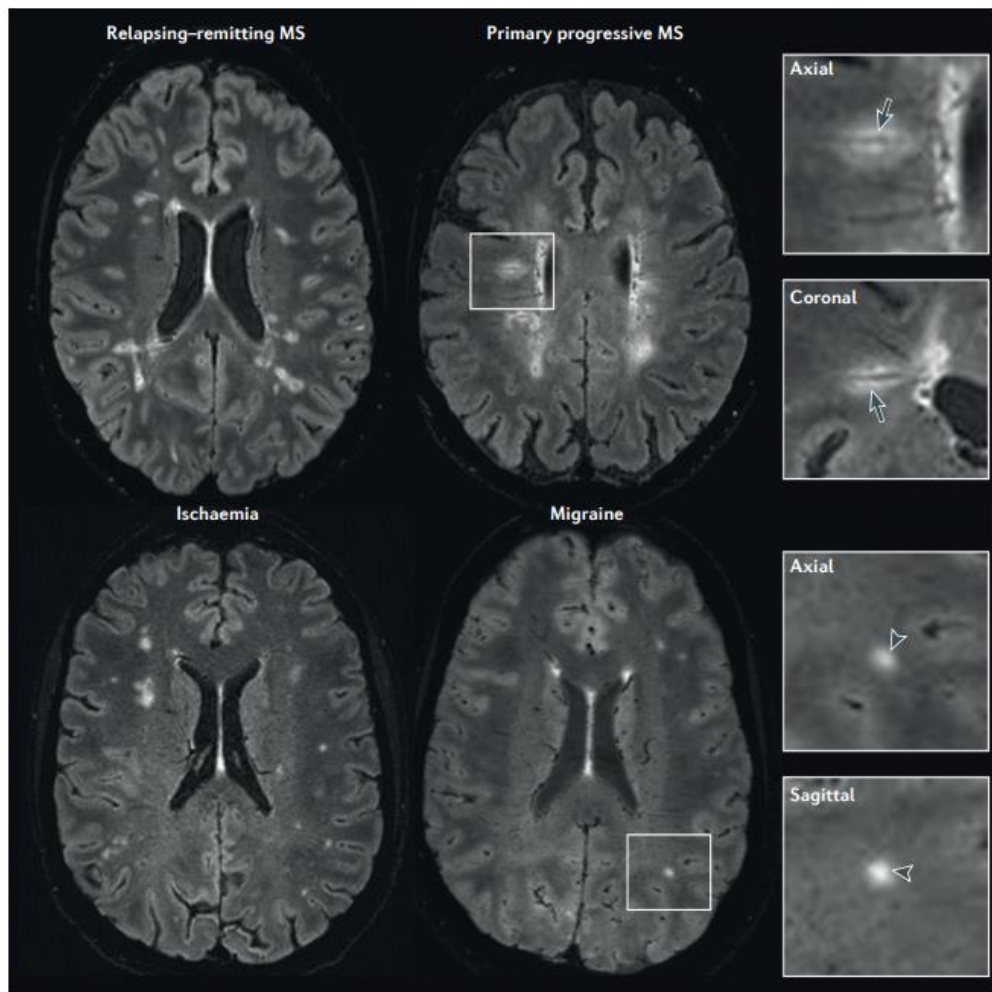


FIGURE 5 PERIVENOUS DISTRIBUTION OF MULTIPLE SCLEROSIS LESIONS

In the patients with relapsing–remitting or primary progressive multiple sclerosis (MS), a central vessel is visible in most hyperintense lesions. The dark veins are located centrally in the lesion and can be visualized in at least two perpendicular planes (arrows in magnified boxes). On the other hand, a central vein is absent from most of the lesions (arrowheads in magnified boxes) in the patient with and the patient with ischaemic small vessel disease. (data from Sati et al., “The central vein sign and its clinical evaluation for the diagnosis of multiple sclerosis: a consensus statement from the North American Imaging in Multiple Sclerosis Cooperative”, Nature Reviews Neurology 2016)

Interestingly, existing studies demonstrated good agreement when defining the radiological characteristics of a central vein^{70,71,73,74,81,82,85,95,97,101}:

- [1] the vein should appear as a thin line or dot
- [2] when technically possible, the vein should be visualized in at least two perpendicular planes
- [3] the vein can run partially or entirely through the lesion but must be located centrally regardless of the lesion's shape.

On the basis of a review of the existing literature on the CVS and the consensus opinion of the members of the North American Imaging in Multiple Sclerosis (NAIMS) Cooperative, statements and recommendations aimed at helping radiologists and neurologists to better understand, refine, standardize and evaluate the CVS in the diagnosis of MS have been published⁶⁵.

Radiological definition of a central vein⁶⁵

A central vein exhibits the following properties on T2*-weighted images:

- Appears as a thin hypointense line or small hypointense dot
- Can be visualized in at least two perpendicular MRI planes, and appears as a thin line in at least one plane
- Has a small apparent diameter (<2mm)
- Runs partially or entirely through the lesion
- Is positioned centrally in the lesion (that is, located approximately equidistant from the lesion's edges and passing through the edge at no more than two places), regardless of the lesion's shape

Exclusion criteria for lesions:

- Lesion is < 3 mm r in any plane
- Lesion merges with another lesion (confluent lesions)
- Lesion has multiple distinct veins
- Lesion is poorly visible (owing to motion or other MRI-related artefacts)

Examples of WM lesions eligible and not eligible for the CVS assessment are shown in

Figure 6

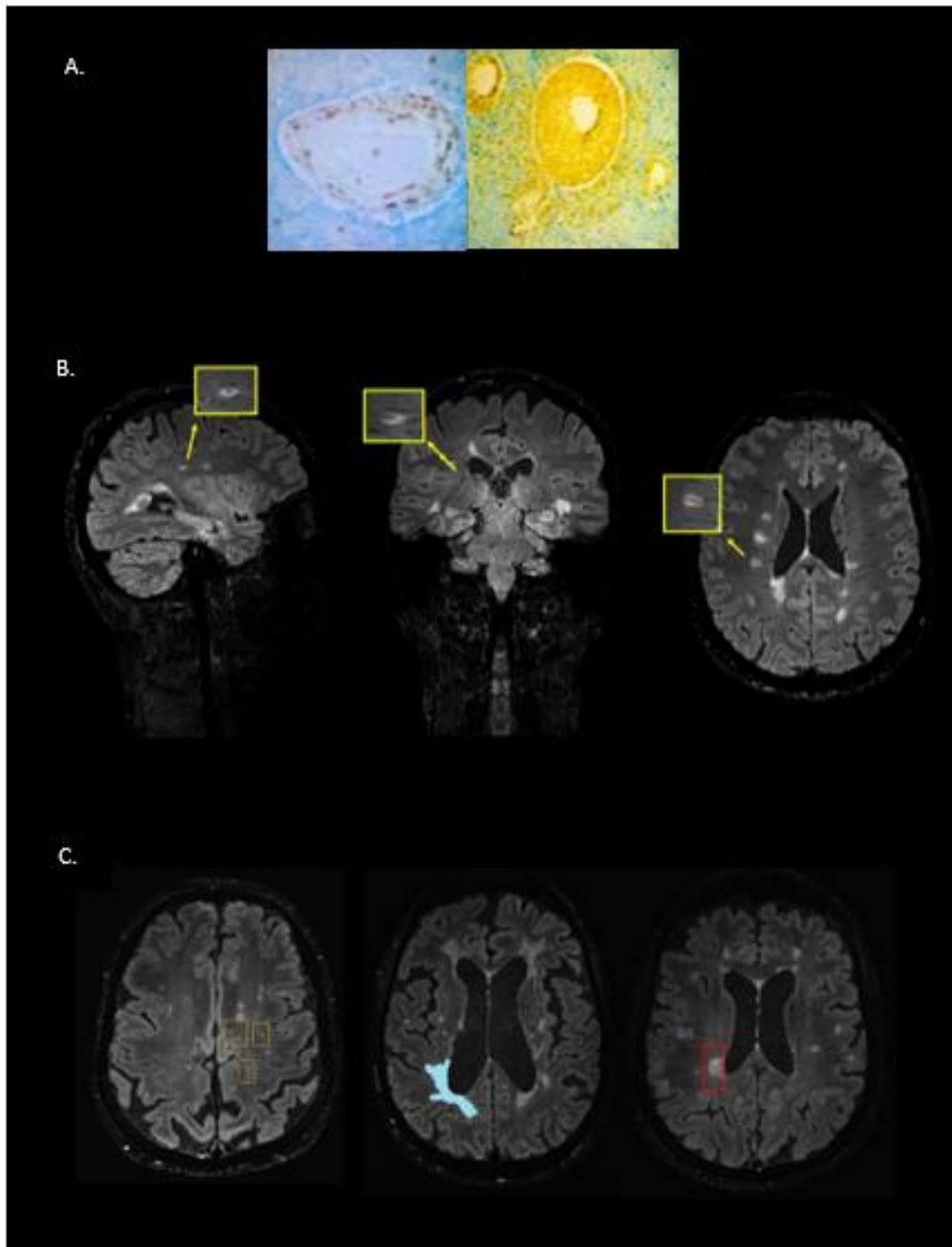


FIGURE 6 INCLUSION AND EXCLUSION CRITERIA FOR CENTRAL VEIN SIGN ASSESSMENT
 A. Hystopathological examination from a patient of our Center in Genoa (Courtesy of Dott. E. Capello) revealing inflammatory cells infiltrates around a central venule within WM lesions. B. Example of WM lesion with CVS: central venule appears as a thin hypointense line in the coronal and axial planes and as a small hypointense dot in the sagittal plane. C. WM lesions excluded from CVS assessment: from left to right, lesions < 3mm, confluent lesions, lesion with multiple distinct vein (data from University of Genoa cohort)

Several efforts have been made to define how to use the CVS to differentiate MS from its mimics may be useful in the everyday clinical practice. One proposed definition is the '40% rule', firstly proposed by Evangelou and colleagues⁹⁷, which evaluates the proportion of CVS+ lesions with respect to the total of lesions and considers a cut-off value of 40% to radiologically differentiate MS from its mimics. This simple threshold approach confirmed its potential (100% positive and negative predictive value for MS) in a prospective study including patients with a diagnosis of possible MS, clinically isolated syndrome (CIS) and insufficient MRI findings, or an atypical CIS presentation with MRI findings suggestive of MS⁸¹.

In a recent study, including MS, non-MS patients and healthy subjects, showed how the diagnostic certainty could be increased by combining the current MRI criteria with the above-mentioned 40% rule¹⁰⁴.

However, this rule is not without limitations, considering that the count of the number of lesions is very time-consuming particularly in patients with high lesion load and, as highlighted above, >40% of brain lesions may be CVS-positive also in patients suffering from diseases different from MS. Another method, first investigated by Kilsdonk et al., associate the number and location of lesions with the proportion of CVS+ lesions¹⁰¹. The reliability of the CVS to differentiate MS and non-MS WM lesions was confirmed in another study, in which very good results were reported (sensitivity 84%, specificity 89%, diagnostic accuracy of 86%)⁸². However, this approach is still based on the counting of the total number of lesions.

In the attempt to overcome this issue, that assessment of ten lesions per patient has been proposed. By using of this approach, a diagnosis of MS could be predicted with an accuracy of 90% accuracy⁹⁷.

More recently, a simpler and time-saving approach for CVS was introduced (“pick 6” rule), consisting of the following three criteria⁹⁹:

- if there are six or more morphologically characteristic lesions, the diagnosis is inflammatory demyelination
- if there are fewer than six morphologically characteristic lesions, but morphologically characteristic lesions outnumber non-perivenous lesions, the diagnosis is inflammatory demyelination
- if neither of these conditions are met, inflammatory demyelination should not be diagnosed.

Solomon et al ¹⁰⁵ suggested a 3–central vein sign lesion threshold as rapid method to distinguish MS from other diseases. According to this rule, a patient may be diagnosed with MS if FLAIR* images show at least 3 lesions restricted to subcortical, deep WM and juxtacortical areas exhibiting the CVS.

Nevertheless, a lower specificity for the differentiation between MS and non-MS for the 3 central vein sign lesions or 6 central vein sign lesions criteria compared with a proportion-based threshold have been detected¹⁰⁶. In this study ¹⁰⁶, a higher median number of analysed lesions per patient was reported. These finding suggested that a proportion-based threshold may be more suitable in patients with higher lesion burden.

2.3 Advanced Diffusion MRI in Multiple Sclerosis

Conventional MRI (including T2-weighted, pre- and post-contrast T1-weighted scans) had an essential impact on MS by enabling earlier diagnosis, and by providing surrogate markers for monitoring response to current disease-modifying treatments and upcoming experimental agents.

Despite its increasing role in the clinical management and scientific investigation of MS, conventional MRI is limited by low pathological specificity and low sensitivity to diffuse damage in Normal Appearing White Matter (NAWM) and Normal Appearing Grey Matter (NAGM). In addition, conventional MRI shows only limited associations with clinical status.

Diffusion MRI (dMRI) is a powerful quantitative technique that probes information on the movement of water molecules within brain tissues¹⁰⁷ and can thus provide markers of different types of microstructural alterations. Since its introduction and with the establishment of multishell sequences, many microstructural models and signal representations have been proposed¹⁰⁸ and applied to study how different neurological diseases affect the integrity of brain tissues.

2.3.1 Diffusion Tensor Imaging (DTI)

Lesions and NAWM microstructure MS were among the first neurological diseases to be investigated with dMRI. Indeed, ever since the introduction of diffusion tensor imaging (DTI), the scalar indices derived from the tensor, such as the axial, radial, and mean diffusivity (AD, RD, and MD, respectively), which quantify the magnitude of principal, radial, and average diffusion within a voxel, and the fractional anisotropy (FA), which measures the directionality of diffusion,

have been applied to study MS alone or compare its microstructural alterations with those caused by other neurological pathologies ¹⁰⁹⁻¹¹² .

DTI has proven to be a valuable tool for investigating the variety of pathological features of T2-visible lesions. Increased MD and RD, and decreased FA are always more pronounced in lesions than in NAWM; however, their values are highly heterogeneous, indicating the variable degrees of tissue damage occurring within MS lesions ¹⁰⁹. Examples of DTI indices obtained with the 3T MAGNETOM Prisma scanner (Siemens Healthcare, Erlangen, Germany) sited in IRCCS Ospedale Policlinico San Martino, in a patient with MS are shown in **FIGURE 7**. These results are consistent with increased water content, loss of myelin and axons, and the presence of gliosis. More interestingly, abnormal DTI parameter values are typically found in the NAWM of patients relative to age-matched healthy controls, consistent with subtle but widespread damage known to occur in MS.

These initial findings have contributed to the knowledge that white matter damage is widespread in MS, even in the early phases, although they did not provide a clear definition of the substrate underpinning these abnormalities ¹⁰⁹⁻¹¹³. Although DTI has been proven to have good sensitivity to disease changes over time, it has low pathological specificity, which does not allow to discriminate between the different pathological processes underlying MS pathogenesis ¹¹⁴. To overcome these issues, multishell dMRI sequences and many multicompartement microstructural models and signal representations have been proposed ¹⁰⁸.

Among them, the Neurite Orientation Dispersion and Density Imaging (NODDI) ¹¹⁵ model and the multicompartement Spherical Mean Technique (SMT) ¹¹⁶ model have also been proven to be sensitive to MS ¹¹⁷.

2.3.2 Neurite Orientation Dispersion and Density Imaging

(NODDI)

NODDI distinguishes between three microstructural environments: intracellular (or intra-axonal), extracellular (or extra axonal), and cerebrospinal fluid compartments. All these compartments have fixed diffusivities (with a relationship between the external axial and radial diffusivities), and geometrical assumptions that affect diffusion in a unique way, resulting in three separate dMRI signals ¹¹⁷.

The intradendrites and intra-axonal spaces represent the intracellular component. Due to the highly restricted nature of diffusion in this space, the intracellular component is modelled as a set of geometric “sticks,” or infinitely thin cylinders, with diffusion completely restricted perpendicular to these sticks but unhindered along them. The extracellular component includes the space around the neurites or axons, characterized by glial cells and neuronal cell bodies. In contrast to the restricted intracellular space, the diffusion in this space is “hindered” by neurites and is modelled as a simple anisotropic Gaussian distribution (as in DTI). Also the CSF compartment is modelled as isotropic Gaussian diffusion with a fixed isotropic diffusivity. Thus, NODDI model is able to provide metrics useful to describe orientation, shape, diffusivities, and fractions of the different compartments. These metrics are: 1) the intracellular volume fraction (ICVF), represented by the neurite density index, whose value ranges from 0 to 1, denoting complete loss or full preservation of axons, respectively; 2) the neurite orientation dispersion index (ODI), whose value ranges from 0, representing perfectly coherently oriented WM structures, to 1, representing isotropically dispersed

neurites; and 3) the isotropic volume fraction isoVF), indicating the voxel volume fraction of free water (i.e., CSF) ¹¹⁷.

Several cross-sectional studies demonstrated the clinical feasibility of NODDI to differentiate brain abnormalities in MS and their impacts on patients' clinical status. Previous studies demonstrated that ICVF was lower in lesions compared with NAWM ¹¹⁸⁻¹²⁰, in NAWM compared with the normal WM of healthy subjects (both in brains ¹¹⁹⁻¹²¹ and spinal cord ^{121,122}), and in the spinal cord normal-appearing GM compared with the GM of healthy subjects ¹²². These results were consistent across patients with RRMS ¹¹⁸⁻¹²² or SPMS ^{119,121}. Conversely, ODI values yielded more contradictory findings because ODI measurements were higher in lesions than NAWM in some studies performed on patients with RRMS ^{120,122,123} and lower in others focused on relapsing-remitting or mixed MS populations ^{118,124}. Similarly, while a study¹¹⁸ showed lower levels of ODI in the brain NAWM of RRMS patients, another investigation by By et al ¹²² reported opposite findings in the spinal cord of a similar population of patients. Interestingly, only cortical ODI values were predictor of clinical decline in patients with both RR ^{120,123} and SPMS ¹²³. Thus, it may suggest that ODI is more informative if used to assess longitudinal changes of individual patients rather than to assess comparisons between patients. On the contrary, ICVF seems to capture some degree of change in axonal content, which is also measurable in perilesional tissue ¹¹⁹.

2.3.3 Spherical Mean Technique (SMT)

Similarly to NODDI, the multicompartment SMT estimates microscopic features specific to the intra- and extra-neurite compartments in the WM. The use of the spherical mean average in the fitting allows minimization of the confounding effects derived from axonal fibre crossings, curving, and orientation dispersion. This is particularly important in MS because many WM voxels contain complex fibre configurations, and fibre arrangements widely vary within MS lesions ¹¹⁷. Thus, these fibre orientation-independent diffusion metrics may provide more accurate estimates of axon integrity. Moreover, compared to NODDI, although it can only indirectly capture the potential presence of free water, it does not fix any values for the intra- and extra-neurite axial diffusivities, allowing to estimate them from the measured signal.

SMT is suitable for clinical applications that require information on axonal volume fraction as well as axonal directions if one obtains spherical deconvolution. Thanks to its basic assumptions, SMT can separate intra- and extra-axonal signals and 2 independent microstructural parameters, i.e., the Intra-axonal Volume fraction (V_{ax}) and the apparent intra-axonal diffusivity (D_{ax}) can be fit from the data. Other microstructure parameters, such as extra-axonal RD, can be calculated from V_{ax} and D_{ax} ¹¹⁷.

The feasibility and applicability of SMT has been recently evaluated in MS, focusing on the brain¹²⁵ and spinal cord¹²⁶ and demonstrating to be helpful in differentiating MS lesions damage from the Normal Appearing WM (NAWM) as well as the NAWM of MS patients from that of healthy controls¹¹⁷ and in characterizing pathological features within MS lesions ¹²⁷.

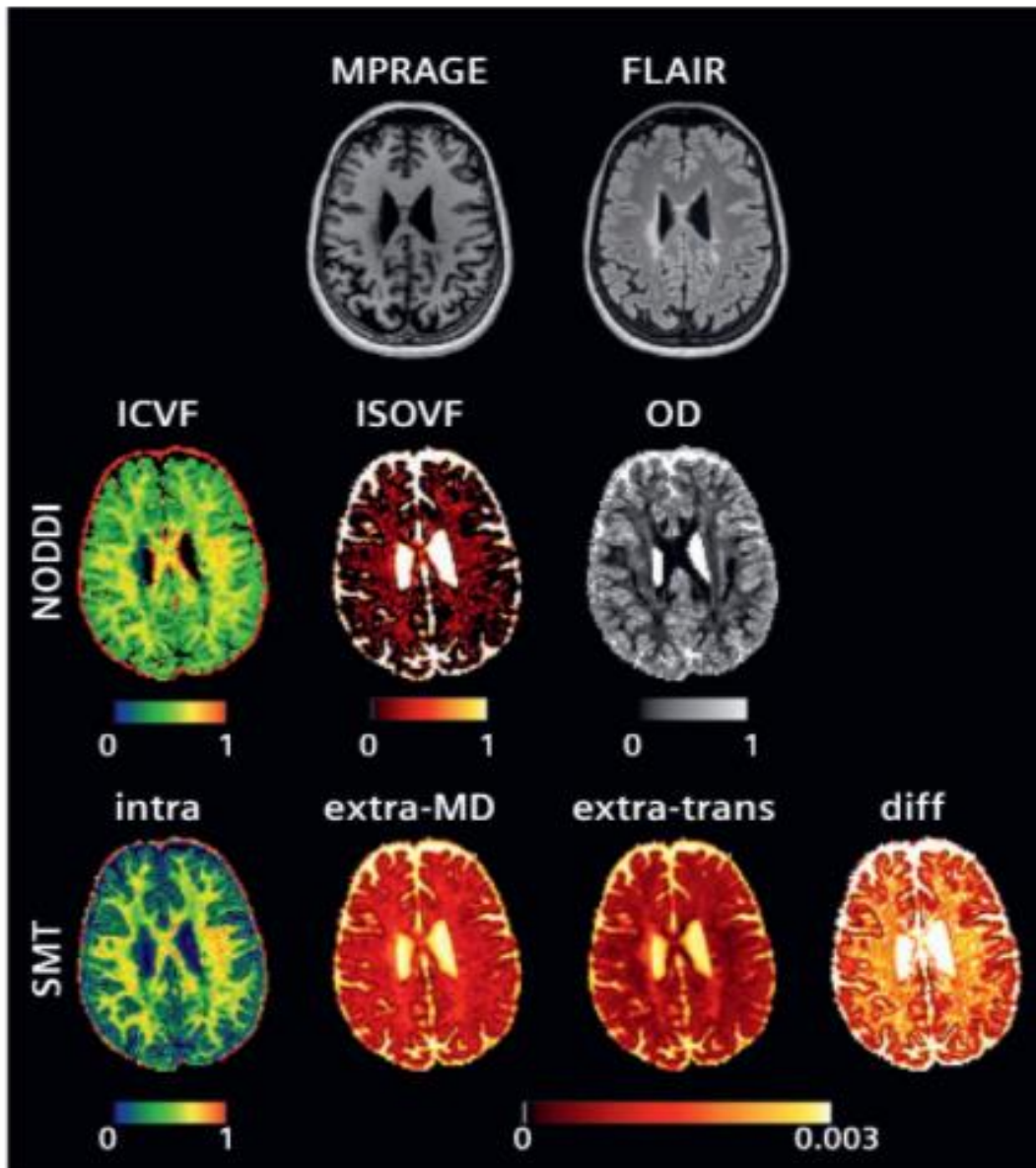


FIGURE 7 MICROSTRUCTURAL MAPS DERIVED FROM NODDI AND SMT MODELS

The top row shows axial views of FLAIR and MPRAGE sequences in which T2 and T1 lesions are visible. The middle row shows axial views of intra-axonal and isotropic signal fractions (ICVF and ISOVF) and the orientation dispersion index (OD) derived from NODDI. The bottom row shows axial views of intra-axonal signal fraction (intra), extra-mean and transversal diffusivities (extra-MD and extra-trans) and axial diffusivity (diff) derived from SMT. Diffusivities are reported in mm²/s. ICVF: Intracellular volume fraction, ISOVF: Isotropic volume fraction (data from University of Genoa)

Chapter 3

3. The Central Vein Sign to differentiate multiple sclerosis from migraine

3.1 Introduction

Multiple sclerosis (MS) is an inflammatory disease of the central nervous system (CNS) characterized by a relapsing or progressing clinical course. The diagnosis of MS relies on the interpretation of clinical and radiographic data, in particular the evaluation of white matter (WM) hyperintensities on T2-weighted magnetic resonance imaging (MRI) of the brain and spinal cord and demonstration of disease dissemination in space (DIS) and in time (DIT) through clinical, laboratory, and MRI criteria. Furthermore, the exclusion of other diseases (the so-called “no better explanation” concept) that can mimic multiple sclerosis (MS) is the cornerstone of current diagnostic criteria¹.

Indeed, misdiagnosis of MS is a persistent issue that results in risk of diagnosing MS in individuals affected by other disorders, such as migraine, cerebral small vessels disease (SVD), neuromyelitis optica spectrum disorder (NMOSD), Susac syndrome, and primary or secondary vasculitis of the CNS. Among them, migraine is the most common mimic of MS⁵⁵. Neuroimaging studies have demonstrated an increased incidence of brain T2 white matter (WM) hyperintensities in patients with migraine, both with and without aura^{128,129}. In order to improve the radiological differential diagnosis of MS and its mimics, several studies investigated the perivenous morphology of MS lesions and the presence of a vein at the centre of WM lesions, the so-called “central vein sign” (CVS), detected on 3T MRI using

FLAIR* sequence⁶⁵. In particular, the North American Imaging in Multiple Sclerosis (NAIMS) Cooperative published consensus recommendations for evaluations of CVS, in order to establish a standard radiological definition of CVS to improve diagnosis of MS⁶⁵. Recent studies investigated CVS with the purpose of differentiating MS from CNS inflammatory vasculopathies¹⁰⁶, seropositive Neuromyelitis Optica Spectrum Disorder (NMOSD)¹³⁰ and microangiopathic brain lesions¹³¹. In these studies, a “threshold-based approach”^{132,133} was used to calculate the percentage of CVS+ lesions able to provide the best differentiation between MS and these other pathological entities. Nevertheless, at the best of our knowledge, no specific threshold capable to distinguish MS from migraine have been yet identified. Thus, the aim of our study is to investigate, in two cohorts including patients with MS and patients with migraine (with and without aura, from now on simply “migraine”): (i) the prevalence of the CVS, (ii) the spatial distribution of CVS+ lesions, (iii) the best threshold able to differentiate MS from migraine.

3.2 Material and Methods

3.2.1 Subjects

Sixty patients with a diagnosis of MS¹ [45 with relapsing-remitting course, 15 with progressive (Primary Progressive, PP and Secondary Progressive, SP, from now on “PMS”) disease course², 49 females (81.7%), mean age 45.3±13.8 years, range 19-77 years, mean disease duration 11.5± 9.8 years] and 50 age and gender-matched patients with migraine diagnosed applying the International Classification of Headache Disorders criteria, 3rd edition. [9 with aura and 41 without aura, 41 females (82%), mean age 45±12.8 years,

range 20-64 years, mean disease duration 16.1 ± 11.2 years] were prospectively enrolled between November 2020 and November 2021 at the Department of Neuroscience, Rehabilitation, Ophthalmology, Genetics, Maternal and Child Health (University of Genoa). MS patients with migraine as comorbidity were excluded from the analysis. Risk factors (RFs) for Small Vessel Disease (SVD) were recorded for patients included in both patients' cohorts.

3.2.2. MRI acquisition

All patients underwent MRI on a Siemens Prisma 3T scanner (Siemens, Erlangen, Germany) with a 64-channel head coil. The MRI protocol included: (i) 3D sagittal T2-FLAIR (repetition time/ inversion time/ echo time (TR/TI/TE): 5000 ms/1800 ms/393 ms; resolution $0.4 \times 0.4 \times 1$ mm³); (ii) 3D sagittal T1 MPRAGE (2300 ms/919 ms/2.96 ms; resolution $1 \times 1 \times 1$ mm³); (iii) 3D sagittal segmented echo-planar imaging (EPI) providing T2* magnitude and phase contrasts (TR/TE: 64 ms/35 ms; resolution $0.65 \times 0.65 \times 0.65$ mm³).

3.2.3 MRI analysis

CVS assessment was performed on FLAIR* images obtained by co-registration and voxel-wise multiplication of the high-resolution 3D T2* EPI and the 3D T2-FLAIR, as previously described ¹³⁴ (**Figure 8**).

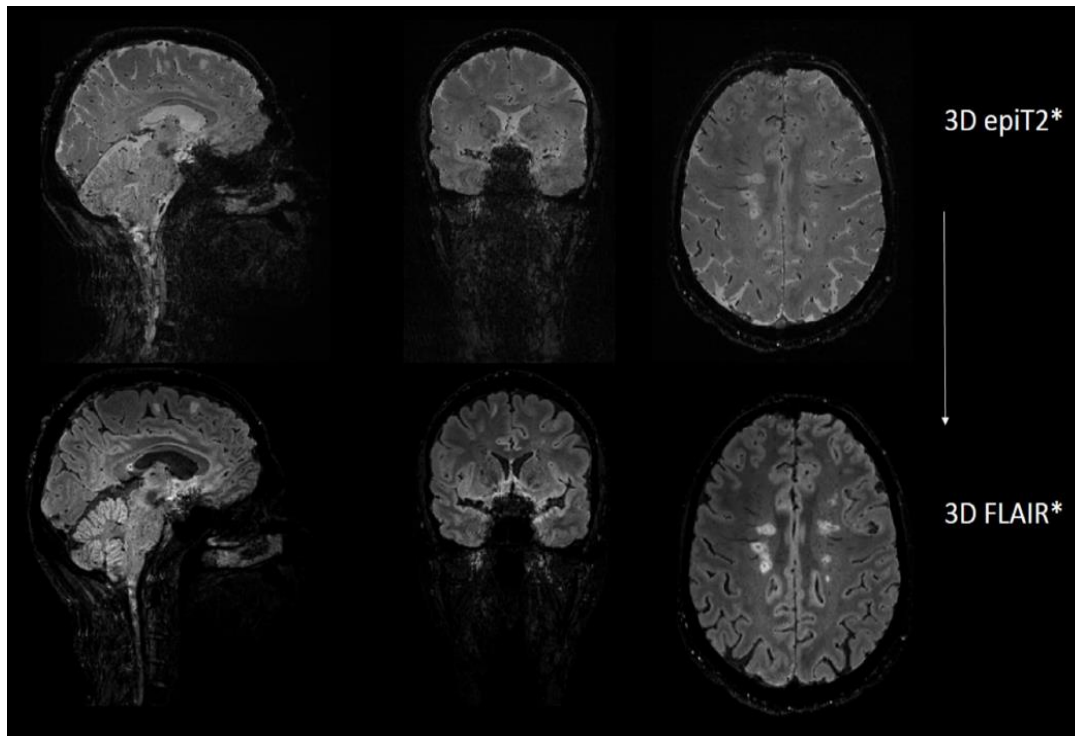


FIGURE 8 3D-FLAIR* CREATION FROM 3D-epiT2* AND 3D-FLAIR IMAGES

The co-registration between 3D-FLAIR and 3D-epiT2* images, followed by interpolation of the registered 3D-FLAIR image to match the high-spatial-resolution of the 3D-epiT2* image, and finally the multiplication of the coregistered interpolated 3D-FLAIR image by the 3D-epiT2* image were performed to obtain 3D-FLAIR* images (data from University of Genoa cohort)

FLAIR* images were reformatted in the axial, coronal and sagittal plane maintaining the native section thickness of 0.65 mm to improve visualisation of vessels within WM lesions and were used for the assessment of the presence of the CVS. For each patient, brain WM matter lesions were selected for CVS assessment according to NAIMS guideline⁶⁵. Exclusion criteria were (i) lesions <3 mm in diameter in any plane, (ii) lesions with multiple distinct veins, (iii) confluent lesions⁶⁵. The presence or absence of the CVS was blindly and independently evaluated by two raters (neurologists with expertise in neuroimaging of MS), according to the NAIMS guidelines⁶⁵ and a consensus was reached in challenging cases. Then, CVS+ and CVS- lesions were manually segmented on native FLAIR* images using Jim software (Jim

7.0, Xinapse System; <http://www.xinapse.com>). An in-house algorithm based on priors about tissues segmentation was used to automatically subdivide CVS+ and CVS- lesions according to their location: (i) deep/subcortical WM, (ii) periventricular, (iii) juxtacortical and (iv) infratentorial. The spatial distribution of lesions was also visually checked to ensure the accuracy of the automatic approach. To further investigate the clinical feasibility of the CVS, we tested “pick 6” and “pick 3” algorithms^{99,105} proposed as less time-consuming methods of counting lesions with the CVS to predict the diagnosis of MS.

3.2.4 Statistical analysis

Results were reported as mean with standard deviation (SD) or median with range and as median with interquartile range (IQR) for total FLAIR and CVS+ lesion number and volumes and for the %CVS+ lesions.

Total FLAIR and CVS+ lesion number and volumes and the %CVS+ lesions were compared between MS and migraine patients using Mann-Whitney test. Univariable and multivariable logistic regression models were fitted, where the type of disease was the dependent variable and the proportion of lesions with the CVS was the independent variable. In the multivariable model the proportion of lesions with the CVS was adjusted for demographic or clinical characteristics that resulted different between MS and migraine patients at the univariable analysis. A ROC-curve analysis was performed to identify the best threshold of %CVS+ lesions and the number of CVS+ lesions able to differentiate MS from migraine patients. P-values <0.001 were considered significant. Stata (v.16; Statacorp) was used for the computation.

3.3 Results

3.3.1 Demographic and clinical data

A summary of the demographic and clinical features of the enrolled subjects is reported in **Table 1** Demographic and clinical features of MS and migraine patients' cohorts. No differences were present in terms of age and gender distribution. Disease duration was different between MS and migraine patients ($p < 0.001$).

Demographic	Migraine (n=50)	MS (n=60)	p-value
Age, mean (SD); range	45.0 (12.8); 20-64	45.3 (13.8); 19-77	0.91
Females, n (%)	41 (82)	49 (81.7)	0.96
Disease duration, median (IQR; range)	20 (10-30; 0.5-50)	11.5 (5-17; 3-38)	<0.001
Clinical features			
Diabetes, n (%)	1 (2)	0	0.46
Dyslipidemia, n (%)	1 (2)	12 (20)	0.006
Smoking, n (%)	7 (14)	30 (50)	<0.001
Hypertension, n (%)	12 (24)	8 (13.3)	0.21
N. risk factors, n (%)			0.029
0	32 (64)	25 (41.7)	
1	15 (30)	23 (38.3)	
2+	3 (6)	12 (20)	
Aura, n (%)	9 (18)	-	

TABLE 1 DEMOGRAPHIC AND CLINICAL FEATURES OF MS AND MIGRAINE PATIENTS' COHORTS

3.3.2 CVS assessment: global and data and inter-raters' agreement

For MS patients, a total of 3467 brain WM lesions were analysed with a median of 56 (IQR:29-80) lesions per patient. For migraine patients, a total of 775 brain WM lesions were analysed with a median of 4.5 (IQR:2-16) lesions per patient. Eight (16%) migraine patients did not show any WM hyperintensities on FLAIR images. Among the 3467 lesions (MS cohort), 2687 (77.5%) were selected for CVS assessment after consensus agreement, with a median of 38 (IQR:20-65) lesions per patient. Among the 775 lesions (migraine cohort), 579 (74.7%) were selected for CVS assessment after consensus agreement, with a median of 3 (IQR:1-11) lesions per patient. Of the 2687 lesions (MS cohort), 1836 (68.3%) were CVS+. Of the 579 lesions (migraine cohort), 93 (16.1%) were CVS+. The median frequency of CVS+ lesions per patient was 72.3% (range: 27.7%-100%) in MS patients and 10% (range: 0%-100%) in migraine patients. The inter-rater agreement for the percentage of CVS+ lesions was “substantial/good” with a Cohen’s κ of 0.7 and agreement of 92%.

Lesion volume was different between CVS+ and CVS- lesions (median = 1273 mm³, range: 26–5840 mm³ vs 181.5 mm³, range: 17–1651 mm³ for MS cohort; median = 35.1 mm³, range: 3.6–883.5 mm³ vs 52.2 mm³, range: 5.0–3721 mm³ for migraine cohort; $p < 0.001$). CVS+ lesions volume and number were higher in MS with respect to migraine patients both considering the whole brain and the 4 brain subregions analysed ($p < 0.001$) (**Figure 9**).

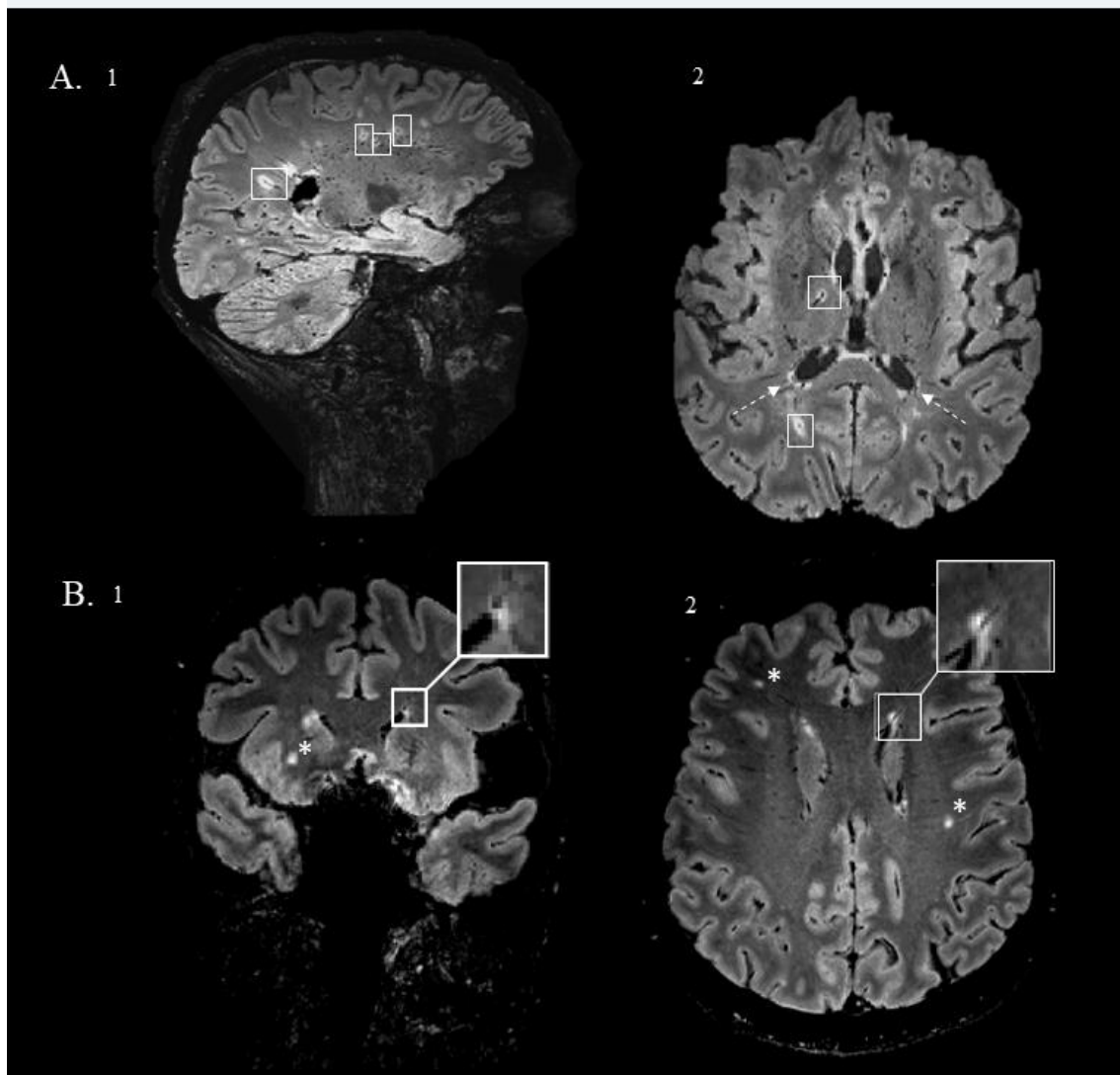


FIGURE 9 CENTRAL VEIN SIGN IN MULTIPLE SCLEROSIS AND MIGRAINE

A.3D-FLAIR* sagittal (1) and axial (2) planes of a patient with MS. Note the considerable number of WM lesions exhibiting the CVS (frames) and the higher density of periventricular vein structures (dotted arrows) that exclude surrounding WM lesions from the CVS assessment. B. 3D-FLAIR* coronal (1) and axial (2) planes of a patient with migraine. Note a periventricular WM lesion exhibiting the CVS (white box) and several deep WM lesions without the CVS (stars) (data from University of Genoa cohort)

3.3.3 CVS assessment: brain location

In migraine cohort, the highest proportion of CVS+ lesions, out of the total number of CVS+ lesions, was found in deep/subcortical (63.4%), as also in MS (55 %). MS patients, with respect to migraine patients, showed significantly ($p < 0.001$) higher: (i) FLAIR total lesion number and volume, (ii) FLAIR* total lesion number and volume, (iii) CVS+ lesion number, volume and percentage, (iv) infratentorial, periventricular, juxtacortical, deep/subcortical CVS+ lesion number.

The proportion of CVS+ lesions in the (i) deep/subcortical WM, out of the total number of FLAIR* selected lesions in the same location, was slightly higher in migraine than MS but without significant differences (63.4% vs 55%, respectively; $p = 0.11$); (ii) juxtacortical area, out of the total number of FLAIR* selected lesions in the same location, was higher in MS than migraine (17.0% vs 7.5%, respectively; $p = 0.016$); (iii) infratentorial area, out of the total number of FLAIR* selected lesions in the same location, was higher in MS than migraine (13.8% vs 3.2%, respectively; $p = 0.034$); (iv) periventricular area, out of the total number of FLAIR* selected lesions in the same location, was higher in migraine than MS (25.8% vs 14.3%, respectively; $p = 0.023$) (**Table 2**) (**Figure10**).

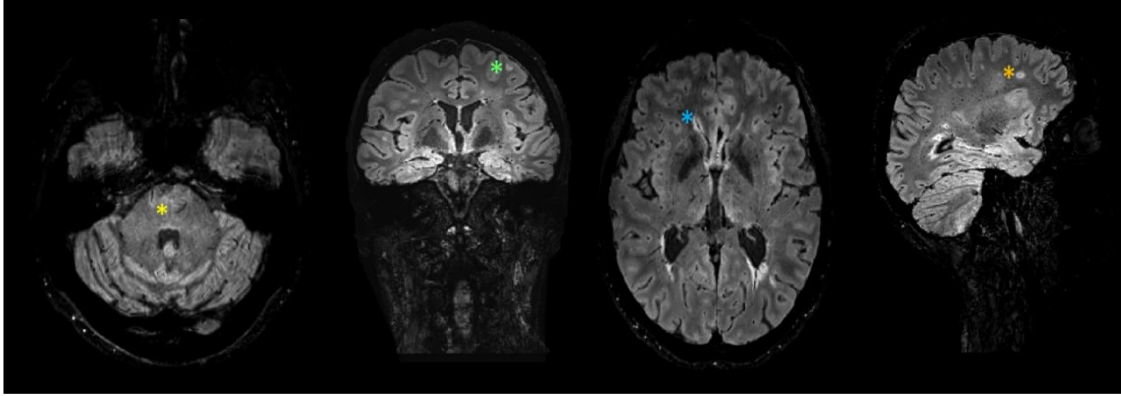


FIGURE 10 BRAIN LOCATION OF WM LESIONS EXHIBITING THE CENTRAL VEIN SIGN IN MULTIPLE SCLEROSIS

From left to right: infratentorial (yellow star), juxtacortical (green star), periventricular (blue star) and deep/subcortical WM (orange star) WM lesions exhibiting the CVS (from a MS patient, University of Genoa cohort)

	Migraine (n=50)	MS (n=60)	p-value
FLAIR lesion number, mean; median (IQR)	15.4; 4.5 (2-16)	57.8; 56 (29-80)	<0.001
FLAIR* lesion number, mean; median (IQR)	11.6; 3 (1-11)	44.8; 38 (20-65)	<0.001
FLAIR* lesion volume, mean; median (IQR)	271; 40.7 (12.4-181.0)	819; 224.5 (76.5-947)	<0.001
CVS+ lesions (%), median (IQR)	10 (0-28.6)	72.3 (60.8-81.8)	<0.001
CVS+ lesion number mean; median (IQR)	3.7; 2 (1-5)	30.6; 25 (13-47.5)	<0.001
CVS+ lesion volume, mean; median (IQR)	185; 35.1 (12.7-392.1)	1617; 1273 (539-2299)	<0.001
Infratentorial CVS+ lesion number, mean (SD); median (range)	0.08 (0.28); 0 (0-1) [n=25 CVS+]	4.22 (3.14); 3.5 (0-14)*	<0.001
Periventricular CVS+ lesion number, mean (SD); median (range)	0.96 (1.21); 1 (0-4) [n=25 CVS+]	4.37 (4.01); 3.5 (0-17)*	<0.001
Juxtacortical CVS+ lesion, mean (SD); median (range)	0.28 (0.68); 0 (0-2) [n=25 CVS+]	5.2 (5.9); 3 (0-27)*	<0.001
Deep/subcortical CVS+ lesion number, mean (SD); median (range)	2.36 (3.13); 1 (0-11) [n=25 CVS+]	16.8 (15.8); 14 (0-91)*	<0.001

8 patients in the migraine group had not Flair lesions; *All MS patients had CVS positive % > 0

TABLE 2 TOTAL WHITE MATTER AND CVS+ LESIONS NUMBER AND VOLUME IN MIGRAINE AND MS PATIENTS

3.3.4 Prediction of MS versus migraine according to the current criteria for MS and CVS related approaches

A higher proportion of CVS+ lesions was associated to a higher probability to be diagnosed as MS (OR 1.12, 95% CI 1.07–1.18, $p < 0.001$): per each percent, unit increase in the proportion of CVS+ lesions, this patient had a 12% higher risk of having MS instead of migraine. When this model was adjusted for disease duration, RFs (dyslipidaemia, smoking) for SVD and total number of lesions, comparable results were obtained (OR=1.11; 95% CI: 1.05-1.17, $p < 0.001$).

The best cut-off value in terms of the proportion of CVS+ lesions able to predict the diagnosis of MS was 23% (Sensitivity 90%, Specificity 90.5%) (**Figure 11; Table 3**). Maximizing on specificity the best cut-off was 25% (Sensitivity: 88.3%; Specificity: 97.6%). The AUC was 0.963 (95% CI: 0.916-1.000).

To further investigate the clinical feasibility of the CVS, we tested “pick 6” and “pick 3” algorithms^{99,105} which were proposed as less time-consuming methods of counting lesions with the CVS to predict the diagnosis of MS. All MS patients would be correctly diagnosed by using both approaches. After selecting migraine patients in which these rules were applicable, we found that 1/42 (2.4%) and 3/28 (10.7%) migraine patients would have been misdiagnosed as having MS, respectively.

Considering the absolute number of CVS+ lesions, regardless of brain location, 5 was identified as the number of CVS+ associated with the best performance in terms of sensitivity and specificity in differentiating MS from migraine (Sensitivity: 93.3%; Specificity: 80%). All MS patients would be

correctly diagnosed by using this approach. Conversely, after selecting migraine patients in which this approach was applicable (at least 5 FLAIR* lesions), we found that 7/25 (28%) migraine patients would have been misdiagnosed as having MS. However, in all these patients, the number of CVS+ lesions were lower than that of CVS- lesions (**Table 3**).

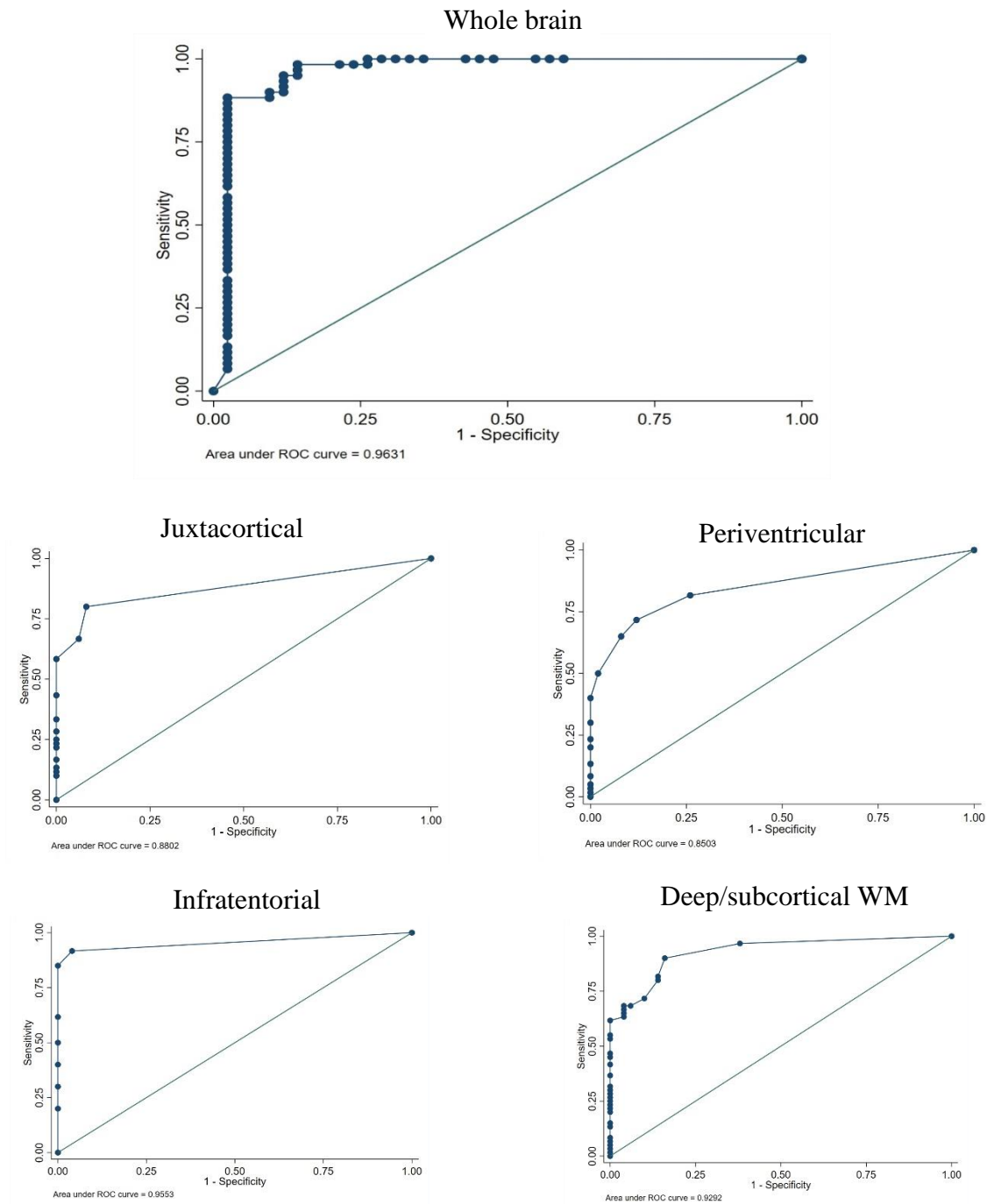


FIGURE 11 ROC CURVE OF THE DIFFERENT CVS+ LESION THRESHOLDS DIFFERENTIATING MS FROM MIGRAINE

Table 3

Marker	%		LR		Youden J Index
	Specificity	Sensitivity	Positive	Negative	
Threshold, %					
15	78.6	98.3	4.59	0.021	0.769
20	88.1	93.3	7.84	0.076	0.814
25	97.6	88.3	37.1	0.129	0.859
30	97.6	80.0	33.6	0.205	0.776
35	97.6	71.7	30.1	0.29	0.693
40	97.6	63.3	26.6	0.376	0.609
45	97.6	53.3	22.4	0.478	0.509
50	97.6	45.0	18.9	0.563	0.426
Positive CVS lesions, No.					
1	0	100	1.00	-	0
2	44.0	100	1.79	0.000	0.44
3	56.0	96.7	2.19	0.059	0.527
4	72.0	95.0	3.39	0.069	0.67
5	80.0	93.3	4.67	0.083	0.733
6	80.0	90.0	4.50	0.125	0.700
8	88.0	83.3	6.94	0.189	0.713
10	92.0	78.3	9.79	0.236	0.703
15	100.0	65.0	-	0.350	-

TABLE 3. PERFORMANCE OF DIFFERENT CVS+ LESION THRESHOLDS AND ABSOLUTE NUMBER OF CVS+ LESIONS

3.4 Discussion

Misdiagnosis of MS is a persistent issue that results in diagnosing MS in individuals affected by other disorders of the CNS. The diagnostic criteria for MS are periodically updated¹ to obtain the best combination of diagnostic sensibility and specificity. Indeed, if on the one hand it has been demonstrated that starting specific treatment for MS as early as possible has a great impact on delaying the progressive phase of the disease¹³⁵, the risk of diagnosing MS in individuals affected by other disorders is also substantial^{136,137}. In this context, increasing scientific evidences demonstrated that advanced imaging techniques could be able to overcome these issues^{1,65} and a lively debate is about their applicability in the clinical setting. In this context, the “central vein sign” (CVS) has been proposed as a highly sensitive and specific biomarker for MS^{138,139}. Advanced and optimised gradient-echo MRI techniques, initially applied at high and ultra-high field MRI^{139,140} and, then, at 3T MRI scans^{103,130,131,134,139,141} showed that the CVS may be very helpful to differentiate MS from its common mimics, as inflammatory vasculopathies¹⁰⁶, NMOSD¹³⁰ and SVD¹³¹. To guide radiologists and neurologists to better understand, standardize and evaluate the CVS in the diagnosis of MS, a consensus statement from the North American Imaging in Multiple Sclerosis Cooperative clearly established the radiological definition of the CVS⁶⁵. However, the traditional “proportion threshold” based approach may be particularly challenging and time-consuming when applied in MS patients with conspicuous lesion burden.

Therefore, simplified CVS algorithms based on the absolute number of lesions exhibiting the CVS (from now on “CVS+”), i.e. the 3¹⁰⁵ and 6⁹⁹ CVS lesions threshold, demonstrated lower sensibility¹⁴². Machine learning approaches for automated CVS assessment in MS has been proposed in the attempt to evaluate the benefit of introducing the CVS marker into MS diagnostic criteria, but their applicability must be evaluated in larger multicenter trials¹⁴³.

To the best of our knowledge, although migraine represents the first mimic of MS⁵⁵, counting for the 22% of MS misdiagnosis, no specific threshold capable to distinguish MS from migraine have been yet identified. A previous study performed in a small cohort of patients, found a significantly higher proportion of CVS+ lesions in MS with respect to migraine patients and finally highlighted the need of larger studies to define the best threshold to differentiate them¹⁰³.

As expected, in our study we showed that MS patients exhibit a significantly higher number of total WM lesion number detected on FLAIR images with respect to migraine patients. In line with previous findings, also in our study, the number, volume and proportion of CVS+ lesions (68.3% vs 16.1%) were clearly prominent in MS cohort.

Focusing on spatial distribution of CVS+ lesions, we found that the highest proportion of CVS+ lesions, out of the total number of FLAIR* detected lesions, was in the deep/subcortical region both in MS and migraine patients (55% vs 63.4%). Interestingly, the proportion of CVS+ lesions in the deep/subcortical WM was slightly lower in MS than migraine patients, although without reaching statistical significance. On the contrary, the proportion of CVS+ lesions in the juxtacortical and infratentorial areas was significantly higher in MS than migraine patients. These findings reflect the well-known topographical distribution of WM lesions in MS, where infratentorial and juxtacortical, but not the deep/subcortical

WM, are included in DIS criteria¹. Periventricular location of WM lesions in patients with migraine represents another issue, as demonstrated in previous studies focused on MS criteria^{144,145}. The anatomical high density of veins around ventricles may be a possible explanation of the high proportion of periventricular CVS+ lesions also in migraine patients. On the other side, the exclusion of a considerable number of periventricular WM lesion from CVS analysis due to their features (i.e., confluent, more than 1 vein passing through the lesion) and the previously suggested reduced periventricular venous visibility in MS, as a consequence of more extensive brain parenchymal gliosis¹⁴⁶, may explain our findings.

Although the features of WM lesions in patients with migraine are the main cause of radiological misdiagnosis with MS at conventional MRI scans, our study demonstrates how the CVS may represent a biomarker capable to distance these two pathological entities. Indeed, we found that the best threshold able to differentiate MS from migraine, maximizing both sensitivity and specificity, was 23% (Sensitivity 90%, Specificity 90.5%), a lower value than those identified in other pure inflammatory CNS diseases, as NMOSD and inflammatory vasculopathies, reflecting -at least partly- their different underlying pathophysiological mechanisms¹²⁹. Maximizing on specificity, a cut-off of 25% was able to reach an almost ideal specificity without a significant impact on sensitivity (Sensitivity: 88.3%; Specificity: 97.6%) and may be also used as valid approach.

The clear role of the CVS in orienting radiological diagnosis toward MS instead of migraine seems to be confirmed by the increase in having MS at the increase of CVS+ lesions proportion: per each percent, unit increase in the proportion of CVS+ lesions, this patient had a 12% higher risk of having MS instead of migraine. Similar

findings were observed after correcting regression analysis for smoke and dyslipidaemia, whose prevalence was significantly different between MS and migraine patients and whose role, as risk factors for SVD, in the reduction of CVS+ lesions proportion in MS cannot be excluded¹⁴⁷. We may explain the different prevalence of these two comorbidities in MS and migraine cohorts considering that smoke is strongly contraindicated in patients with migraine and, on the other side, the reduced mobility due to disability in MS may favour the development of dysmetabolic syndrome¹⁴⁸.

In the attempt to evaluate whether less time-consuming approaches were comparable to the threshold-based approach, we used pick 6⁹⁹ and pick 3¹⁰⁵ algorithms, finding that all MS patients would have been correctly diagnosed, while 2.4% and 10.7% of migraine patients would have been misdiagnosed as having MS respectively. Thus, we suggest that, among the time-saving approaches, the “6-rule”⁹⁹ may be preferable to the “3-rule”¹⁰⁵, in which also lesion location must be considered, thus requiring more time for analysis.

Furthermore, we found that the absolute count of 5 CVS+ lesions was able to minimize the risk to underestimate MS diagnosis (sensitivity 93.3%). Conversely, it was associated with a poorer performance in terms of specificity, as a considerable proportion (28%) of migraine patients would have been misdiagnosed with MS. This data is not negligible, and underlines that a significant proportion of migraine patients may exhibit a concrete number of WM lesions with heterogeneous pathophysiology¹⁰³. Indeed, although the pathophysiology of migraine-related WM hyperintensities is poorly understood, both ischemic and inflammatory mechanisms have been proposed, as there is increased cerebral vulnerability to ischemia in migraineurs, as well as evidence of blood brain barrier (BBB) disruption during migraine attacks¹²⁹

Our study is not without limitations. Our analysis was limited to the brain and did not consider the spinal cord in the assessment of DIS criteria for MS. In vivo imaging studies on CVS in the spinal cord are still lacking, mainly due to the challenge of obtaining high-quality T2*-weighted images of the cord⁶⁵. In addition, in our migraine cohort, patients with and without aura coexisted. Nevertheless, the presence of WM hyperintensities have been described in both conditions^{128,129}, thus no significant impact of migraine type on CVS assessment may be expected.

In conclusion, the central vein assessment provided by susceptibility-based MRI is a useful tool when attempting to differentiate MS from migraine. This latter condition represents the most common mimic of MS, as it can have similarities with MS, especially from a radiological point of view. Thus, the addition of the central vein sign assessment to the existing clinical and radiological workup can reduce the risk of misdiagnosis and aid therapeutic strategies. In our study, we demonstrated that a threshold of 23% is capable to distinguish MS from migraine with a particularly satisfactory performance in terms of sensitivity and specificity. Furthermore, the pick 6 seemed to be preferable to the pick 3 approach as time saving algorithm to differentiate MS from migraine. Nevertheless, the implementation of automated imaging postprocessing approaches (ie, automated FLAIR* reconstruction and CVS detection) remains essential to allow direct translation of the central vein sign into the everyday clinical practice.

Chapter 4

4. White matter lesions and comorbidities in multiple sclerosis: central vein sign and diffusion MRI

4.1 Introduction

Multiple sclerosis (MS) is an inflammatory disease of the central nervous system (CNS) characterized by a relapsing or progressing clinical course. Although focal hyperintensities on T2-weighted magnetic resonance imaging (MRI) detected within the brain and spinal cord represent the radiological hallmarks of the disease¹⁴⁹, they lack of histopathological specificity and may hide heterogenous pathological substrates.

The perivenular location of MS lesions has been known for more than a century. From the histopathological point of view, MS lesions are characterized by cellular infiltrates that rise around small-to-medium-sized parenchymal venules¹⁵⁰- the so called “perivascular cuffs”- mainly characterized by mononuclear cells that enter CNS throughout the damage of the blood brain barrier (BBB) as waves of inflammatory invasion¹⁵¹. The essential transition from the histopathological evidence to the “in vivo” demonstration of the presence of a central venule within MS lesions has been made possible by advanced gradient-echo MRI techniques^{139,140}. Thus, this “Central Vein Sign” (CVS) has been suggested as a potential biomarker able to improve diagnostic specificity in MS. The so-called “threshold-

based” approach, consisting in the calculation of the percentage of white matter (WM) lesion exhibiting the CVS (from now on “%CVS+ lesions”), has been applied to differentiate MS from its most common mimics. Particularly, a 50% threshold of lesions with CVS has been demonstrated to be able to differentiate MS from inflammatory vasculopathies¹⁰⁶, a 54% threshold from Neuromyelitis Optica Spectrum Disorder (NMOSD)¹³⁰ and a 45% threshold from and small vessel disease (SVD) associated lesions¹³¹, thus supporting the potential use of CVS for improving MS diagnosis.

Nevertheless, the presence of cardiovascular comorbidities, which are particularly frequent in older patients with progressive MS, introduces an extra challenge in the conventional radiological setting, where advanced and specific MRI biomarkers may be needed to distinguish whether a new T2-weighted lesion is due to MS or to age-related comorbidities. The prevalence of SVD-related WM hyperintensities increases from about 5% for people aged 50 years to nearly 100% for people aged 90 years¹⁵². In addition to age, arterial hypertension (HT)¹⁵³, current and former smoking and diabetes mellitus¹⁵⁴ are considered modifiable risk factors (RFs) for SVD.

However, data about the impact of age and, more generically, of the SVD on CVS performance in MS patients are still scarce. In a recent study, performed on a relatively small cohort of MS patients, the %CVS+ lesions significantly decreased in older and hypertensive MS patients¹⁴⁷.

Besides SVD, migraine is a frequent comorbidity in MS patients¹⁵⁵. It is well-known that WM T2-weighted hyperintensities are frequently detected in patients with migraine and persist over time¹⁵⁶, with the deep/subcortical WM of the frontal lobes typically involved¹⁵⁷. Despite the similar features shared by MS, migraine and SVD-related WM T2-weighted hyperintensities on conventional MRI, ex-vivo

studies showed the heterogeneity of the underlying histopathological substrates^{158,159}.

To overcome the limited pathological specificity of conventional MRI, several advanced MRI techniques have been developed and applied to characterize microstructural alterations due to tissue disruptions caused by MS^{117,160}. Among all the proposed multicompartiment models, the Spherical Mean Technique (SMT) has been successfully applied to characterize the brain¹²⁵ and spinal cord¹²⁶ of MS patients. Nevertheless, at the best of our knowledge, whether CVS+ lesions show distinctive microstructural features with respect to CVS- lesions has not yet been investigated.

Therefore, the aims of our study were: a) to investigate the impact of SVD and migraine on the global and subregional brain CVS assessment in a large cohort of MS patients as a whole and stratified according to age; b) to investigate the pathological substrate of CVS+ and CVS- lesions using advanced diffusion metrics (SMT); c) to determine whether the use of SMT-derived metrics can differentiate perivenular lesions, typical of MS, from non-perivenular lesions, possibly associated with different pathophysiological mechanisms.

4.2 Material and Methods

4.2.1 Subjects

One hundred and twenty patients with a diagnosis of MS¹ [84 with relapsing-remitting (RRMS), 36 with progressive (Primary Progressive, PP and Secondary Progressive, SP, from now on “PMS”) disease course², were prospectively enrolled between January 2019 and September 2020 at the Department of Neuroscience, Rehabilitation, Ophthalmology, Genetics,

Maternal and Child Health (University of Genoa). Inclusion criteria were: (I) age >18 years and (II) MS diagnosis according to revisions of McDonald's criteria¹. Exclusion criteria were: (i) absence of capability to sign the informed consent and (ii) suboptimal MRI image quality.

Moreover, we stratified the included subjects as follows: (i) Group 1: 18-30 years (n=30); (ii) Group 2: 31-44 years (n=30); (iii) Group 3: 45-55 years (n=30); (iv) Group 4: 56-77 years (n=30).

All patients underwent neurological examination with the assessment the Expanded Disability Status Scale (EDSS). In addition, the following RFs for SVD were recorded: body mass index (BMI; measured as weight-to-height ratio, cut-off ≥ 25 kg/m²), smoking (at the time of MRI examination or in the past), diagnosis of arterial hypertension (at the time of MRI examination or in the past) and its medications, diabetes or glucose intolerance (at the time of MRI examination or in the past) and its medications, hypercholesterolemia (at the time of MRI examination or in the past) and its medications. The cumulative number of RFs was calculated for each patient. Furthermore, the presence of migraine (or history of migraine) with or without aura (from now on simply "migraine") was also recorded.

4.2.2 MRI acquisition

All patients underwent MRI on a 3T Siemens MAGNETOM Prisma (Siemens Healthcare, Erlangen, Germany) with a 64-channel head and neck coil.

The MRI protocol included: (i) 3D sagittal T2-FLAIR (repetition time/inversion time/echo time (TR/TI/TE): 5000 ms/1800 ms/393 ms; resolution $0.4 \times 0.4 \times 1$ mm³); (ii) 3D sagittal T1 MPRAGE (TR/TI/TE: 2300 ms/919 ms/2.96 ms; resolution $1 \times 1 \times 1$ mm³); (iii) twice-refocused spin echo

echo-planar imaging sequence for multi-shell diffusion-weighted images (TR/TE: 4500 ms/75 ms; 107 diffusion directions distributed in 5 shells with b-value up to 3000s/mm² plus 7 non weighted images acquired with both anterior-posterior and posterior-anterior phase encoding directions; spatial resolution 1.8 × 1.8 × 1.8 mm³); (iv) 3D sagittal segmented echo-planar imaging (EPI) providing T2* magnitude and phase contrasts (TR/TE: 64 ms/35 ms; resolution 0.65 × 0.65 × 0.65 mm³) after intravenous contrast injection of 10 ml of 0.5 mmol/ml gadoteric acid contrast agent.

4.2.3 Lesion segmentation and CVS assessment

CVS assessment was performed on FLAIR* images obtained by rigid co-registration¹⁶¹ and voxel-wise multiplication of the high-resolution 3D T2* EPI and the 3D T2-FLAIR, as previously described⁷⁵.

FLAIR* images were analysed in the native section thickness of 0.65 mm to improve visualisation of vessels within MS lesions and were used for the assessment of the presence of the CVS. For each patient, brain WM matter lesions were selected for CVS assessment according to NAIMS guideline⁶⁵. The presence or absence of the CVS (CVS+ lesions or “perivenular” and CVS- lesions or “non-perivenular” respectively) was blindly and independently evaluated by two raters (neurologists with expertise in neuroimaging of MS), according to the NAIMS guidelines⁶⁵. In case of disagree between raters, lesions were reviewed by a third rater (with great expertise in neuroimaging) and a consensus was reached. Then, CVS+ and CVS- lesions were manually segmented on native FLAIR* images using Jim software (Jim 7.0, Xinapse System; <http://www.xinapse.com>), creating CVS+ and CVS- lesion masks, respectively.

In addition, MS patients were classified in “perivenular positive” versus “perivenular negative” according to the previously proposed criteria: the 35% and 40% CVS proportion-based diagnostic thresholds^{132,133}, the “6-lesion rule”⁹⁹ and the “3-lesion rule”¹⁰⁵.

An in-house algorithm based on priors about tissues segmentation was used to automatically subdivide CVS+ and CVS- lesions according to their location: (i) Deep/subcortical WM, (ii) Periventricular, (iii) Juxtacortical and (iv) Infratentorial. To avoid mislabelling, a quality check on the resulting classification was then made by a Neurologist with more than 5 years of experience.

Finally, whole brain and subregion-specific CVS+ and CVS- lesion masks were registered on T1- weighted images using the automated FMRIB's Linear Image Registration Tool (FLIRT) with boundary-based registration¹⁶².

4.2.4 Diffusion processing

Diffusion MR images were first denoised using the Marchenko-Pastur principal component analysis algorithm¹⁶³ available in MRtrix3¹⁶⁴. Then they were corrected for movement artifacts and susceptibility induced distortions using eddy and top-up commands from FMRIB Software Library (FSL)^{165–168}. As last step of pre-processing we also performed B1 field inhomogeneity correction to all the dMRI volumes¹⁶⁹. To compute the microstructural maps derived from SMT model, we used the open-source code available at (<https://github.com/ekaden/smt>). To register the different lesions masks on the SMT maps, first diffusion weighted images were registered on T1-weighted images using FLIRT with boundary-based registration¹⁶², then the resulting transformations were inverted and applied to the lesion masks to

register them in the diffusion weighted image space. Similar to¹⁷⁰ to compensate for the variable partial volume effects caused by the different resolution between the images, only lesions larger than three voxels after registration on diffusion space were included in the final data analysis. All the registrations were visually checked by a trained professional with more than 5 years of experience in neuroimaging. Finally, we extracted the mean values inside each type of lesions of the following SMT microstructural maps: intraneurite signal fraction (INTRA), extraneurite transverse diffusivity (EXTRATRANS), and extraneurite mean diffusivity (EXTRAMD) that describe the fraction of signal coming from the intra-axonal compartment as well as the properties of the anisotropic extraneurite compartment via its transverse microscopic diffusivity and mean diffusion outside the axons, respectively^{116,171}.

4.2.5 Statistical analysis

Results were reported as mean with standard deviation (SD) or median with range. Differences on lesion volume and lesion location frequencies were compared between CVS+ and CVS- using a Generalized Estimating Equation (GEE) model to take in account multiple lesions from the same patients. Association of demographic and clinical characteristics of patients on percentage of CVS lesions was assessed using Mann-Whitney test for binary variables or Kruskal-Wallis test for categorical variables. Spearman's rank correlation was used for continuous characteristics as age, disease duration and BMI. All significant ($p < 0.05$) characteristics at the univariable analyses were included in a multivariable linear regression model. Single lesions

microstructural metrics comparisons between CVS+ and CVS- and according to age Groups was performed using the GEE model for the same reasons reported above. Mean and SD of each microstructural metric were estimated from a multivariable GEE model also including age, gender and MS type. P-values were adjusted for multiple comparisons using the false-discovery rate (FDR) approach. Stata (v.16; Statacorp) was used for the computation.

4.3 Results

6.3.1 Demographic and clinical data

In our cohort, 66 MS patients were females (55%), mean (\pm SD) age was 43.8 ± 14.4 years and mean disease duration was 13.4 ± 10.6 years. A more detailed summary of the demographic and clinical features of the enrolled subjects is reported in **Table 4**. No differences were present in terms of gender distribution. Disease duration was different between age Group 4 vs age Group 1 and age Group 2 ($p<0.001$ for both, $>$ in age Group 4) and between age Group 3 vs age Group 1 ($p=0.001$, $>$ in age Group 3) and age Group 2 ($p<0.001$, $>$ in age Group 3). No differences in disease duration were present between age Group 1 vs age Group 2 and age Group 3 vs age Group 4. MS phenotype was different between age Group 1 vs Age Group 3 and age Group 4 [RRMS $>$ PMS, $p<0.001$ for both] and between age Group 2 vs age Group 4 (RRMS $>$ PMS, $p=0.002$). HT was prevalent in age Group 4 vs age Group 3 ($p=0.04$), age Group 2 and age Group 1 ($p<0.001$ for both). A difference in prevalence of hypercholesterolemia was observed between age Group 4 vs

age Group 1 ($p=0.021$). As concerns migraine, smoke and diabetes or glucose intolerance no differences between age Groups were observed.

Demographic and MS clinical data	
Patients, n	120
Female, %	55
Age, years, mean (<i>SD</i>)	43.8 (14.4)
EDSS score, median (<i>range</i>)	2 (1-7)
MS phenotype, n (%)	
RRMS	84 (70)
SPMS	21 (17.5)
PPMS	15 (12.5)
Disease duration, years, mean (<i>SD</i>)	13.4 (10.6)
Comorbidities clinical data	
Age Groups, n	4
Age Group 1, n. patients (range, years)	30 (18-30 years)
Age Group 2, n. patients (range, years)	30 (31-44 years)
Age Group 3, n. patients (range, years)	30 (45-55 years)
Age Group 4, n. patients (range, years)	30 (56-77 years)
HT, n (%)	17 (14.2)
Diabetes or glucose intolerance, n (%)	2 (1.7)
Smoke, n (%)	63 (52.5)
BMI ≥ 25 kg/m ² , n (%)	10 (8.3)
Hypercholesterolemia, n (%)	21 (17.5)
Cumulative number of RFs for SVD, median (<i>range</i>)	1 (0-4)
Migraine, n (%)	34 (28.3)
Demographic and clinical features according to age Groups¹	
Disease duration	1 vs 4 (p<0.001) 2 vs 4 (p<0.001) 1 vs 3 (p=0.001) 2 vs 3 (p<0.001) (> in age Group 4 and age Group 3)
MS phenotype	1 vs 3 (p<0.001) 1 vs 4 (p<0.001) 2 vs 4 (p=0.002) (RRMS>PMS in age Group 1)
HT	1 vs 4 (p<0.001) 2 vs 4 (p<0.001) 3 vs 4 (p=0.04) (>HT in age Group 4)
Hypercholesterolemia	1 vs 4 (p=0.021) (>hypercholesterolemia in age Group 4)

¹only significant comparisons among Age Groups were reported

TABLE 4 BASELINE DEMOGRAPHIC AND CLINICAL CHARACTERISTICS

4.3.2 CVS assessment: global data and inter-raters' agreement

A total of 7445 brain WM lesions were analysed with a median of 27.3 (range: 4–51) lesions per patient. Among the 7445 lesions, 5303 (71.2%) were selected for CVS assessment after consensus agreement, with a median of 38 (range: 4-20) lesions per patient. Of the 5303 lesions, 3645 (68.7%) were CVS+. The median frequency of CVS+ lesions per patient was 73.5% (range: 27.7%-100%). The inter-rater agreement for the percentage of CVS+ lesions was “substantial/good” with a Cohen’s κ of 0.7 and agreement of 89%.

Lesion volume was different between CVS+ and CVS– lesions (median = 1292 mm³, range: 26–7969 mm³ vs 224 mm³, range: 17–1713 mm³, respectively; $p < 0.001$). CVS+ lesions had significant higher volume and number with respect to CVS- lesions in all the 4 brain regions analysed [deep/subcortical WM, periventricular, juxtacortical and infratentorial; ($p < 0.001$ for all, both for volume and number), **Table 5**]

	CVS+	CVS-	p-value
Total lesions, n (%)	3645 (68.7)	1658 (31.3)	-
Whole cohort, Lesion volume (mm³), median (range)	1292 (26-7969)	224 (17-1713)	<0.001
Periventricular	296 (110-555)	45 (13-88)	<0.001
Infratentorial	161 (75-273)	34 (16-54)	<0.001
Juxtacortical	283 (72-526)	74 (29-255)	<0.001
Deep/subcortical WM	596 (158-1229)	141 (56-270)	
Whole cohort, Lesion location, n (%)			
Periventricular	584 (80)	146 (20)	<0.001
Infratentorial	527 (85.6)	89 (14.4)	<0.001
Juxtacortical	640 (61.3)	404 (38.7)	<0.001
Deep/subcortical WM	1894 (65.1)	1019 (34.9)	<0.001
Age Group 1 (18-30), Lesion location, n (%)			
Periventricular	136 (84.5)	25 (15.5)	<0.001
Infratentorial	112 (85.5)	19 (14.5)	<0.001
Juxtacortical	171 (67.6)	82 (32.4)	<0.001
Deep/subcortical WM	411 (72.1)	159 (27.9)	<0.001
Age Group 2 (31-44), Lesion location, n (%)			
Periventricular	178 (84)	34 (16)	<0.001
Infratentorial	161 (88.5)	21 (11.5)	<0.001
Juxtacortical	187 (64.9)	101 (35.1)	<0.001
Deep/subcortical WM	570 (73.4)	207 (26.6)	<0.001
Age Group 3 (45-55), Lesion location, n (%)			
Periventricular	123 (75.9)	39 (24.1)	<0.001
Infratentorial	113 (85)	20 (15)	<0.001
Juxtacortical	161 (59.2)	111 (40.8)	0.033
Deep/subcortical WM	558 (67.1)	273 (32.9)	<0.001
Age Group 4 (56-77), Lesion location, n (%)			
Periventricular	147 (75.4)	48 (24.6)	<0.001
Infratentorial	141 (82.9)	29 (17.1)	<0.001
Juxtacortical	121 (52.4)	110 (47.6)	0.19
Deep/subcortical WM	355 (48.3)	380 (51.7)	0.085

TABLE 5 VOLUME AND TOPOGRAPHY OF CVS+ AND CVS- LESIONS IN THE WHOLE COHORT AND ACCORDING TO AGE GROUPS

4.3.3 CVS proportion-based diagnostic thresholds versus simplified algorithms

Applying the 35% and the 40% CVS proportion-based diagnostic thresholds^{132,133} 119 of the 120 included patients were, for both thresholds, perivenular positive. In one patient, %CVS+ lesions was 28% (age Group 4, secondary progressive phenotype, history of migraine); in the other one it was 39% (age Group 2, secondary progressive phenotype, smoke and migraine). When applying the simplified algorithms, 6-lesion¹³¹ and 3-lesion rules¹⁰⁵, 119 and 111 of the 120 included patients were perivenular positive, respectively.

4.3.4 CVS relationship with MS phenotype, RFs for SVD and migraine

RRMS patients showed a higher percentage of CVS+ lesions with respect to PMS patients (76.9%, range 40-100% vs 67.3%, range 27.7-100%; $p=0.002$). The median percentage of CVS+ lesions decreased from age Group 1 to age Group 4 (for age Group 1: median 79.7%, range 60.3-100%; for age Group 2: median 79.1%, range 39.1-100%; for age Group 3: median 71.8%, range 40-100%; for age Group 4: median 57.7%, range 27.7-100%). Differences in median percentage of CVS+ lesions were observed among all Age Groups, except for Age Group 2 vs Age Group 3 (**Table 6**).

	CVS+ (% lesions), median (range)	p-value
Age		1 vs 2 p=0.026
Age Group 1: 18-30 (n=30) ¹	79.7 (60.3-100)	1 vs 3 p<0.001
Age Group 2: 31-44 (n=30) ²	79.1 (39.1-100)	1 vs 4 p<0.001
Age Group 3: 45-55 (n=30) ³	71.8 (40-100)	2 vs 4 p<0.001
Age Group 4: 56-77 (n=30) ⁴	57.7 (27.7-100)	3 vs 4 p=0.017
MS type		
RR (n=84)	76.9 (40-100)	0.002
PMS (n=36)	67.3 (27.7-100)	
HT		
No (n=103)	74.7 (27.7-100)	0.031
Yes (n=17)	61.9 (43.3-100)	
Diabetes or glucose intolerance		
No (n=118)	74.0 (27.7-100)	0.33
Yes (n=2)	60.8 (49.2-72)	
Smoke		
No (n=57)	72.4 (27.7-100)	0.84
Yes (n=63)	75 (39.1-100)	
BMI		
18-24.9 (n=79)	75 (27.7-100)	0.27
≥25 (n=41)	72 (40-100)	
Hypercholesterolemia		
No (n=99)	74.7 (27.7-100)	0.078
Yes (n=21)	68 (43.1-100)	
Cumulative RFs number		
0 (n=31)	74.7 (40-100)	0.55
1 (n=52)	77.1 (27.7-100)	
2 (n=20)	65.8 (39.1-93.3)	
3-4 (n=17)	66.7 (43.5-88.1)	
Migraine (with or without aura)		
No (n=86)	76.4 (40-100)	0.032
Yes (n=34)	65.8 (27.7-100)	

TABLE 6 CVS+ LESIONS PERCENTAGE COMPARISONS AMONG AGE GROUPS, MS PHENOTYPE, RFs FOR SVD AND MIGRAINE

When MS patients were stratified according to the Age Groups, we found that, in all Age Groups and brain subregions, CVS+ lesion number was higher than CVS- lesions [$p < 0.001$ for all, except for: (i) juxtacortical area in Age Group 3 ($p = 0.033$) and (ii) juxtacortical area in Age Group 4 where the difference was not significant], excluding the deep/subcortical WM in Age Group 4, where CVS- lesion number was higher than CVS+ lesions, although not reaching statistical significance (**Table 2**). (**Figure 12**)

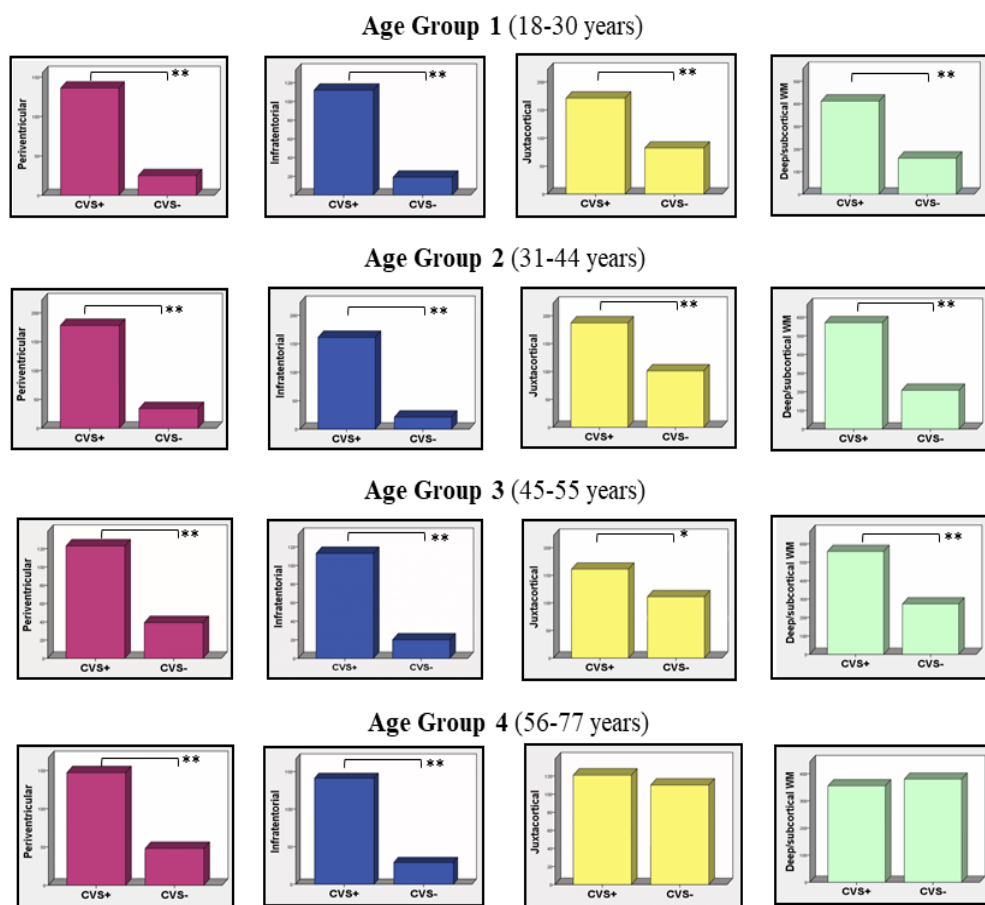


FIGURE 12 CVS+ AND CVS- LESION DISTRIBUTION ACCORDING TO AGE GROUPS AND BRAIN SUBREGIONS

In all Age Groups and brain subregions CVS+ lesion number is higher than CVS- lesions (** $p < 0.001$; * $p = 0.033$), except for juxtacortical area in Age Group 4 where the difference is not significant. Note the deep/subcortical WM in Age Group 4 (57-77 years), where CVS- lesion number rises and becomes higher than CVS+ lesions, although not reaching statistical significance.

Patients with HT showed a lower percentage of CVS+ lesions (median: 61.9%, range 43.3-100%) compared with patients without diagnosis of HT (median: 74.7%, range 27.7-100%; $p=0.031$). Migraine patients had a lower percentage of CVS+ lesions (median: 65.8%, range 27.7%–100%) compared with patients without migraine (median: 76.4%, range 40%–100%; $p=0.032$). A trend was observed between hypercholesteraemic and no hypercholesteraemic patients (median: 68%, range 43.1%–100% vs median 74.7%, range 27.7%–100% respectively; $p=0.078$). For smoke, BMI \geq 25, diabetes or glucose intolerance and cumulative number of RFs for SVD no differences were observed in CVS+ vs CVS- lesion median percentage (**Table 3**).

A negative correlation was found between %CVS+ lesions and age ($r=-0.46$; $p<0.001$; **Figure 13**) and between %CVS+ lesions and disease duration ($r=-0.24$; $p=0.008$), while a trend was observed with BMI ($r= -0.17$; $p=0.058$).

In the multivariable model, including age, migraine, the cumulative number of RFs for SVD, HT, MS phenotype and disease duration, age and migraine were independently associated with the %CVS+ lesions (model R^2 0.25; $p<0.001$ for age and $p=0.013$ for migraine).

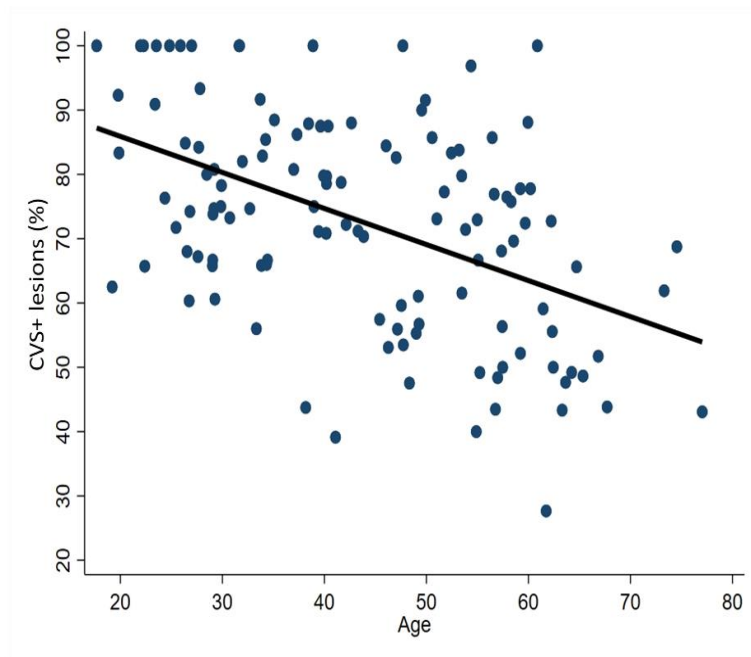


FIGURE 13 ASSOCIATION BETWEEN PATIENT'S AGE AND THE FREQUENCY OF CVS+ LESIONS

An inverse correlation was found between %CVS+ lesions and age ($r = -0.46$; $p < 0.001$)

4.3.5 Microstructural features of CVS+ and CVS- lesions evaluated by SMT diffusion model

With respect to CVS- lesions, CVS+ lesions showed higher EXTRAMD ($p=0.001$), higher EXTRATRANS ($p=0.001$) and lower INTRA ($p=0.02$). In the deep/subcortical WM, juxtacortical and infratentorial areas, EXTRAMD was higher in CVS+ lesions with respect to CVS- lesions ($p=0.001$, $p=0.01$ and $p=0.05$ respectively), while in periventricular region we observed the opposite result ($p=0.001$). In the deep/subcortical WM and infratentorial areas, EXTRATRANS was higher in CVS+ lesions with respect to CVS- lesions ($p=0.001$ and $p=0.04$ respectively), while in periventricular and juxtacortical regions no differences were observed. In the deep/subcortical

WM and periventricular areas, INTRA was lower in CVS+ lesions with respect to CVS- lesions (p=0.001 for both), while in infratentorial and juxtacortical regions no differences were observed (**Table 7**).

	CVS+	CVS-	p-value*	p-value adjusted for m.c.^
EXTRAMD, mean (SD) mm ² /sec	0.00144 (0.000245)	0.00139 (0.000228)	< 0.001	0.001
Deep/subcortical WM	0.00139 (0.000128)	0.00135 (0.000114)	< 0.001	0.001
Periventricular	0.00154 (0.000226)	0.00163 (0.000301)	0.007	0.010
Juxta	0.00132 (0.000175)	0.00129 (0.000190)	0.035	0.050
Infratentorial	0.00141 (0.000251)	0.00134 (0.000260)		
EXTRATRANS mean (SD) mm ² /sec	0.00117 (0.000288)	0.00111 (0.000252)	< 0.001	0.001
Deep/subcortical WM	0.00109 (0.000182)	0.00105 (0.000145)	0.130	0.150
Periventricular	0.00131 (0.000252)	0.00135 (0.000333)	0.080	0.110
Juxta	0.00114 (0.000176)	0.00112 (0.000194)	0.027	0.040
Infratentorial	0.00103 (0.000293)	0.000952 (0.000296)		
INTRA mean (SD)	0.399 (0.129)	0.409 (0.124)	0.012	0.020
Deep/subcortical WM	0.425 (0.113)	0.449 (0.0976)	< 0.001	0.001
Periventricular	0.341 (0.0969)	0.378 (0.109)	0.170	0.190
Juxta	0.309 (0.0932)	0.301 (0.0894)	0.110	0.140
Infratentorial	0.507 (0.122)	0.530 (0.138)		

TABLE 7 SMT METRICS COMPARISONS BETWEEN CVS+ AND CVS- LESIONS
m.c.: multiple comparisons; *P-value obtained from GEE model and adjusted for age, MS phenotype and gender; ^Adjustment for multiple comparisons using the false-discovery rate approach.

SMT-metrics maps within representative CVS+ and CVS-lesions are showed in **Figure 14** .

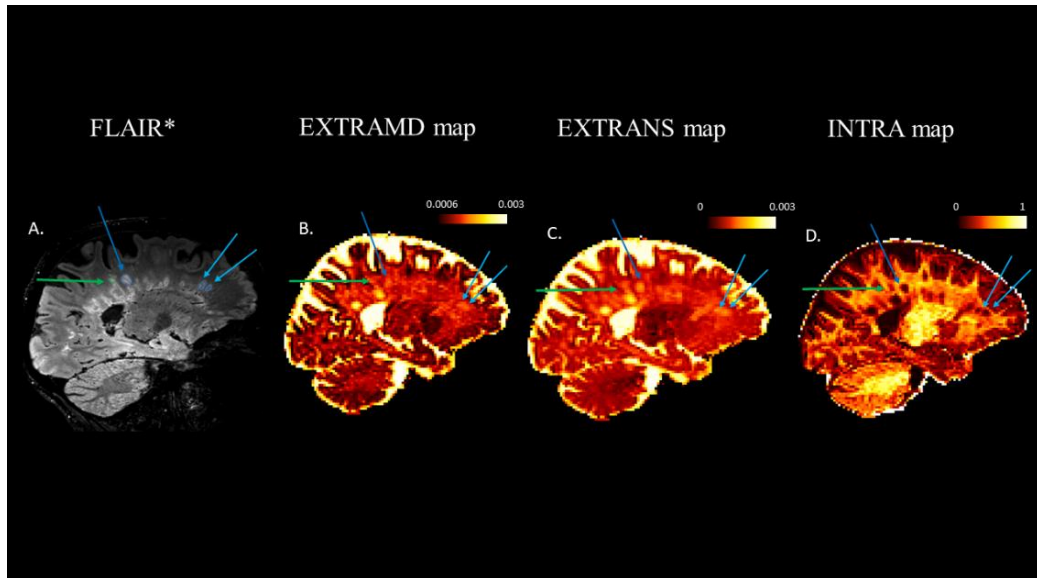


FIGURE 14 SELECTED SAGITTAL FLAIR* AND SMT-DERIVED EXTRAMD, EXTRATRANS AND INTRA MAPS OF A 62-YEAR-OLD PATIENT DIAGNOSED WITH MULTIPLE SCLEROSIS.

The colour bar expresses each SMT-metric: adimensional unit for INTRA, mm^2/sec for EXTRAMD and EXTRATRANS measures. Arrows indicate the presence of representative CVS+ lesions (blue arrows) and CVS- lesion (green arrows) to highlight the differences in SMT metrics among them.

4.4 Discussion

In this study, we investigated the impact of RFs for SVD and migraine on the global and subregional brain CVS assessment in a large cohort of MS patients stratified according to age and thus applied SMT diffusion model to evaluate whether perivenular lesions show distinctive microstructural features with respect to non-perivenular lesions. We focused on SVD and migraine, due to their high prevalence in common population, including MS patients^{155,172}. Unlike MS, histopathological studies in SVD revealed that the anatomical target of tissue damage is mostly represented by the arteriolar side of vascular microcirculation^{159,173}, where vessel lumen restriction and chronic hypoperfusion mainly occur. Although the pathophysiology of migraine-related deep WM hyperintensities is poorly understood, both ischemic and inflammatory mechanisms have been proposed, as there is increased cerebral vulnerability to ischemia in migraineurs, as well as evidence of BBB disruption during migraine attacks¹⁵⁸.

Among the RFs for SVD, age was the strongest inverse predictor of the percentage of CVS+ lesions, while HT, although associated with a lower prevalence of CVS+ lesions, did not survive as a significant predictor in the regression analysis. The low percentage of MS patients with HT in our sample (as for diabetes, smoke and higher BMI) may explain these findings. One of the most novel aspects of our study was the investigation of migraine impact on the percentage of CVS+ lesions. MS patients with migraine showed a lower percentage of CVS+ lesions with respect to MS patients without migraine. Furthermore, migraine also survived as inverse predictor of the percentage of perivenular lesions in the regression analysis. Interestingly, analysing demographic and clinical features of MS patients who did not fulfil the 35% and 40% thresholds approach in our sample, we observed that both MS patients had suffered or suffered from migraine. Although our data

confirmed that the previously proposed 35% and 40% CVS proportion-based thresholds^{132,133} remain valid for differential diagnosis, they may suggest that migraine, beside aging, could be able to affect CVS performance and, thus, it should be carefully considered in the radiological workflow of patients with high clinical suspicion of MS.

Furthermore, in order to investigate whether older age has a preferential impact on the CVS assessment in some brain subregions rather than in others, we considered the distribution of the CVS+ and CVS- lesions in brain areas considered specific (periventricular, infratentorial, juxtacortical) and not specific (deep/subcortical WM) for MS. CVS+ lesion volume was higher than CVS- lesion volume, both considering the global brain and the four subregions analysed, where CVS+ lesions were also numerically prevalent. In a recent study¹⁴⁷, it was reported that CVS+ lesion volume in the whole brain and CVS+ lesion number in the deep/subcortical WM were higher than CVS- lesion volume and CVS- lesion number in the global brain and deep/subcortical WM respectively, although this difference did not reach statistical significance. The larger sample size and the higher number of lesions analysed in our study may partially explain these different findings. Nevertheless, conflicting results emerged also in the juxtacortical area, where Guisset *et al.*¹⁴⁷ found that CVS- lesions were numerically prevalent with respect to CVS+ lesions. CVS evaluation in the juxtacortical area may be challenging due to the possible effect of distortion artefacts intrinsic to EPI-T2* images. To improve the detection rate of CVS+ lesions, we decided to perform EPI-T2* images after contrast agent administration, following the suggestion of previous studies^{70,80,94,174,175}. It is possible that T1 shortening, due to gadolinium administration, may lead to an increase in the phase effects around blood vessels, thus improving the visibility of the central vein^{94,176}. In our study, the CVS assessment in gadolinium enhanced

susceptibility images could have helped to optimize the detection of perivenular lesions on the whole brain but also in challenging areas.

By adding the stratification of MS patients according to age to the evaluation of the CVS in the different brain subregions, we found that in brain subregions considered typical of MS (periventricular, infratentorial, juxtacortical), the relationship between CVS+/CVS- lesion number showed a clear prevalence of CVS+ on CVS- lesions in all age Groups, except for juxtacortical areas in the 56-77 years Group. An overestimation of CVS- lesion in the juxtacortical area throughout all age Groups due to the abovementioned technical issues, despite our attempt to improve CVS detection acquiring EPI-T2* images after contrast injection, may partially explain our findings. Furthermore, despite both SVD and migraine related WM T2-weighted hyperintensities are mostly located in the deep/subcortical WM, different studies showed that also juxtacortical areas may be involved^{145,177,178}. Interestingly, we found that in age Group 4 (56-77 years) CVS- lesion number increased to become higher than CVS+ lesions, although not reaching statistical significance. Therefore, driven by our findings about the impact of age and migraine on the percentage of CVS+ lesions and the inversion of CVS+/CVS- lesions prevalence in deep/subcortical WM in older MS patients, we decided to use SMT model to investigate the pathological substrate of CVS+ and CVS- lesions. The choice to use SMT relied on its interesting basic assumptions and its encouraging recent results in MS^{116,117,126}. Overcoming the issue represented by the fixed intrinsic diffusivity of other multicompartment models¹¹⁷, SMT considers WM as a two-compartment (intra- and extra-axonal) tissue and provides signal fraction and diffusion metrics per axon without confounds from fibre direction, crossing, or dispersion¹¹⁶. This is particularly important in MS because many WM voxels contain complex fibre configurations, and fibre arrangements widely vary within MS lesions. Thus, these

fibre orientation-independent diffusion metrics may provide more accurate estimates of axon integrity. SMT has been already applied in different studies focusing on the brain¹²⁵ and spinal cord¹²⁶ of MS patients, demonstrating to be helpful in differentiating MS lesions damage from the Normal Appearing WM (NAWM) as well as the NAWM of MS patients from that of healthy controls¹¹⁷ and in characterizing pathological features within MS lesions¹²⁷. In this study, we demonstrated that SMT was able to investigate the pathological substrates of CVS+ and CVS- lesions and to detect distinctive features capable in differentiating them from each other. Compared to CVS- lesions, perivenular lesions showed higher EXTRAMD, indirectly reflecting higher free water content, higher EXTRATRANS, indirect expression of a decrease in myelin content and lower INTRA, suggestive of a higher degree of axonal damage and fibre disruption. Thus, we could suggest that perivenular lesions, typical of MS, are characterized by a more severe degree of inflammation, demyelination and fibre disruption than non-perivenular lesions, possibly associated by different pathophysiological mechanisms. Similar strong evidence was found comparing all SMT metrics within CVS+ and CVS- lesions clustered in the deep/subcortical WM. Fibber disruption seemed to be higher also in perivenular lesions located in periventricular areas, while cerebrospinal fluid (CSF) contamination could have affected extraneurite compartment metrics (EXTRAMD >in CVS- lesions; no difference between CVS+ and CVS- lesions in EXTRATRANS). Similar, although weaker, differences were found in juxtacortical and infratentorial areas; a higher inflammatory component was detected in CVS+ lesions located in both regions and a more pronounced degree of demyelination was found in infratentorial CVS+ lesions. The lower mean volume of juxtacortical and infratentorial T2-weighted hyperintensities may

explain why SMT metrics seem to perform worse in differentiating perivenular from non-perivenular lesions in these areas.

This study is not without limitation. Firstly, the presence of a comparison group including non-MS patients suffering from RFs for SVD and/or migraine would have been extremely helpful to investigate whether CVS- lesions in MS and non-MS patients possibly share microstructural features, thus potentially contributing to validate our findings. Moreover, the cross-sectional design of this study does not allow to evaluate how and where the new T2-weighted hyperintensities develop over time and their temporal relationships with aging and other comorbidities in patients with MS. Finally, the relatively low incidence of MS patients with RFs for SVD in our sample may have underestimated the role of HT, above all, in reducing the percentage of CVS+ lesions and thus affecting CVS performance.

In conclusion, this study demonstrated that aging has a relevant impact on reducing the percentage of CVS+ lesions in MS patients. This effect is already clear when whole brain is considered but becomes even more evident when the deep/subcortical WM, a region not typical of MS, is specifically analysed. Indeed, in this site non-perivenular lesions become prevalent on perivenular lesions in older MS patients. Among the other comorbidities, for the first time we showed that migraine may play a significant role in increasing the amount of non-perivenular lesions also in younger MS patients. Furthermore, we demonstrated that SMT-derived metrics may provide a deep characterization of microstructural features within WM lesions and, for the first time, that these metrics are able to differentiate perivenular lesions, characterized by higher levels of inflammation, demyelination and fibre disruption, from non-perivenular lesions, for which other pathophysiological mechanisms could be suggested. These findings have not an

immediate impact on the diagnostic accuracy of the CVS but may be very useful to deepen our knowledge about MS lesions pathophysiology.

Therefore, in our opinion, the development of a new non-perivenular T2-weighted hyperintensity, especially if located in the deep/subcortical WM in older MS patients, should be considered a “red flag” for a different -other than MS disease activity- pathophysiology. A careful evaluation of comorbidities during CVS assessment for the diagnosis and monitoring of MS should be mandatory, to avoid misleading interpretations and potentially inappropriate therapeutic strategies.

5. Bibliography

1. Thompson AJ, Banwell BL, Barkhof F, et al. Diagnosis of multiple sclerosis: 2017 revisions of the McDonald criteria. *Lancet Neurol.* 2018;17(2):162-173. doi:10.1016/S1474-4422(17)30470-2
2. Lublin FD, Reingold SC, Cohen JA, et al. Defining the clinical course of multiple sclerosis: the 2013 revisions. *Neurology.* 2014;83(3):278-286. doi:10.1212/WNL.0000000000000560
3. Reich DS, Lucchinetti CF, Calabresi PA. Multiple Sclerosis. *N Engl J Med.* 2018;378(2):169-180. doi:10.1056/NEJMra1401483
4. Global, regional, and national burden of neurological disorders, 1990-2016: a systematic analysis for the Global Burden of Disease Study 2016. *Lancet Neurol.* 2019;18(5):459-480. doi:10.1016/S1474-4422(18)30499-X
5. Browne P, Chandraratna D, Angood C, et al. Atlas of Multiple Sclerosis 2013: A growing global problem with widespread inequity. *Neurology.* 2014;83(11):1022-1024. doi:10.1212/WNL.0000000000000768
6. Koch-Henriksen N, Soerensen P. Koch-Henriksen, N. & Sorensen, P. S. The changing demographic pattern of multiple sclerosis epidemiology. *Lancet Neurol.* 9, 520-532. *Lancet Neurol.* 2010;9:520-532. doi:10.1016/S1474-4422(10)70064-8
7. Orton S-M, Herrera BM, Yee IM, et al. Sex ratio of multiple sclerosis in Canada: a longitudinal study. *Lancet Neurol.* 2006;5(11):932-936. doi:10.1016/s1474-4422(06)70581-6
8. Kingwell E, van der Kop M, Zhao Y, et al. Relative mortality and survival in

- multiple sclerosis: findings from British Columbia, Canada. *J Neurol Neurosurg & Psychiatry*. 2012;83(1):61 LP - 66. doi:10.1136/jnnp-2011-300616
9. Leray E, Vukusic S, Debouverie M, et al. Excess Mortality in Patients with Multiple Sclerosis Starts at 20 Years from Clinical Onset: Data from a Large-Scale French Observational Study. *PLoS One*. 2015;10(7):e0132033. doi:10.1371/journal.pone.0132033
 10. Kjetil B, Marianna C, C. HB, et al. Longitudinal analysis reveals high prevalence of Epstein-Barr virus associated with multiple sclerosis. *Science (80-)*. 2022;375(6578):296-301. doi:10.1126/science.abj8222
 11. Belbasis L, Bellou V, Evangelou E, Ioannidis JPA, Tzoulaki I. Environmental risk factors and multiple sclerosis: an umbrella review of systematic reviews and meta-analyses. *Lancet Neurol*. 2015;14(3):263-273. doi:10.1016/S1474-4422(14)70267-4
 12. Dendrou CA, Fugger L, Friese MA. Immunopathology of multiple sclerosis. *Nat Rev Immunol*. 2015;15(9):545-558. doi:10.1038/nri3871
 13. Ebers GC, Bulman DE, Sadovnick AD, et al. A Population-Based Study of Multiple Sclerosis in Twins. *N Engl J Med*. 1986;315(26):1638-1642. doi:10.1056/NEJM198612253152603
 14. Hollenbach JA, Oksenberg JR. The immunogenetics of multiple sclerosis: A comprehensive review. *J Autoimmun*. 2015;64:13-25. doi:10.1016/j.jaut.2015.06.010
 15. Koch MW, Ilnytsky Y, Golubov A, Metz LM, Yong VW, Kovalchuk O. Global transcriptome profiling of mild relapsing-remitting versus primary

- progressive multiple sclerosis. *Eur J Neurol.* 2018;25(4):651-658.
doi:10.1111/ene.13565
16. Lassmann H. Pathogenic Mechanisms Associated With Different Clinical Courses of Multiple Sclerosis. *Front Immunol.* 2018;9:3116.
doi:10.3389/fimmu.2018.03116
 17. Trapp BD, Nave K-A. Multiple sclerosis: an immune or neurodegenerative disorder? *Annu Rev Neurosci.* 2008;31:247-269.
doi:10.1146/annurev.neuro.30.051606.094313
 18. Stys PK, Zamponi GW, van Minnen J, Geurts JGG. Will the real multiple sclerosis please stand up? *Nat Rev Neurosci.* 2012;13(7):507-514.
doi:10.1038/nrn3275
 19. Miller DH, Chard DT, Ciccarelli O. Clinically isolated syndromes. *Lancet Neurol.* 2012;11(2):157-169. doi:10.1016/S1474-4422(11)70274-5
 20. Montalban X, Gold R, Thompson AJ, et al.ECTRIMS/EAN Guideline on the pharmacological treatment of people with multiple sclerosis. *Mult Scler.* 2018;24(2):96-120. doi:10.1177/1352458517751049
 21. Lipp I, Tomassini V. Neuroplasticity and motor rehabilitation in multiple sclerosis. *Front Neurol.* 2015;6:59. doi:10.3389/fneur.2015.00059
 22. Polman CH, Reingold SC, Edan G, et al. Diagnostic criteria for multiple sclerosis: 2005 revisions to the “McDonald Criteria”. *Ann Neurol.* 2005;58(6):840-846. doi:10.1002/ana.20703
 23. Polman CH, Reingold SC, Banwell B, et al. Diagnostic criteria for multiple sclerosis: 2010 revisions to the McDonald criteria. *Ann Neurol.*

- 2011;69(2):292-302. doi:10.1002/ana.22366
24. McDonald WI, Compston A, Edan G, et al. Recommended diagnostic criteria for multiple sclerosis: guidelines from the International Panel on the diagnosis of multiple sclerosis. *Ann Neurol.* 2001;50(1):121-127. doi:10.1002/ana.1032
 25. Miller DH, Grossman RI, Reingold SC, McFarland HF. The role of magnetic resonance techniques in understanding and managing multiple sclerosis. *Brain.* 1998;121 (Pt 1):3-24. doi:10.1093/brain/121.1.3
 26. Klawiter EC. Current and new directions in MRI in multiple sclerosis. *Continuum (Minneap Minn).* 2013;19(4 Multiple Sclerosis):1058-1073. doi:10.1212/01.CON.0000433283.00221.37
 27. Filippi M, Rocca MA, Ciccarelli O, et al. MRI criteria for the diagnosis of multiple sclerosis: MAGNIMS consensus guidelines. *Lancet Neurol.* 2016;15(3):292-303. doi:10.1016/S1474-4422(15)00393-2
 28. Odenthal C, Coulthard A. The prognostic utility of MRI in clinically isolated syndrome: a literature review. *AJNR Am J Neuroradiol.* 2015;36(3):425-431. doi:10.3174/ajnr.A3954
 29. Brownlee WJ, Miller DH. Clinically isolated syndromes and the relationship to multiple sclerosis. *J Clin Neurosci Off J Neurosurg Soc Australas.* 2014;21(12):2065-2071. doi:10.1016/j.jocn.2014.02.026
 30. Okuda DT, Mowry EM, Beheshtian A, et al. Incidental MRI anomalies suggestive of multiple sclerosis: the radiologically isolated syndrome. *Neurology.* 2009;72(9):800-805. doi:10.1212/01.wnl.0000335764.14513.1a

31. Granberg T, Martola J, Kristoffersen-Wiberg M, Aspelin P, Fredrikson S. Radiologically isolated syndrome--incidental magnetic resonance imaging findings suggestive of multiple sclerosis, a systematic review. *Mult Scler*. 2013;19(3):271-280. doi:10.1177/1352458512451943
32. Giovannoni G, Butzkueven H, Dhib-Jalbut S, et al. Brain health: time matters in multiple sclerosis. *Mult Scler Relat Disord*. 2016;9 Suppl 1:S5-S48. doi:10.1016/j.msard.2016.07.003
33. Freedman MS, Comi G, De Stefano N, et al. Moving toward earlier treatment of multiple sclerosis: Findings from a decade of clinical trials and implications for clinical practice. *Mult Scler Relat Disord*. 2014;3(2):147-155. doi:10.1016/j.msard.2013.07.001
34. Singh H, Graber ML. Improving Diagnosis in Health Care — The Next Imperative for Patient Safety. *N Engl J Med*. 2015;373(26):2493-2495. doi:10.1056/NEJMp1512241
35. Zwaan L, Schiff GD, Singh H. Advancing the research agenda for diagnostic error reduction. *BMJ Qual & Saf*. 2013;22(Suppl 2):ii52 LP-ii57. doi:10.1136/bmjqs-2012-001624
36. Graber ML. The incidence of diagnostic error in medicine. *BMJ Qual Saf*. 2013;22 Suppl 2(Suppl 2):ii21-ii27. doi:10.1136/bmjqs-2012-001615
37. Solomon AJ, Weinshenker BG. Misdiagnosis of multiple sclerosis: frequency, causes, effects, and prevention. *Curr Neurol Neurosci Rep*. 2013;13(12):403. doi:10.1007/s11910-013-0403-y
38. Hankey GJ, Stewart-Wynne EG. Pseudo-multiple sclerosis: a clinico-epidemiological study. *Clin Exp Neurol*. 1987;24:11-19.

39. Engell T. A clinico-pathoanatomical study of multiple sclerosis diagnosis. *Acta Neurol Scand.* 1988;78(1):39-44. doi:10.1111/j.1600-0404.1988.tb03616.x
40. Rudick RA, Schiffer RB, Schwetz KM, Herndon RM. Multiple sclerosis. The problem of incorrect diagnosis. *Arch Neurol.* 1986;43(6):578-583. doi:10.1001/archneur.1986.00520060042015
41. Poser CM. Misdiagnosis of multiple sclerosis and beta-interferon. *Lancet (London, England).* 1997;349(9069):1916. doi:10.1016/S0140-6736(05)63920-7
42. Solomon AJ, Klein EP, Bourdette D. “Undiagnosing” multiple sclerosis: the challenge of misdiagnosis in MS. *Neurology.* 2012;78(24):1986-1991. doi:10.1212/WNL.0b013e318259e1b2
43. Confavreux C, Vukusic S. Natural history of multiple sclerosis: a unifying concept. *Brain.* 2006;129(Pt 3):606-616. doi:10.1093/brain/awl007
44. Miller DH, Weinshenker BG, Filippi M, et al. Differential diagnosis of suspected multiple sclerosis: a consensus approach. *Mult Scler.* 2008;14(9):1157-1174. doi:10.1177/1352458508096878
45. Charil A, Yousry TA, Rovaris M, et al. MRI and the diagnosis of multiple sclerosis: expanding the concept of “no better explanation”. *Lancet Neurol.* 2006;5(10):841-852. doi:10.1016/S1474-4422(06)70572-5
46. Liu S, Kullnat J, Bourdette D, et al. Prevalence of brain magnetic resonance imaging meeting Barkhof and McDonald criteria for dissemination in space among headache patients. *Mult Scler.* 2013;19(8):1101-1105. doi:10.1177/1352458512471874

47. Kim SS, Richman DP, Johnson WO, Hald J, Agius MA. Limited utility of current MRI criteria for distinguishing multiple sclerosis from common mimickers: primary and secondary CNS vasculitis, lupus and Sjogren_s syndrome. *Mult Scler J*. 2014;20:57-63.
48. Stangel M, Fredrikson S, Meinl E, Petzold A, Stüve O, Tumani H. The utility of cerebrospinal fluid analysis in patients with multiple sclerosis. *Nat Rev Neurol*. 2013;9(5):267-276. doi:10.1038/nrneurol.2013.41
49. Petzold A. Intrathecal oligoclonal IgG synthesis in multiple sclerosis. *J Neuroimmunol*. 2013;262(1-2):1-10. doi:10.1016/j.jneuroim.2013.06.014
50. Dobson R, Ramagopalan S, Davis A, Giovannoni G. Cerebrospinal fluid oligoclonal bands in multiple sclerosis and clinically isolated syndromes: a meta-analysis of prevalence, prognosis and effect of latitude. *J Neurol Neurosurg Psychiatry*. 2013;84(8):909-914. doi:10.1136/jnnp-2012-304695
51. Selchen D, Bhan V, Blevins G, et al. MS, MRI, and the 2010 McDonald criteria: a Canadian expert commentary. *Neurology*. 2012;79(23 Suppl 2):S1-15. doi:10.1212/WNL.0b013e318277d144
52. Schiffer RB, Giang DW, Mushlin A, et al. Perils and pitfalls of magnetic resonance imaging in the diagnosis of multiple sclerosis. The Rochester-Toronto MRI Study Group. *J Neuroimaging*. 1993;3(2):81-88. doi:10.1111/jon19933281
53. Boster A, Caon C, Perumal J, et al. Failure to develop multiple sclerosis in patients with neurologic symptoms without objective evidence. *Mult Scler*. 2008;14(6):804-808. doi:10.1177/1352458507088156
54. Uitdehaag BMJ, Kappos L, Bauer L, et al. Discrepancies in the interpretation

- of clinical symptoms and signs in the diagnosis of multiple sclerosis. A proposal for standardization. *Mult Scler.* 2005;11(2):227-231. doi:10.1191/1352458505ms1149oa
55. Solomon AJ, Bourdette DN, Cross AH, et al. The contemporary spectrum of multiple sclerosis misdiagnosis: A multicenter study. *Neurology.* 2016;87(13):1393-1399. doi:10.1212/WNL.0000000000003152
56. Hawkes CH, Giovannoni G. The McDonald Criteria for Multiple Sclerosis: time for clarification. *Mult Scler.* 2010;16(5):566-575. doi:10.1177/1352458510362441
57. Lumley R, Davenport R, Williams A. Most Scottish neurologists do not apply the 2010 McDonald criteria when diagnosing multiple sclerosis. *J R Coll Physicians Edinb.* 2015;45(1):23-26. doi:10.4997/JRCPE.2015.106
58. Gooch CL, Pracht E, Borenstein AR. The burden of neurological disease in the United States: A summary report and call to action. *Ann Neurol.* 2017;81(4):479-484. doi:10.1002/ana.24897
59. Ontaneda D, Tallantyre E, Kalincik T, Planchon SM, Evangelou N. Early highly effective versus escalation treatment approaches in relapsing multiple sclerosis. *Lancet Neurol.* 2019;18(10):973-980. doi:10.1016/S1474-4422(19)30151-6
60. Midaglia L, Sastre-Garriga J, Pappolla A, et al. The frequency and characteristics of MS misdiagnosis in patients referred to the multiple sclerosis centre of Catalonia. *Mult Scler J.* 2021;27(6):913-921. doi:10.1177/1352458520988148
61. Teunissen CE, Malekzadeh A, Leurs C, Bridel C, Killestein J. Body fluid

- biomarkers for multiple sclerosis--the long road to clinical application. *Nat Rev Neurol*. 2015;11(10):585-596. doi:10.1038/nrneurol.2015.173
62. Raphael I, Webb J, Stuve O, Haskins W, Forsthuber T. Body fluid biomarkers in multiple sclerosis: how far we have come and how they could affect the clinic now and in the future. *Expert Rev Clin Immunol*. 2015;11(1):69-91. doi:10.1586/1744666X.2015.991315
63. D'Ambrosio A, Pontecorvo S, Colasanti T, Zamboni S, Francia A, Margutti P. Peripheral blood biomarkers in multiple sclerosis. *Autoimmun Rev*. 2015;14(12):1097-1110. doi:10.1016/j.autrev.2015.07.014
64. Comabella M, Montalban X. Body fluid biomarkers in multiple sclerosis. *Lancet Neurol*. 2014;13(1):113-126. doi:10.1016/S1474-4422(13)70233-3
65. Sati P, Oh J, Todd Constable R, et al. The central vein sign and its clinical evaluation for the diagnosis of multiple sclerosis: A consensus statement from the North American Imaging in Multiple Sclerosis Cooperative. *Nat Rev Neurol*. 2016;12(12):714-722. doi:10.1038/nrneurol.2016.166
66. Rae-Grant AD, Wong C, Bernatowicz R, Fox RJ. Observations on the brain vasculature in multiple sclerosis: A historical perspective. *Mult Scler Relat Disord*. 2014;3(2):156-162. doi:10.1016/j.msard.2013.08.005
67. Barnett MH, Prineas JW. Relapsing and remitting multiple sclerosis: pathology of the newly forming lesion. *Ann Neurol*. 2004;55(4):458-468. doi:10.1002/ana.20016
68. Adams CW. The onset and progression of the lesion in multiple sclerosis. *J Neurol Sci*. 1975;25(2):165-182. doi:10.1016/0022-510x(75)90138-0

69. Reichenbach JR, Venkatesan R, Schillinger DJ, Kido DK, Haacke EM. Small vessels in the human brain: MR venography with deoxyhemoglobin as an intrinsic contrast agent. *Radiology*. 1997;204(1):272-277. doi:10.1148/radiology.204.1.9205259
70. Tan IL, van Schijndel RA, Pouwels PJ, et al. MR venography of multiple sclerosis. *AJNR Am J Neuroradiol*. 2000;21(6):1039-1042.
71. Tallantyre EC, Brookes MJ, Dixon JE, Morgan PS, Evangelou N, Morris PG. Demonstrating the perivascular distribution of MS lesions in vivo with 7-Tesla MRI. *Neurology*. 2008;70(22):2076-2078. doi:10.1212/01.wnl.0000313377.49555.2e
72. Hammond KE, Metcalf M, Carvajal L, et al. Quantitative in vivo magnetic resonance imaging of multiple sclerosis at 7 Tesla with sensitivity to iron. *Ann Neurol*. 2008;64(6):707-713. doi:10.1002/ana.21582
73. Kuchling J, Ramien C, Bozin I, et al. Identical lesion morphology in primary progressive and relapsing-remitting MS--an ultrahigh field MRI study. *Mult Scler*. 2014;20(14):1866-1871. doi:10.1177/1352458514531084
74. Kilsdonk ID, Lopez-Soriano A, Kuijjer JPA, et al. Morphological features of MS lesions on FLAIR* at 7 T and their relation to patient characteristics. *J Neurol*. 2014;261(7):1356-1364. doi:10.1007/s00415-014-7351-6
75. Sati P, George IC, Shea CD, Gaitán MI, Reich DS. FLAIR*: a combined MR contrast technique for visualizing white matter lesions and parenchymal veins. *Radiology*. 2012;265(3):926-932. doi:10.1148/radiol.12120208
76. Dawson JW. The Histology of Disseminated Sclerosis. *Edinb Med J*. 1916;17(4):229-241.

<https://www.ncbi.nlm.nih.gov/pmc/articles/PMC5273367/>

77. Zivadinov R, Weinstock-Guttman B, Hashmi K, et al. Smoking is associated with increased lesion volumes and brain atrophy in multiple sclerosis. *Neurology*. 2009;73(7):504-510. doi:10.1212/WNL.0b013e3181b2a706
78. Weinstock-Guttman B, Zivadinov R, Horakova D, et al. Lipid profiles are associated with lesion formation over 24 months in interferon- β treated patients following the first demyelinating event. *J Neurol Neurosurg Psychiatry*. 2013;84(11):1186-1191. doi:10.1136/jnnp-2012-304740
79. Chavhan GB, Babyn PS, Thomas B, Shroff MM, Haacke EM. Principles, techniques, and applications of T2*-based MR imaging and its special applications. *Radiogr a Rev Publ Radiol Soc North Am Inc*. 2009;29(5):1433-1449. doi:10.1148/rg.295095034
80. Sati P, Thomasson DM, Li N, et al. Rapid, high-resolution, whole-brain, susceptibility-based MRI of multiple sclerosis. *Mult Scler*. 2014;20(11):1464-1470. doi:10.1177/1352458514525868
81. Mistry N, Dixon J, Tallantyre E, et al. Central veins in brain lesions visualized with high-field magnetic resonance imaging: a pathologically specific diagnostic biomarker for inflammatory demyelination in the brain. *JAMA Neurol*. 2013;70(5):623-628. doi:10.1001/jamaneurol.2013.1405
82. Kau T, Taschwer M, Deutschmann H, Schönfelder M, Weber JR, Hausegger KA. The “central vein sign”: is there a place for susceptibility weighted imaging in possible multiple sclerosis? *Eur Radiol*. 2013;23(7):1956-1962. doi:10.1007/s00330-013-2791-4
83. Ge Y, Zohrabian VM, Grossman RI. Seven-Tesla Magnetic Resonance

- Imaging: New Vision of Microvascular Abnormalities in Multiple Sclerosis. *Arch Neurol.* 2008;65(6):812-816. doi:10.1001/archneur.65.6.812
84. Sinnecker T, Dörr J, Pfueller CF, et al. Distinct lesion morphology at 7-T MRI differentiates neuromyelitis optica from multiple sclerosis. *Neurology.* 2012;79(7):708-714. doi:10.1212/WNL.0b013e3182648bc8
85. Kister I, Herbert J, Zhou Y, Ge Y. Ultrahigh-Field MR (7 T) Imaging of Brain Lesions in Neuromyelitis Optica. *Mult Scler Int.* 2013;2013:398259. doi:10.1155/2013/398259
86. Grabner G, Dal-Bianco A, Schernthaner M, Vass K, Lassmann H, Trattnig S. Analysis of multiple sclerosis lesions using a fusion of 3.0 T FLAIR and 7.0 T SWI phase: FLAIR SWI. *J Magn Reson Imaging.* 2011;33(3):543-549. doi:10.1002/jmri.22452
87. Dal-Bianco A, Hametner S, Grabner G, et al. Veins in plaques of multiple sclerosis patients - a longitudinal magnetic resonance imaging study at 7 Tesla. *Eur Radiol.* 2015;25(10):2913-2920. doi:10.1007/s00330-015-3719-y
88. Haacke EM, Xu Y, Cheng Y-CN, Reichenbach JR. Susceptibility weighted imaging (SWI). *Magn Reson Med.* 2004;52(3):612-618. doi:10.1002/mrm.20198
89. Denk C, Rauscher A. Susceptibility weighted imaging with multiple echoes. *J Magn Reson Imaging.* 2010;31(1):185-191. doi:10.1002/jmri.21995
90. Sati P, Cross AH, Luo J, Hildebolt CF, Yablonskiy DA. In vivo quantitative evaluation of brain tissue damage in multiple sclerosis using gradient echo plural contrast imaging technique. *Neuroimage.* 2010;51(3):1089-1097. doi:10.1016/j.neuroimage.2010.03.045

91. Luo J, Yablonskiy DA, Hildebolt CF, Lancia S, Cross AH. Gradient echo magnetic resonance imaging correlates with clinical measures and allows visualization of veins within multiple sclerosis lesions. *Mult Scler.* 2014;20(3):349-355. doi:10.1177/1352458513495935
92. Zwanenburg JJM, Versluis MJ, Luijten PR, Petridou N. Fast high resolution whole brain T2* weighted imaging using echo planar imaging at 7T. *Neuroimage.* 2011;56(4):1902-1907. doi:10.1016/j.neuroimage.2011.03.046
93. Dixon JE, Simpson A, Mistry N, Evangelou N, Morris PG. Optimisation of T2*-weighted MRI for the detection of small veins in multiple sclerosis at 3 T and 7 T. *Eur J Radiol.* 2013;82(5):719-727. doi:10.1016/j.ejrad.2011.09.023
94. Maggi P, Mazzoni LN, Moretti M, Grammatico M, Chiti S, Massacesi L. SWI enhances vein detection using gadolinium in multiple sclerosis. *Acta Radiol Open.* 2015;4(3):204798161456093. doi:10.1177/2047981614560938
95. Massacesi L. Evaluation by brain MRI of white matter perivenular lesions in inflammatory microangiopathic ischemia and in demyelinating multiple sclerosis lesions. [abstract O2217] *Eur J Neurol* 23 (Suppl 2), 86. 2012;5(1):13-22. doi:10.1177/1756285611425694
96. Lummel N, Boeckh-Behrens T, Schoepf V, Burke M, Brückmann H, Linn J. Presence of a central vein within white matter lesions on susceptibility weighted imaging: a specific finding for multiple sclerosis? *Neuroradiology.* 2011;53(5):311-317. doi:10.1007/s00234-010-0736-z
97. Tallantyre EC, Dixon JE, Donaldson I, et al. Ultra-high-field imaging distinguishes MS lesions from asymptomatic white matter lesions.

- Neurology*. 2011;76(6):534-539. doi:10.1212/WNL.0b013e31820b7630
98. Samaraweera APR, Clarke MA, Whitehead A, et al. The Central Vein Sign in Multiple Sclerosis Lesions Is Present Irrespective of the T2* Sequence at 3 T. *J Neuroimaging*. 2017;27(1):114-121. doi:10.1111/jon.12367
99. Mistry N, Abdel-Fahim R, Samaraweera A, et al. Imaging central veins in brain lesions with 3-T T2*-weighted magnetic resonance imaging differentiates multiple sclerosis from microangiopathic brain lesions. *Mult Scler*. 2016;22(10):1289-1296. doi:10.1177/1352458515616700
100. Lane JJ, Bolster B, Campeau NG, Welker KM, Gilbertson JR. Characterization of multiple sclerosis plaques using susceptibility-weighted imaging at 1.5 T: can perivenular localization improve specificity of imaging criteria? *J Comput Assist Tomogr*. 2015;39(3):317-320. doi:10.1097/RCT.0000000000000233
101. Kilsdonk ID, Wattjes MP, Lopez-Soriano A, et al. Improved differentiation between MS and vascular brain lesions using FLAIR* at 7 Tesla. *Eur Radiol*. 2014;24(4):841-849. doi:10.1007/s00330-013-3080-y
102. Wuerfel J, Sinnecker T, Ringelstein EB, et al. Lesion morphology at 7 Tesla MRI differentiates Susac syndrome from multiple sclerosis. *Mult Scler*. 2012;18(11):1592-1599. doi:10.1177/1352458512441270
103. Solomon AJ, Schindler MK, Howard DB, et al. "Central vessel sign" on 3T FLAIR* MRI for the differentiation of multiple sclerosis from migraine. *Ann Clin Transl Neurol*. 2016;3(2):82-87. doi:10.1002/acn3.273
104. George IC, Sati P, Absinta M, et al. Clinical 3-tesla FLAIR* MRI improves diagnostic accuracy in multiple sclerosis. *Mult Scler*. 2016;22(12):1578-

1586. doi:10.1177/1352458515624975
105. Solomon AJ, Watts R, Ontaneda D, Absinta M, Sati P, Reich DS. Diagnostic performance of central vein sign for multiple sclerosis with a simplified three-lesion algorithm. *Mult Scler.* 2018;24(6):750-757. doi:10.1177/1352458517726383
106. Maggi P, Absinta M, Grammatico M, et al. Central vein sign differentiates Multiple Sclerosis from central nervous system inflammatory vasculopathies. *Ann Neurol.* 2018;83(2):283-294. doi:10.1002/ana.25146
107. Basser PJ, Mattiello J, LeBihan D. MR diffusion tensor spectroscopy and imaging. *Biophys J.* 1994;66(1):259-267. doi:10.1016/S0006-3495(94)80775-1
108. Alexander DC, Dyrby TB, Nilsson M, Zhang H. Imaging brain microstructure with diffusion MRI: practicality and applications. *NMR Biomed.* 2019;32(4):e3841. doi:10.1002/nbm.3841
109. Inglese M, Bester M. Diffusion imaging in multiple sclerosis: research and clinical implications. *NMR Biomed.* 2010;23(7):865-872. doi:10.1002/nbm.1515
110. Filippi M, Cercignani M, Inglese M, Horsfield MA, Comi G. Diffusion tensor magnetic resonance imaging in multiple sclerosis. *Neurology.* 2001;56(3):304-311. doi:10.1212/wnl.56.3.304
111. Hygino da Cruz LCJ, Batista RR, Domingues RC, Barkhof F. Diffusion magnetic resonance imaging in multiple sclerosis. *Neuroimaging Clin N Am.* 2011;21(1):71-88, vii-viii. doi:10.1016/j.nic.2011.02.006

112. Cercignani M, Iannucci G, Filippi M. Diffusion-weighted imaging in multiple sclerosis. *Ital J Neurol Sci.* 1999;20(5 Suppl):S246-9. doi:10.1007/s100729970005
113. Cercignani M, Gandini Wheeler-Kingshott C. From micro- to macro-structures in multiple sclerosis: what is the added value of diffusion imaging. *NMR Biomed.* 2019;32(4):e3888. doi:10.1002/nbm.3888
114. Pagani E, Bammer R, Horsfield MA, et al. Diffusion MR Imaging in Multiple Sclerosis: Technical Aspects and Challenges. *Am J Neuroradiol.* 2007;28(3):411 LP - 420. <http://www.ajnr.org/content/28/3/411.abstract>
115. Zhang H, Schneider T, Wheeler-Kingshott CA, Alexander DC. NODDI: practical in vivo neurite orientation dispersion and density imaging of the human brain. *Neuroimage.* 2012;61(4):1000-1016. doi:10.1016/j.neuroimage.2012.03.072
116. Kaden E, Kelm ND, Carson RP, Does MD, Alexander DC. Multi-compartment microscopic diffusion imaging. *Neuroimage.* 2016;139:346-359. doi:10.1016/j.neuroimage.2016.06.002
117. Lakhani DA, Schilling KG, Xu J, Bagnato F. Advanced multicompartment diffusion MRI models and their application in multiple sclerosis. *Am J Neuroradiol.* 2020;41(5):751-757. doi:10.3174/AJNR.A6484
118. Schneider T, Brownlee W, Zhang H, Ciccarelli O, Miller DH, Wheeler-Kingshott CG. Sensitivity of multi-shell NODDI to multiple sclerosis white matter changes: a pilot study. *Funct Neurol.* 2017;32(2):97-101. doi:10.11138/fneur/2017.32.2.097
119. Mustafi SM, Harezlak J, Kodiweera C, et al. Detecting white matter

- alterations in multiple sclerosis using advanced diffusion magnetic resonance imaging. *Neural Regen Res.* 2019;14(1):114-123. doi:10.4103/1673-5374.243716
120. Granberg T, Fan Q, Treaba CA, et al. In vivo characterization of cortical and white matter neuroaxonal pathology in early multiple sclerosis. *Brain.* 2017;140(11):2912-2926. doi:10.1093/brain/awx247
121. Collorone S, Cawley N, Grussu F, et al. Reduced neurite density in the brain and cervical spinal cord in relapsing-remitting multiple sclerosis: A NODDI study. *Mult Scler.* 2020;26(13):1647-1657. doi:10.1177/1352458519885107
122. By S, Xu J, Box BA, Bagnato FR, Smith SA. Application and evaluation of NODDI in the cervical spinal cord of multiple sclerosis patients. *NeuroImage Clin.* 2017;15:333-342. doi:https://doi.org/10.1016/j.nicl.2017.05.010
123. Spanò B, Giulietti G, Pisani V, et al. Disruption of neurite morphology parallels MS progression. *Neurol - Neuroimmunol Neuroinflammation.* 2018;5(6):e502. doi:10.1212/NXI.0000000000000502
124. Chen A, Franco G, Smith S, Dortch R, Xu J, Bagnato F. Measuring White Matter Axonal Injury in Patients with Multiple Sclerosis (S31.007). *Neurology.* 2019;92(15 Supplement):S31.007. http://n.neurology.org/content/92/15_Supplement/S31.007.abstract
125. Bagnato F, Franco G, Li H, et al. Probing axons using multi-compartmental diffusion in multiple sclerosis. *Ann Clin Transl Neurol.* 2019;6(9):1595-1605. doi:10.1002/acn3.50836
126. By S, Xu J, Box BA, Bagnato FR, Smith SA. Multi-compartmental diffusion characterization of the human cervical spinal cord in vivo using the spherical

- mean technique. *NMR Biomed.* 2018;31(4):1-12. doi:10.1002/nbm.3894
127. Devan SP, Jiang X, Bagnato F, Xu J. Optimization and numerical evaluation of multi-compartment diffusion MRI using the spherical mean technique for practical multiple sclerosis imaging. *Magn Reson Imaging.* 2020;74:56-63. doi:10.1016/j.mri.2020.09.002
128. Dobrynina LA, Suslina AD, Gubanova M V, et al. White matter hyperintensity in different migraine subtypes. *Sci Rep.* 2021;11(1):10881. doi:10.1038/s41598-021-90341-0
129. Eikermann-Haerter K, Huang SY. White Matter Lesions in Migraine. *Am J Pathol.* 2021;191(11):1955-1962. doi:10.1016/j.ajpath.2021.02.007
130. Cortese R, Magnollay L, Tur C, et al. Value of the central vein sign at 3T to differentiate MS from seropositive NMOSD. *Neurology.* 2018;90(14):e1183-e1190. doi:10.1212/WNL.0000000000005256
131. Mistry N, Abdel-Fahim R, Samaraweera A, et al. Imaging central veins in brain lesions with 3-T T2*-weighted magnetic resonance imaging differentiates multiple sclerosis from microangiopathic brain lesions. *Mult Scler.* 2016;22(10):1289-1296. doi:10.1177/1352458515616700
132. Maggi P, Absinta M, Sati P, et al. The “central vein sign” in patients with diagnostic “red flags” for multiple sclerosis: A prospective multicenter 3T study. *Mult Scler.* 2020;26(4):421-432. doi:10.1177/1352458519876031
133. Sinnecker T, Clarke MA, Meier D, et al. Evaluation of the Central Vein Sign as a Diagnostic Imaging Biomarker in Multiple Sclerosis. *JAMA Neurol.* 2019;76(12):1446-1456. doi:10.1001/jamaneurol.2019.2478

134. Sati P, George IC, Shea CD, Gaitán MI, Reich DS. FLAIR*: A combined MR contrast technique for visualizing white matter lesions and parenchymal veins. *Radiology*. 2012;265(3):926-932. doi:10.1148/radiol.12120208
135. Giovannoni G. Disease-modifying treatments for early and advanced multiple sclerosis: A new treatment paradigm. *Curr Opin Neurol*. 2018;31(3):233-243. doi:10.1097/WCO.0000000000000561
136. Solomon AJ, Watts R, Ontaneda D, et al. Sclerosis with a Simplified Three Lesion Algorithm. 2019;24(6):750-757. doi:10.1177/1352458517726383.Diagnostic
137. Geraldes R, Ciccarelli O, Barkhof F, et al. The current role of MRI in differentiating multiple sclerosis from its imaging mimics. *Nat Rev Neurol*. 2018;14(4):199-213. doi:10.1038/nrneurol.2018.14
138. Kollia K, Maderwald S, Putzki N, et al. First clinical study on ultra-high-field MR imaging in patients with multiple sclerosis: Comparison of 1.5T and 7T. *Am J Neuroradiol*. 2009;30(4):699-702. doi:10.3174/ajnr.A1434
139. Tallantyre EC, Morgan PS, Dixon JE, et al. A comparison of 3T and 7T in the detection of small parenchymal veins within MS lesions. *Invest Radiol*. 2009;44(9):491-494. doi:10.1097/rli.0b013e3181b4c144
140. Kuchling J, Ramien C, Bozin I, et al. Identical lesion morphology in primary progressive and relapsing-remitting MS -an ultrahigh field MRI study. *Mult Scler J*. 2014;20(14):1866-1871. doi:10.1177/1352458514531084
141. Sparacia G, Agnello F, Iaia A, Banco A, Galia M, Midiri M. Multiple sclerosis: prevalence of the 'central vein' sign in white matter lesions on gadolinium-enhanced susceptibility-weighted images. *Neuroradiol J*.

142. Sinnecker T, Clarke MA, Meier D, et al. Evaluation of the Central Vein Sign as a Diagnostic Imaging Biomarker in Multiple Sclerosis. *JAMA Neurol.* 2019;76(12):1446-1456. doi:10.1001/jamaneurol.2019.2478
143. Maggi P, Fartaria MJ, Jorge J, et al. CVSnet: A machine learning approach for automated central vein sign assessment in multiple sclerosis. *NMR Biomed.* 2020;33(5):e4283. doi:10.1002/nbm.4283
144. Lapucci C, Saitta L, Bommarito G, et al. How much do periventricular lesions assist in distinguishing migraine with aura from CIS? *Neurology.* 2019;92(15):e1739-e1744. doi:10.1212/WNL.00000000000007266
145. Absinta M, Rocca MA, Colombo B, et al. Patients with migraine do not have MRI-visible cortical lesions. *J Neurol.* 2012;259(12):2695-2698. doi:10.1007/s00415-012-6571-x
146. Schumacher S, Pache F, Bellmann-Strobl J, et al. Neuromyelitis optica does not impact periventricular venous density versus healthy controls: a 7.0 Tesla MRI clinical study. *MAGMA.* 2016;29(3):535-541. doi:10.1007/s10334-016-0554-3
147. Guisset F, Lolli V, Bugli C, et al. The central vein sign in multiple sclerosis patients with vascular comorbidities. *Mult Scler J.* 2021;27(7):1057-1065. doi:10.1177/1352458520943785
148. Sicras-Mainar A, Ruíz-Beato E, Navarro-Artieda R, Maurino J. Comorbidity and metabolic syndrome in patients with multiple sclerosis from Asturias and Catalonia, Spain. *BMC Neurol.* 2017;17(1):134. doi:10.1186/s12883-017-0914-2

149. Inglese M, Petracca M. MRI in multiple sclerosis: clinical and research update. *Curr Opin Neurol*. 2018;31(3). https://journals.lww.com/co-neurology/Fulltext/2018/06000/MRI_in_multiple_sclerosis__clinical_and_research.4.aspx
150. Adams CWM, Poston RN, Buk SJ. Pathology, histochemistry and immunocytochemistry of lesions in acute multiple sclerosis. *J Neurol Sci*. 1989;92(2-3):291-306. doi:10.1016/0022-510X(89)90144-5
151. Hohlfeld R, Londei M, Massacesi L, Salvetti M. T-cell autoimmunity in multiple sclerosis. *Immunol Today*. 1995;16(6):259-261. doi:10.1016/0167-5699(95)80176-6
152. van der Knaap MS, Valk J. White Matter Lesions of the Elderly. *Magn Reson Myelination Myelin Disord*. Published online 2005:759-766. doi:10.1007/3-540-27660-2_98
153. Hilal S, Mok V, Youn YC, Wong A, Ikram MK, Chen CLH. Prevalence, risk factors and consequences of cerebral small vessel diseases: Data from three Asian countries. *J Neurol Neurosurg Psychiatry*. 2017;88(8):669-674. doi:10.1136/jnnp-2016-315324
154. Khan U, Porteous L, Hassan A, Markus HS. Risk factor profile of cerebral small vessel disease and its subtypes. *J Neurol Neurosurg Psychiatry*. 2007;78(7):702-706. doi:10.1136/jnnp.2006.103549
155. Applebee A. The clinical overlap of multiple sclerosis and headache. *Headache*. 2012;52 Suppl 2:111-116. doi:10.1111/j.1526-4610.2012.02243.x
156. Zaidat OO, Kruit MC, Van Buchem MA, Ferrari MD, Launer LJ. Migraine

- as a Risk Factor for Subclinical Brain Lesions [1] (multiple letters). *J Am Med Assoc.* 2004;291(17):2072-2073. doi:10.1001/jama.291.17.2072-b
157. De Benedittis G, Lorenzetti A, Sina C, Bernasconi V. Magnetic Resonance Imaging in Migraine and Tension-Type Headache. *Headache J Head Face Pain.* 1995;35(5):264-268. doi:10.1111/j.1526-4610.1995.hed3505264.x
158. Eikermann-Haerter K, Huang SY. White Matter Lesions in Migraine. *Am J Pathol.* Published online 2021. doi:10.1016/j.ajpath.2021.02.007
159. Pantoni L. Cerebral small vessel disease: from pathogenesis and clinical characteristics to therapeutic challenges. *Lancet Neurol.* 2010;9(7):689-701. doi:10.1016/S1474-4422(10)70104-6
160. Schiavi S, Petracca M, Sun P, et al. Non-invasive quantification of inflammation, axonal and myelin injury in multiple sclerosis. *Brain.* 2021;144(1):213-223. doi:10.1093/brain/awaa381
161. Jenkinson M, Bannister P, Brady M, Smith S. Improved Optimization for the Robust and Accurate Linear Registration and Motion Correction of Brain Images. *Neuroimage.* 2002;17(2):825-841. doi:10.1006/nimg.2002.1132
162. Greve DN, Fischl B. Accurate and robust brain image alignment using boundary-based registration. *Neuroimage.* 2009;48(1):63-72. doi:10.1016/j.neuroimage.2009.06.060
163. Veraart J, Novikov DS, Christiaens D, Ades-aron B, Sijbers J, Fieremans E. Denoising of diffusion MRI using random matrix theory. *Neuroimage.* 2016;142:394-406. doi:10.1016/j.neuroimage.2016.08.016
164. Tournier JD, Smith R, Raffelt D, et al. MRtrix3: A fast, flexible and open

- software framework for medical image processing and visualisation. *Neuroimage*. 2019;202(January):116137. doi:10.1016/j.neuroimage.2019.116137
165. Andersson JLR, Sotiropoulos SN. An integrated approach to correction for off-resonance effects and subject movement in diffusion MR imaging. *Neuroimage*. 2016;125:1063-1078. doi:10.1016/j.neuroimage.2015.10.019
166. Andersson JLR, Graham MS, Zsoldos E, Sotiropoulos SN. Incorporating outlier detection and replacement into a non-parametric framework for movement and distortion correction of diffusion MR images. *Neuroimage*. 2016;141:556-572. doi:10.1016/j.neuroimage.2016.06.058
167. Andersson JLR, Skare S, Ashburner J. How to correct susceptibility distortions in spin-echo echo-planar images: Application to diffusion tensor imaging. *Neuroimage*. 2003;20(2):870-888. doi:10.1016/S1053-8119(03)00336-7
168. Smith SM, Jenkinson M, Woolrich MW, et al. Advances in functional and structural MR image analysis and implementation as FSL. *Neuroimage*. 2004;23(SUPPL. 1):208-219. doi:10.1016/j.neuroimage.2004.07.051
169. Tustison NJ, Cook PA, Gee JC. N4Itk. 2011;29(6):1310-1320. doi:10.1109/TMI.2010.2046908.N4ITK
170. Inglese M, Madelin G, Oesingmann N, et al. Brain tissue sodium concentration in multiple sclerosis: A sodium imaging study at 3 tesla. *Brain*. 2010;133(3):847-857. doi:10.1093/brain/awp334
171. Kaden E, Kruggel F, Alexander DC. Quantitative mapping of the per-axon diffusion coefficients in brain white matter. *Magn Reson Med*.

- 2016;75(4):1752-1763. doi:10.1002/mrm.25734
172. Zhang CE, Wong SM, Van De Haar HJ, et al. Blood-brain barrier leakage is more widespread in patients with cerebral small vessel disease. *Neurology*. 2017;88(5):426-432. doi:10.1212/WNL.0000000000003556
173. Caunca MR, De Leon-Benedetti A, Latour L, Leigh R, Wright CB. Neuroimaging of cerebral small vessel disease and age-related cognitive changes. *Front Aging Neurosci*. 2019;11(JUN):1-15. doi:10.3389/fnagi.2019.00145
174. Sparacia G, Agnello F, Iaia A, Banco A, Galia M, Midiri M. Multiple sclerosis: prevalence of the “central vein” sign in white matter lesions on gadolinium-enhanced susceptibility-weighted images. *Neuroradiol J*. 2021;34(5):470-475. doi:10.1177/19714009211008750
175. Champion T, Smith RJP, Altmann DR, et al. FLAIR* to visualize veins in white matter lesions: A new tool for the diagnosis of multiple sclerosis? *Eur Radiol*. 2017;27(10):4257-4263. doi:10.1007/s00330-017-4822-z
176. Gaitán MI, Yañez P, Paday Formenti ME, et al. SWAN-venule: An optimized MRI technique to detect the central vein sign in MS Plaques. *Am J Neuroradiol*. 2020;41(3):456-460. doi:10.3174/ajnr.A6437
177. Dobrynina LA, Suslina AD, Gubanov M V., et al. White matter hyperintensity in different migraine subtypes. *Sci Rep*. 2021;11(1):1-9. doi:10.1038/s41598-021-90341-0
178. Lapucci C, Saitta L, Bommarito G, et al. How much do periventricular lesions assist in distinguishing migraine with aura from CIS? *Neurology*. 2019;92(15):1-6. doi:10.1212/WNL.0000000000007266

